THE UNIVERSITY OF QUEENSLAND

AUSTRALIA

Understanding and overcoming monoterpene toxicity in *Saccharomyces cerevisia* for the production of sustainable jet fuels

Timothy Charles Reiss Brennan

Bachelor of Science, Chemical Engineering, UC Berkeley

A thesis submitted for the degree of Doctor of Philosophy at

The University of Queensland in 2014

Australian Institute for Bioengineering and Nanotechnology (AIBN)

Abstract

Monoterpenes are liquid hydrocarbons that can serve as light component precursors for drop-in jet fuels. Fermentative production of monoterpene products in engineered microorganisms, such as *Saccharomyces cerevisiae*, has gained attention as a potential route to deliver these next-generation fuels from renewable biomass. However, end product toxicity presents a formidable problem for microbial synthesis. Due to their hydrophobicity, monoterpene inhibition has long been attributed to membrane interference but the molecular mechanism remains largely unsolved. This thesis applied tools in biochemical engineering, evolution engineering and systems and synthetic biology to: (1) gain a better understanding of the mechanism behind monoterpene inhibition and (2) detail specific strategies to overcome toxicity restraints for improved production.

Contrary to the accepted mechanism of membrane deterioration, these data demonstrate that the plasma membrane is not a target for monoterpene inhibition. Hallmark molecular inhibitory effects, such as increased membrane fluidity and changes in fatty acid content, were not observed during limonene exposure. Analysis of the global transcriptional response to limonene revealed a compensatory reaction to cell wall damage through overexpression of several genes (*ROM1, RLM1, PIR3, CTT1, YGP1, MLP1, PST1, CWP1*) involved in the cell wall integrity signalling pathway. Further studies, including cell wall integrity staining and cell wall sensitivity assays, demonstrated that limonene can disrupt cell wall properties. These findings underscore the position that monoterpene inhibition is not at the molecular level (e.g., membrane interference effects), and that the mechanism of action must stem from the physical interaction between an insoluble monoterpene phase and the surface of a cell.

The inhibitory cell-solvent contact mechanism is not yet understood, but by presenting an inert solvent to the system, toxicity can be significantly reduced. In particular, the nontoxic extractant farnesene, which is already produced in yeast for diesel markets, can be blended with monoterpene precursors to make a terpene-derived biojet fuel. This work describes a biphasic system that can not only relieve product toxicity *in situ* but can also consolidate recovery and downstream purification steps to produce terpene fuel blends that match Jet-A fuel properties.

In addition, adaptive laboratory evolution was used to generate several limonene-tolerant strains. Whole-genome resequencing revealed a number of genetic targets for engineering tolerance. The mutations were constructed in the reference strain and their fitness was evaluated. A truncated version of Tcb3p protein was proven to be responsible

for limonene resistance. This provides new metabolic engineering strategies for further strain improvement.

Lastly, product toxicity affects key production parameters such as yield, titer and rate. Monoterpene-derived jet fuel production will not be viable unless the toxicity challenge is met. To this end, this thesis represents a starting point for the development of both cellular and biochemical engineering techniques to address this problem, while also improving our fundamental understanding of solvent toxicity in *S. cerevisiae.*

Declaration by author

This thesis is composed of my original work, and contains no material previously published or written by another person except where due reference has been made in the text. I have clearly stated the contribution by others to jointly-authored works that I have included in my thesis.

I have clearly stated the contribution of others to my thesis as a whole, including statistical assistance, survey design, data analysis, significant technical procedures, professional editorial advice, and any other original research work used or reported in my thesis. The content of my thesis is the result of work I have carried out since the commencement of my research higher degree candidature and does not include a substantial part of work that has been submitted to qualify for the award of any other degree or diploma in any university or other tertiary institution. I have clearly stated which parts of my thesis, if any, have been submitted to qualify for another award.

I acknowledge that an electronic copy of my thesis must be lodged with the University Library and, subject to the General Award Rules of The University of Queensland, immediately made available for research and study in accordance with the *Copyright Act 1968*.

I acknowledge that copyright of all material contained in my thesis resides with the copyright holder(s) of that material. Where appropriate I have obtained copyright permission from the copyright holder to reproduce material in this thesis.

Publications during candidature

Brennan, T.C.R., Turner, C.D., Krömer, J.O. & Nielsen, L.K. Alleviating monoterpene toxicity using a two-phase extractive fermentation for the bioproduction of jet fuel mixtures in *Saccharomyces cerevisiae. Biotechnol Bioeng* **109**, 2513-2522 (2012).

Brennan, T.C.R., Krömer, J.O. & Nielsen, L.K. Physiological and Transcriptional Responses of Saccharomyces cerevisiae to d-Limonene Show Changes to the Cell Wall but Not to the Plasma Membrane. *Appl Environ Microbiol* **79**, 3590-3600 (2013).

Publications included in this thesis

Brennan, T.C.R., Turner, C.D., Krömer, J.O. & Nielsen, L.K. Alleviating monoterpene toxicity using a two-phase extractive fermentation for the bioproduction of jet fuel mixtures in *Saccharomyces cerevisiae. Biotechnol Bioeng* **109**, 2513-2522 (2012).

Incorporated as Chapter 2

Contributor	Statement of contribution
Brennan, T.C.R. (Candidate)	Designed experiments (80%) Wrote the paper (80%)
Turner, C.D.	Carried out thermodynamic modelling of jet fuel properties (Table V)
Krömer, J.O.	Designed experiments (20%) Wrote and edited the paper (20%)
Nielsen, L.K.	Designed experiments (20%) Wrote and edited the paper (20%)

Brennan, T.C.R., Krömer, J.O. & Nielsen, L.K. Physiological and Transcriptional Responses of Saccharomyces cerevisiae to d-Limonene Show Changes to the Cell Wall but Not to the Plasma Membrane. *Appl Environ Microbiol* **79**, 3590-3600 (2013).

Incorporated as Chapter 3

Contributor	Statement of contribution
Brennan, T.C.R. (Candidate)	Designed experiments (80%)

	Wrote the paper (80%)
Krömer, J.O.	Designed experiments (20%)
	Wrote and edited the paper (20%)
Nielsen, L.K.	Designed experiments (20%)
	Wrote and edited the paper (20%)

Contributions by others to the thesis

Chapter 2:

1.   Brennan TCR, Turner CD, Krömer JO, & Nielsen LK (2012) Alleviating monoterpene toxicity using a two-phase extractive fermentation for the bioproduction of jet fuel mixtures in *Saccharomyces cerevisiae. Biotechnol Bioeng* 109(10):2513-2522.

TCRB, JK and LKN designed the experiments. TCRB carried out the experiments and analysis. CDT performed the thermodynamic modelling of jet fuel properties. TCRB, JK and LKN wrote the paper.

Chapter 3:

2.   Brennan TCR, Krömer JO, & Nielsen LK (2013) Physiological and Transcriptional Responses of Saccharomyces cerevisiae to d-Limonene Show Changes to the Cell Wall but Not to the Plasma Membrane. *Appl Environ Microbiol* 79(12):3590-3600.

TCRB, JK and LKN designed the experiments. TCRB carried out the experiments and analysis. TCRB, JK and LKN wrote the paper.

Chapter 4:

3.   Timothy C. R. Brennan, Thomas C. Williams, Benjamin L. Schulz, Robin W Palfreyman, Jens Kromer, Lars K. Nielsen. Evolutionary engineering improves tolerance towards jet fuel replacements in yeast. (*In preparation*)

TCRB, JK and LKN designed the experiments. TCRB carried out the experiments and analysis. TCW designed the molecular engineering experiments and carried the molecular

engineering experiments. RWP performed the genome mapping. BS, TCRB designed and analyzed the cell wall proteomics experiment. TCRB, JK and LKN wrote the paper.

Statement of parts of the thesis submitted to qualify for the award of another degree

None

Acknowledgements

Australian and New Zealand Standard Research Classifications (ANZSRC)

ANZSRC code: 090499 Chemical Engineering not elsewhere classified, 60%

ANZSRC code: 060114 Systems Biology, 20%

ANZSRC code: 060199, Biochemistry and Cell Biology not elsewhere classified, 20%

Fields of Research (FoR) Classification

FoR code: 0601, Biochemistry and Cell Biology, 50%

FoR code: 0904 Chemical Engineering, 50%

Table of Contents

List of Figures

Chapter 5

List of Tables

Chapter 2

Chapter 3

Chapter 4

List of Abbreviations

ISPR	In situ product recovery
YPD	Rich medium
CBS	Chemically defined medium
Kd	Monoterpene partitioning coefficient
PI	Propidium iodide
MIC	Minimum inhibitory concentration
log Pow	Octanol-water partitioning coefficient
Slimonene	Aqueous solubility for limonene
CFW	Calcofluor white
MFI	Mean fluorescence intensity
DMF	Dimethylformamide
ALE	Adaptive laboratory evolution
IPP	Isopentenyl pyrophosphate
DMAPP	Dimethyllallyl pyrophosphate
GPP	Geranyl pyrophosphate
FPP	Farnesyl pyrophosphate

$\Delta_c H°$ Heat of combustion

OW   oil-in-water emulsion system

Chapter 1: General introduction

Petroleum dominates the world's energy and transportation industries. Environmental concerns and energy security have become two of the most pressing issues the international community faces today. Numerous nations and governments around the globe have set goals to reduce their carbon emissions and dependence on imported oil. For example, the U.S. plans on displacing 30% of its petroleum demand with biofuels by 2030 [1]. Achieving these targets relies on the cooperation and execution of multiple facets of today's complex society including research and development, industry investment, education and political will. However, the ultimate success of these targets will depend on the development of efficient and viable technologies.

Aviation is one of the transportation sectors leading the surge for renewable fuel research [2]. The aviation industry is a cornerstone of the modern economy with global economic impact estimated at USD 3,560 billion, equivalent to 7.5% of world gross domestic product [2]. Globally, the industry is growing, with airline traffic expected to rise 5% annually over the next 20 years [3]. This growth has escalated concerns around fuel resources, given that fuel represents airlines highest operating cost (34%) [3]. Along with the uncertainties of future fuel reserves the industry is also committed to decreasing its environmental impact. Roughly 3% of the world's carbon emissions is caused by aviation and this number is expected to increase in the future [4]. However, coming up with sustainable alternatives for aviation is more difficult than other transportation sectors, which currently have an array of renewable options (e.g., electric engines, natural gas). Planes differ in that they require energy dense liquid fuel. Turbine aviation fuel has specific physio-chemical properties and engine performance requirements [5]. The goal of producing an alternative jet fuel replacement is to make fuels that meet or exceed the current fuel requirements without negative environmental, economic or social impacts.

Metabolic engineering in *Saccharomyces cerevisiae* (baker's yeast) offers an attractive route for the production of replacement jet fuels. Yeast fermentation has been used for millennia for the production of alcohol beverages and to leaven bread. Yeast is the world's most well studied organism. The knowledge base and readily available genetic tools enables researchers to exploit the metabolic capabilities in *S. cerevisiae* more than ever [6, 7]. Recently, petroleum-compatible products (e.g., bisabolene [8] and farnesene [9]) have been successfully produced in yeast as renewable diesel and gasoline fuels. The maturity of both the sugar industry and yeast fermentation was reflected in a recent

techno-economic analysis showing that in Australia, renewable jet fuel production via yeast fermentation from sugarcane was economically superior to production from algae and oil seed [10].

Monoterpenes are C_{10} isoprenoids built from two isoprene (C_5) units. These complex olefins and their derivatives are major constituents of essential oils and find applications as flavours and fragrances (e.g. menthol), antiseptics (e.g. thymol), and solvents (e.g. pinene, limonene, turpentine) [11]. Saturated paraffins generated from monoterpenes have properties similar to the light end fraction of traditional kerosene aviation fuel (Jet-A) making them ideal components for 'drop in' replacements [12, 13]. Engineering heterologous metabolic pathways for the synthesis of monoterpenes and other isoprenoids, has gained attention recently as a route to produce fuels, drugs and chemicals from non-petroleum resources [12, 14]. Reprogramming microbes to produce monoterpenes should be no more difficult than the already completed engineering of *S. cerevisiae* to produce farnesene, a C_{15} sesquiterpene replacement for diesel fuel, that uses the same precursors in the cell [9]. Unlike farnesene, monoterpenes are highly toxic and this core issue must be overcome in order to realize microbial jet fuel production. This problem is the focal point of this thesis. The central aim of the work was to better understand the mode(s) of action monoterpenes have on yeast cells to develop more effective solutions in addressing toxicity and increasing productivity.

Monoterpenes are lipophilic compounds and toxicity has to been attributed to the interference with membrane properties [15-17]. For example, β-pinene inhibits the respiration and essential ion (K^+ and H^+) transport in whole yeast cells, while loss of respiratory control, ATP synthesis inhibition and increased membrane fluidity is observed in isolated yeast mitochondria [16]. These observations indicate that β-pinene interferes with mitochondrial membrane integrity and ATP production, while release of cytoplasmic material in the presence of α-pinene [17] indicates that monoterpenes also can cause severe damage to the plasma membrane. Limonene similarly causes severe interference with cell functions. Cell viability and ethanol production by *S. cerevisiae* using enzymatically digested citrus peel waste was significantly reduced in the presence of 0.02-0.10% orange peel oil, which contains 95-97% limonene [18-20]. Although growth inhibition by orange peel oil, limonene and other nonsubstituted monoterpenes in yeast and bacteria is well-established [15, 16, 20-23], the exact mechanism remains poorly understood.

In order to gain a greater understanding of the toxic actions monoterpenes elicit on cellular function it is useful to differentiate between molecular and phase toxicity [24].

Molecular toxicity in microorganisms is well described. For aqueous-soluble compounds in equilibrium, molecular toxicity increases with a solvent's aqueous concentration, which is proportional to its membrane concentration. Hydrophobic compounds can interchelate into membranes and interfere with membrane properties [25]. Increases in membrane fluidity, membrane permeability, denaturation of membrane-bound proteins, loss of transport mechanisms and reduced energy transduction are some of the consequences of molecular toxicity [26-29]. A compounds critical membrane concentration can be calculated for some common microorganisms given the compounds octanol-water partitioning coefficient (log P_{ow}) [30]. With the membrane and aqueous phases in equilibrium, molecular toxicity peaks when the solvents aqueous solubility has been reached.

Monoterpenes are poorly soluble in water (e.g., $S_{limonene}$ = 6 mg/l) [31]. Any additional monoterpene added or produced beyond this solubility point results a distinct second phase. Theoretically, this means that the maximum toxicity that can be achieved on the molecular level must occur at very low monoterpene concentrations. The interaction of cells with organic phases causes a second type of toxicity, termed phase toxicity. Phase toxicity is a phenomological rather than mechanistic definition: toxicity occurs in the presence of a second phase after water and membrane saturation [32]. Phase toxicity increases with increasing surface area (e.g., due to mixing), suggesting a significant kinetic component to the phenomenon [15]. The exact mode of action has never been elucidated, though several mechanisms have been proposed: disruptions of outer cellular components by cell-solvent contact, extraction of nutrients from the medium and limited access to nutrients by cell-coating [24].

Understanding the mechanism is vital in order to find solutions to the problem. For example, molecular toxicity (e.g., membrane damage) may be addressed by heterologous expression of solvent efflux pumps from *Pseudomonas putida* [33]. So far this strategy has failed for limonene in yeast, though it is not known if this is due to pump compatability with yeast, pump affinity for limonene, or if limonene simply does not cause molecular toxicity. If phase toxicity is the main cause of toxicity, solutions may include physiological changes at the cell surface, evolution of solventogenic strains or *in situ* product recovery techniques to relieve toxicity during production.

This thesis aims to answer two questions: 1) what is the precise mechanism of monoterpene toxicity in *S. cerevisiae* and 2) what are appropriate strategies to overcome inhibition? This thesis does not focus on the pathway engineering aspects of monoterpene production, although this topic is briefly addressed in the discussion section (Chapter 5).

First, I describe a quantitative measure of the inhibitory limits for five potential monoterpene products (Chapter 2). A biochemical engineering strategy is then outlined as an attractive bioprocessing option to address product toxicity *in situ* (Chapter 2). Second, a more detailed analysis towards a greater mechanistic and physiological understanding of monoterpene toxicity is described in Chapter 3. Chapter 4 describes another strategy, which utilizes evolution engineering and systems biology tools, to identify genetic targets for strain improvement. Finally, the current obstacles and a future perspective for renewable jet fuel production in *S. cerevisiae* are discussed in Chapter 5.

Chapter 1 Reference List:

1.   Biomass as feedstock for a bioenergy and bioproducts industry: The technical feasability of a billion-ton annual supply, April 2005 (http://feedstockreview.ornl.gov/pdf/billion_ton_vision.pdf).

2.   Air Transport Action group, Beginners Guide to Aviation Biofuels (May 2009).

3.   Boeing, Current market outlook 2013-2032; http://www.boeing.com/assets/pdf/commercial/cmo/pdf/Boeing_Current_Market_Outlook_2013.pdf.

4.   *Flight Path To The Future,* National Aviation Policy Green Paper, December 2008; pg 182. (http://www.infrastructure.gov.au/aviation/nap/files/Aviation_Green_Paper.pdf).

5.   ASTM overview; (http://www.astm.org/ABOUT/overview.html).

6.   Lee, J.W. et al. Systems metabolic engineering of microorganisms for natural and non-natural chemicals. *Nat Chem Biol* **8**, 536-546 (2012).

7.   Hong, K.-K. & Nielsen, J. Metabolic engineering of *Saccharomyces cerevisiae*: a key cell factory platform for future biorefineries. *Cell. Mol. Life Sci.* **69**, 2671-2690 (2012).

8.   Peralta-Yahya, P.P. et al. Identification and microbial production of a terpene-based advanced biofuel. *Nat Commun* **2**, 483 (2011).

9.   Renninger, N. & McPhee, D. (USA; 2008).

10.   Klein-Marcuschamer, D. et al. Technoeconomic analysis of renewable aviation fuel from microalgae, Pongamia pinnata, and sugarcane. *Biofuels, Bioproducts and Biorefining*, n/a-n/a (2013).

11.   Krings, U. & Berger, R.G. Biotechnological production of flavours and fragrances. *Applied Microbiology and Biotechnology* **49**, 1-8 (1998).

12.   Fortman, J.L. et al. Biofuel alternatives to ethanol: pumping the microbial well. *Trends in Biotechnology* **26**, 375-381 (2008).

13. Lee, S.K., Chou, H., Ham, T.S., Lee, T.S. & Keasling, J.D. Metabolic engineering of microorganisms for biofuels production: from bugs to synthetic biology to fuels. *Current Opinion in Biotechnology* **19**, 556-563 (2008).

14. Chang, M. & Keasling, J. Production of isoprenoid pharmaceuticals by engineered microbes. *Nat Chem Biol* **2**, 674 - 681 (2006).

15. Uribe, S. & Pena, A. Toxicity of allelopathic monoterpene suspensions on yeast dependence on droplet size. *Journal of Chemical Ecology* **16**, 1399-1408 (1990).

16. Uribe, S., Ramirez, J. & Pena, A. Effects of beta-pinene on yeast membrane functions. *Journal of Bacteriology* **161**, 1195-1200 (1985).

17. Andrews, R.E., Parks, L.W. & Spence, K.D. Some effects of douglas-fir terpenes on certain microorganisms. *Appl Environ Microbiol* **40**, 301-304 (1980).

18. Pourbafrani, M., Talebnia, F., Niklasson, C. & Taherzadeh, M. Protective Effect of Encapsulation in Fermentation of Limonene-contained Media and Orange Peel Hydrolyzate. *International Journal of Molecular Sciences* **8**, 777-787 (2007).

19. Shaw, P.E. Review of quantitative-analysis of citrus essential oils *Journal of Agricultural and Food Chemistry* **27**, 246-257 (1979).

20. Wilkins, M., Suryawati, L., Maness, N. & Chrz, D. Ethanol production by *Saccharomyces cerevisiae* and *Kluyveromyces marxianus* in the presence of orange-peel oil. *World Journal of Microbiology and Biotechnology* **23**, 1161-1168 (2007).

21. Grohmann, K., Baldwin, E.A. & Buslig, B.S. Production of ethanol from enzymatically hydrolyzed orange peel by the yeast *Saccharomyces cerevisiae. Appl Biochem Biotechnol*, 45/46, 315-327 (1994).

22. Murdock, D.I. & Allen, W.E. Germicidal effect of orange peel oil and d-limonene in water and orange juice. *Food Technology* **14**, 441-445 (1960).

23. Subba, M.S., Soumithr.Tc & Rao, R.S. Antimicrobial action of cirtrus oils. *Journal of Food Science* **32**, 225-229 (1967).

24. Bar, R. in Laane, C., J. Tramper and M. D. Lilly (Ed.). Studies in Organic Chemistry, 29. Biocatalysis in Organic Media; International Symposium, Wageningen, Netherlands, December 7-10, 1986. Xii+426p. Elsevier Science Publishers B.V.: Amsterdam, Netherlands (Dist. In the USA and Canada by Elsevier Science Publishing Co., Inc.: New York, N.Y., USA). Illus 147-154 (1987).

25. Sikkema, J., de Bont, J. & Poolman, B. Mechanisms of membrane toxicity of hydrocarbons. *Microbiological reviews* **59**, 201-222 (1995).

26. Sikkema, J., Weber, F.J., Heipieper, H.J. & Bont, J.A.M.d. Cellular toxicity of lipophilic compounds: mechanisms, implications, and adaptations. *Biocatalysis 10 (1994) 113-122.* (1994).

27. Inoue, A. & Horikoshi, K. Estimation of solvent-tolerance of bacteria by the solvent parameter log P. *Journal of Fermentation and Bioengineering* **71**, 194-196 (1991).

28. Vermue, M., Sikkema, J., Verheul, A., Bakker, R. & Tramper, J. Toxicity of homologous series of organic solvents for the gram-positive bacteria *Arthrobacter* and *Nocardia* Sp. and the gram-negative bacteria *Acinetobacter* and *Pseudomonas* Sp. *Biotechnol Bioeng* **42**, 747-758 (1993).

29. León, R., Fernandes, P., Pinheiro, H.M. & Cabral, J.M.S. Whole-cell biocatalysis in organic media. *Enzyme and Microbial Technology* **23**, 483-500 (1998).

30. Osborne, S.J., Leaver, J., Turner, M.K. & Dunnill, P. Correlation of biocatalytic activity in an organic aqueous 2-liquid phase seystem with solvent concentration in the cell-membrane. *Enzyme and Microbial Technology* **12**, 281-291 (1990).

31. Schmid, C., Steinbrecher, R. & Ziegler, H. Partition-coefficients of plant cuticles for monoterpenes. *Trees-Structure and Function* **6**, 32-36 (1992).

32. Brennan, T.C.R., Krömer, J.O. & Nielsen, L.K. Physiological and transcriptional responses of *Saccharomyces cerevisiae* to d-limonene show changes to the cell wall but not to the plasma membrane. *Appl Environ Microbiol* **79**, 3590-3600 (2013).

33. Hu, F. et al. Key cytomembrane ABC transporters of *Saccharomyces cerevisiae* fail to improve the tolerance to *d*-limonene. *Biotechnology Letters* **34**, 1505-1509 (2012).

Chapter 2

Alleviating Monoterpene Toxicity Using a Two-Phase Extractive Fermentation for the Bioproduction of Jet Fuel Mixtures in *Saccharomyces cerevisiae*

Chapter 2 has been published in the Journal of Bioengineering and Biotechnology:

TCRB, JK and LKN designed the experiments. TCRB carried out the experiments and analysis. CDT performed the thermodynamic modelling of jet fuel properties. TCRB, JK and LKN wrote the paper.

ARTICLE

Alleviating Monoterpene Toxicity Using a Two-Phase Extractive Fermentation for the Bioproduction of Jet Fuel Mixtures in *Saccharomyces cerevisiae*

Timothy C.R. Brennan, Christopher D. Turner, Jens O. Krömer, Lars K. Nielsen

Australian Institute for Bioengineering and Nanotechnology (AIBN), University of Queensland, Brisbane Qld 4072, Australia; telephone: 61-7-3346-3222; fax: 61-7-3346-3973; e-mail: j.kromer@uq.edu.au

ABSTRACT: Monoterpenes are a diverse class of compounds with applications as flavors and fragrances, pharmaceuticals and more recently, jet fuels. Engineering biosynthetic pathways for monoterpene production in microbial hosts has received increasing attention. However, monoterpenes are highly toxic to many microorganisms including *Saccharomyces cerevisiae*, a widely used industrial biocatalyst. In this work, the minimum inhibitory concentration (MIC) for *S. cerevisiae* was determined for five monoterpenes: β-pinene, limonene, myrcene, γ-terpinene, and terpinolene (1.52, 0.44, 2.12, 0.70, 0.53 mM, respectively). Given the low MIC for all compounds tested, a liquid two-phase solvent extraction system to alleviate toxicity during fermentation was evaluated. Ten solvents were tested for biocompatibility, monoterpene distribution, phase separation, and price. The solvents dioctyl phthalate, dibutyl phthalate, isopropyl myristate, and farnesene showed greater than 100-fold increase in the MIC compared to the monoterpenes in a solvent-free system. In particular, the MIC for limonene in dibutyl phthalate showed a 702-fold (308 mM, $42.1 \, \mathrm{g \, L^{-1}}$ of limonene) improvement while cell viability was maintained above 90%, demonstrating that extractive fermentation is a suitable tool for the reduction of monoterpene toxicity. Finally, we estimated that a limonane to farnesane ratio of 1:9 has physicochemical properties similar to traditional Jet-A aviation fuel. Since farnesene is currently produced in *S. cerevisiae*, its use as a co-product and extractant for microbial terpene-based jet fuel production in a two-phase system offers an attractive bioprocessing option.

Introduction

Isoprenoids are a large and diverse class of natural compounds derived from a common 5 carbon isoprene unit (Keasling, 2010). Fermentative production of isoprenoids using engineered microorganisms is a potential route to deliver petroleum-compatible fuels [e.g., isopentanol (Hull et al., 2006), farnesene (Renninger and McPhee, 2008), bisabolene (Peralta-Yahya et al., 2011)] from simple sugars supplied by renewable feedstocks such as lignocellulosic biomass and sugarcane (Fortman et al., 2008; Renouf et al., 2008). Monoterpenes are a subclass of isoprenoids built from two isoprene (C_5) units (Fig. 1). These C_{10} olefins and their derivatives are major constituents of essential oils and find applications as flavors and fragrances (e.g., menthol and pinene) (van der Werf et al., 1997), antiseptics (e.g., thymol) (Lambert et al., 2001), and anticancer agents (e.g., limonene and perillyl alcohol) (Gould, 1997). Saturated paraffins generated from monoterpenes have properties similar to the light end of traditional kerosene aviation fuel (Jet-A) making them ideal components for "drop in" replacements (Fortman et al., 2008; Harvey et al., 2009; Renninger et al., 2008). For example, Amyris, Inc. plans to use a mixture of 50% limonane (C_{10} cycloparaffin), 10% cymene (C_{10} aromatic), and 40% farnesane (C_{15} branched chain paraffin), termed AMJ-700, in test flights in 2012 (Amyris, 2009; Ryder, 2009).

Synthesis of monoterpenes in whole cell biocatalysts such as *Escherichia coli* (Carter et al., 2003; Dunlop et al., 2011;
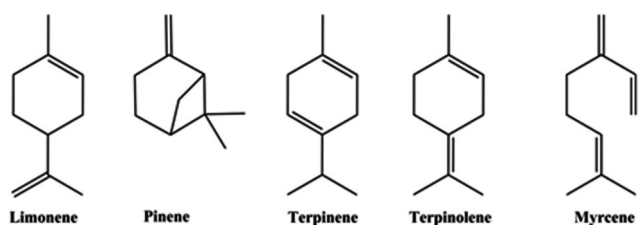
Figure 1. *d*-limonene, β-pinene, γ-terpinene, terpinolene and myrcene were the five monoterpenes analyzed in this work.

Reiling et al., 2004) and *S. cerevisiae* (Carrau et al., 2005; Fischer et al., 2011; Oswald et al., 2007) has been limited (e.g., $30\,\mu g\,L^{-1}$ to $60\,mg\,L^{-1}$ of monoterpene product) by insufficient supply of the monoterpene precursor geranyl pyrophosphate and monoterpene synthase activity (Fischer et al., 2011; Oswald et al., 2007; Reiling et al., 2004). In principle, engineering microbes to produce monoterpenes should be no more difficult than the already completed engineering of *S. cerevisiae* to produce farnesene, a C_{15} sesquiterpene replacement for diesel fuel (Renninger and McPhee, 2008), which is produced from the same precursors in the cell. However, unlike farnesene, monoterpenes are generally highly toxic to microorganisms. Therefore, the realization of microbial monoterpene production will rely extensively on solving this core issue.

Monoterpenes are lipophilic compounds and their toxicity is attributed to the interference with membrane properties (Andrews et al., 1980; Uribe and Pena, 1990; Uribe et al., 1985). For instance, β-pinene inhibits the respiration and essential ion (K^+ and H^+) transport in whole yeast cells, while loss of respiratory control, ATP synthesis inhibition and increased membrane fluidity is observed in isolated yeast mitochondria (Uribe et al., 1985). These observations indicate that β-pinene interferes with mitochondrial membrane integrity and ATP production, while release of cytoplasmic material in the presence of α-pinene (Andrews et al., 1980) indicates that monoterpenes can also cause severe damage to the plasma membrane. Limonene similarly causes severe interference with cell functions. Cell viability and ethanol production by *S. cerevisiae* using enzymatically digested citrus peel waste was significantly reduced in the presence of 0.02–0.10% $v\,v^{-1}$ orange peel oil, which contains 95–97% limonene (Pourbafrani et al., 2007; Wilkins et al., 2007). Although growth inhibition by orange peel oil, limonene, and other non-substituted monoterpenes in yeast and bacteria is well-established (Grohmann et al., 1994; Murdock and Allen, 1960; Subba et al., 1967; Uribe and Pena, 1990; Uribe et al., 1985; Wilkins et al., 2007), quantitative data on monoterpene toxicity are limited and the exact mechanism remains poorly understood.

A physical approach used to overcome toxicity limitations is to remove inhibitory products in situ during fermentation using an extractive solvent. Numerous in situ product recovery (ISPR) techniques (e.g., pervaporation, perstraction, gas stripping) have been reported for the recovery of aromas, alcohols, and organic acids and an extensive review of ISPR projects and process designs have been covered by Stark and von Stockar (2003). Liquid–liquid extraction has shown the greatest potential because it is simple and scalable (Janusz, 2001) and provides the cells with an efficient product sink (Malinowski, 2001). Two-phase extractive fermentation has been reported to enhance the production and recovery of short-chain alcohols [e.g., ethanol (Daugulis et al., 1987), butanol (Roffler et al., 1988)], acetone (Roffler et al., 1988), organic acids (Bar and Gainer, 1987), and volatile sesquiterpene products such as amorpha-4,11-diene (Newman et al., 2006). However, this technique has not been applied to overcome monoterpene inhibition. Solvent selection is the first crucial step in the development of an effective two-phase bioprocess because solvents are generally both product and host specific (Bruce and Daugulis, 1991; León et al., 1998). The solvent needs to meet the following key criteria: Biocompatibility with the producing organism, high product distribution coefficients, favorable phase separation (e.g., low emulsion formation), and low cost (Bruce and Daugulis, 1991).

A proof-of-concept two-phase extractive system for monoterpene production with *S. cerevisiae* was defined in this work. First, we quantitatively determined the inhibitory concentrations for five common monoterpene products in a solvent-free system. In an attempt to evolve a monoterpene tolerant phenotype, we subjected the wild type strain to several hundred generations of limonene challenged chemostat cultivation without significant improvement. We then screened ten organic solvents for biocompatibility, monoterpene distribution, phase separation, and price to select suitable solvent candidates to be used for extractive fermentation. We demonstrated that using this biphasic approach, *S. cerevisiae* was able to withstand significantly higher monoterpene concentrations compared to the solvent-free system and the chemostat challenged strain. Finally, we explored the use of the yeast product farnesene as an extractant and a co-product for jet fuel production by estimating fuel properties of a farnesane-limonane blend.

Materials and Methods

Strains, Media, and Chemicals

The *S. cerevisiae* strain S288C (MATα SUC2 gal2 mal mel flo1 flo8-1 hap1) was kindly provided by the Australian Wine Research Institute (AWRI, Adelaide, SA, Australia). Rich medium (YPD) was used to store cultures at $-80°C$ in 40% glycerol. The YPD medium contained $10\,g\,L^{-1}$ yeast extract, $10\,g\,L^{-1}$ polypeptone, and $20\,g\,L^{-1}$ dextrose (glucose). Cells were reactivated from frozen glycerol stocks by streaking out on chemically defined medium (CDM) agar plates ($15\,g\,L^{-1}$ agar) and incubated at $30°C$. CDM

contained the following components per liter of solution: 5 g sucrose, 1 g $(NH_4)_2HPO_4$, 2 g $(NH_4)_2SO_4$, 0.99 g KCl, 0.15 g $CaCl_2·2H_2O$, 7.8 g NaH_2PO_4, 7.1 g Na_2HPO_4, 0.5 g $MgSO_4·7H_2O$, trace metals: 4.5 mg $ZnSO_4·7H_2O$, 15 mg EDTA, 0.84 mg $MnCl_2·2H_2O$, 0.3 mg $CoCl_2·6H_2O$, 0.3 mg $CuSO_4·5H_2O$, 0.4 mg $Na_2MoO_4·2H_2O$, 4.5 mg $CaCl_2·2H_2O$, 3 mg $FeSO_4·7H_2O$, 1 mg H_3BO_3, 0.1 mg KI, vitamins: 0.05 d-biotin, 1 mg Ca pantothenate, 1 mg nicotinic acid, 1 mg myoinositol, 25 mg thiamine hydrochloride, 1 mg pyridoxal hydrochloride, 0.2 mg p-amino benzoic acid. All experiments were carried out aerobically in CDM. Chemicals where obtained from Sigma Aldrich (Castle Hill, NSW, Australia) and were analytical grade ($\geq$99%) except for the following purities: d-limonene (93%), terpenolene ($\geq$85%), oleyl alcohol (85%), farnesene (mixture of isomers), isopropyl myristate (90%).

Growth Conditions

Single colonies from CDM solid media were used as inocula for the pre-cultures. Pre-cultures in 10 mL of CDM were incubated in 100 mL baffled shake flasks in a shaking incubator (Multitron, Infors, Bottmingen, Switzerland) at 200 rpm (Orbit 25 mm) and 30°C. Pre-cultures were grown overnight until mid-log phase and then appropriate aliquots of the pre-culture broth were used to inoculate 25 mL of fresh CDM medium to a target OD_{660} of 0.2, respectively. Cultures were grown at 30°C aerobically in 250 mL baffled screw top shake flasks sealed with Teflon™ lining to avoid any monoterpene evaporation. Monoterpene evaporation in sealed versus non-sealed shake flasks was determined hourly for 12 h and significant monoterpene losses occurred in non-sealed flasks. For sealed and non-sealed flasks we observed similar growth rates ($0.35 \pm 0.01\,h^{-1}$, respectively) and biomass yields after 12 h of growth ($0.22 \pm 0.02\,g_{DCW}\,g_{sucrose}^{-1}$, respectively), showing that sufficient oxygen was available in the headspace of sealed flasks to ensure aerobic conditions. At 5 h after inoculation ($\sim OD_{660} = 1.0$) varying amounts of monoterpene were added aseptically into the culture medium using a 10 µL glass-syringe. Cell growth was determined by measuring the optical density at 660 nm against water in a spectrophotometer (Libra S4, Cambridge, England) and all growth experiments were performed in triplicate. Specific growth rates were determined from OD_{660} values during the exponential growth phase after the addition of monoterpene. For aqueous-organic two-phase growth conditions an equal volume (10.2 mL) of organic solvent-limonene mixture was added to exponentially growing cultures at 5 h and growth was monitored as described. The following amounts of limonene in the solvent mixture were tested: 1, 2.5, and 5% ($v_{limonene}\,v_{solvent-limonenemix}^{-1}$). Evaporation of limonene from the solvents butyl oleate, dioctyl phthalate, dibutyl phthalate, isopropyl myristate, and farnesene was tested by measuring limonene concentration before and after two-phase cultivation by GC/MS as described below.

Organic Solvent Biocompatibility

Ten organic solvents were tested for biocompatibility with *S. cerevisiae*. A 10% ($v_{solvent}\,v_{culture}^{-1}$) volume of solvent was added to exponentially growing cultures at 5 h and growth was monitored as described previously. The growth rate of cultures with solvent was compared to a control with no solvent and the ratio was reported as $\mu\,\mu_{max}^{-1}$.

GC/MS analysis

Monoterpenes in the organic and aqueous phases were quantified in GC/MS. For this the organic and aqueous phases were separated using centrifugation. The aqueous phase underwent a liquid–liquid extraction using hexane. Equal volumes of hexane and aqueous phase (0.5 mL) were mixed, vortexed for 5 min and allowed to phase-separate at 25°C. Aliquots of the hexane extract of the aqueous phase and of the organic phase were diluted in hexane prior to quantification in order for the signals to fall within the calibration curve. A linear standard curve was achieved for standard solutions of known monoterpene stocks in hexane (100, 250, 500, 750, 1,000 µM). Menthol was used as an internal standard and was added to the hexane samples and the standards with a 10 µL glass-syringe (Gerstel, Mulheim, Germany) to achieve a final concentration of 500 µM prior to injection. For quantification, 3 µL sample was injected into the GC program temperature vaporizer (PTV) inlet in splitless mode at 250°C using helium as a carrier gas with a constant flow rate of $1\,mL\,min^{-1}$. Compounds were separated using a Varian factorFOUR capillary column (VF-5 ms: 0.25 mm inner diameter, 0.25 µm film, 30 m length with a 10 m fused guard column) on an Agilent 7890A gas chromatograph attached to an Agilent 5975C MSD. Initially the oven temperature was set to 40°C and was held for 5 min followed by a temperature ramp of $7.5°C\,min^{-1}$ to 100°C, then $35°C\,min^{-1}$ to 350°C and held for 5 min. Detection was achieved in scan mode at 9.26 scans sec^{-1} from 30 to 300 amu.

Monoterpene Partitioning Coefficients

The partitioning coefficient K_d, is defined as the ratio of monoterpene concentration in the organic phase to aqueous phase. In order to determine K_d, equal volumes (0.5 mL) of aqueous CDM media and each organic solvent were vortexed vigorously overnight at 30°C. Known amounts of monoterpene were added directly into the organic solvent prior to mixing and each monoterpene K_d was determined in triplicate for each solvent. Samples were allowed to phase separate for 5 min after mixing at 30°C. Due to emulsion formation, samples with corn oil, oleyl alcohol, and dodecanol were centrifuged at 5,900 rcf for 5 min at 25°C (Eppendorf centrifuge 5415R, rotor: FA-45-24-11) to separate the two phases. After phase separation, monoterpene quantification in the aqueous and organic phases was determined by GC/MS as described above.

Viability Assessment

Propidium iodide (PI) was used to measure cell viability and membrane integrity. During limonene treated growth experiments, aliquots from the culture broth were analyzed at 2, 4, and 6 h after the addition of limonene or limonene-solvent mixtures. The final PI concentration in the sample was 2.5 $\mu g\, mL^{-1}$ and samples were shaken as set by Quanta Cell Lab software well-prep mode in 96-well plates for 0.5 h at 25°C before analysis. As positive controls non-limonene treated cells were incubated in 70% ethanol at 30°C for 0.5 h, washed and resuspended in PBS. This caused 99.5% of the cells to be stained with PI. Cell suspensions were analyzed using a Beckman Coulter Cell Lab SC MPL flow-cytometer with an argon-ion laser emitting 488 nm beam at 22 mW. The intensity of fluorescence at FL3 (red fluorescence, 620 nm) was recorded using a logarithmic scale and the sample flow rate was 30 $\mu L\, min^{-1}$.

Jet fuel Physicochemical Property Estimation

Physicochemical properties of limonane and limonane-farnesane fuel blends were estimated using suitable modeling software and compared to previously reported (Renninger et al., 2008) fuel specifications. Modeling in AspenPlus® (AspenTech, 2000) was used for transport and vapor liquid equilibrium properties (e.g., density, flash point, enthalpy of combustion, and viscosity) while the Dortmund Data Bank software (Onken et al., 1989) was used for freezing point calculations. The UNIFAC group contribution method (Fredenslund et al., 1977) was used for thermodynamic properties.

Chemostat Adaptation

A sucrose limited continuous fermentation was carried out in a 1.4 L Multifors benchtop bioreactor (InfrosHT, Bottmingen, Switzerland) attached to a HPR-20 QIC gas analysis system (Hiden, Warrington, England). Synthetic media (CBS) containing 2 $g\, L^{-1}$ sucrose, 5 $g\, L^{-1}$ $(NH_4)_2\, SO_4$, 3 $g\, L^{-1}$ KH_2PO_4, 0.5 $g\, L^{-1}$ $MgSO_4 \cdot 7H_2O$, and identical concentrations of vitamins and trace metals of CDM, were used for chemostat experiments. An aerobic culture of 350 mL was run at 30°C, 500 rpm and was sparged with air at 0.35 $L\, h^{-1}$. The pH was maintained at 5 by automatic addition of 2 M NaOH. A dilution rate of 0.2 h^{-1} was used with an inlet feed of 72 $mL\, h^{-1}$. Limonene was continuously fed at 125 $\mu L\, h^{-1}$ directly into the culture using an electronic syringe pump (New Era Pump System Inc., Farmingdale, NY) controlled by the Syringe Pump Pro software program (Version 1.54, Gawler, South Australia). The limonene concentration in the chemostat was determined directly. 1 ml of culture was removed and harvested by centrifugation at 5,900 rcf for 1 min at 25°C. The supernatant was separated from the cell pellet and immediately overlaid with 200 μL of hexane and then

vortexed for 30 s. The limonene concentration in the hexane layer was analyzed by GC/MS. The steady state limonene concentration was measured to be 0.53 ± 0.04 mM ($n = 3$). Culture purity was routinely monitored by light microscopy. Culture from the reactor was used to inoculate shake flask cultures as described in the growth conditions section to determine the MIC for limonene.

Results

Growth Inhibition by Monoterpenes

The toxicity of pure monoterpenes was determined by adding different amounts of the monoterpene to yeast measuring the growth rate over the ensuing 5 hr (Fig. 2). The monoterpene was added to yeast cells already in mid-exponential growth, in order to avoid confounding by lag phase phenomena. The minimum inhibitory concentration (MIC) was defined as the amount of monoterpene required to reduce the specific growth rate by 50% compared to control cultures with no monoterpene present. As shown in Figure 3, very low concentrations (MIC 0.4–2 mM, 0.0075–0.033% v v^{-1}) for all five monoterpenes caused growth inhibition. Limonene was the most toxic (MIC = 0.44 mM) while the acyclic terpene myrcene was the least toxic (MIC = 2.12 mM). Even when growth is completely inhibited by limonene (0.6 mM), viability remains high 6 h after addition; it requires another magnitude increase in concentration to see substantial loss of viability, e.g., 73% reduction in viability at 6 mM (Fig. 2B). In contrast, if limonene is added to cultures immediately after inoculation, significant reduction in viability is seen even at MIC (data not shown).

Though low, the MIC of limonene is approximately an order of magnitude higher than its aqueous saturation point 0.045 mM (Schmid et al., 1992) ($S_{Limonene}$ in Fig. 2 B). Cultures with limonene present in amounts beyond its solubility point (e.g., in Fig. 2 B, the 2nd and 3rd data points are 0.14 mM and 0.34 mM, respectively) were able to grow within 97% of the maximum growth rate with no limonene present. In fact, all five monoterpenes had MICs well above their solubility points (Table I).

An unsuccessful attempt was made to alleviate monoterpene toxicity via cell adaptation. After 885 h (225 generations) of continuous cultivation in the presence of 0.54 mM limonene, no significant improvement in the MIC (0.45 mM) was observed. Shown in Figure 2 B, identical limonene concentrations for the mutant and wild type had very similar impact on growth.

Solvent Selection for a Two-Phase Bioprocess to Reduce Monoterpene Toxicity In situ

In order to alleviate the observed monoterpene toxicity, 10 organic solvents were chosen from the literature based on
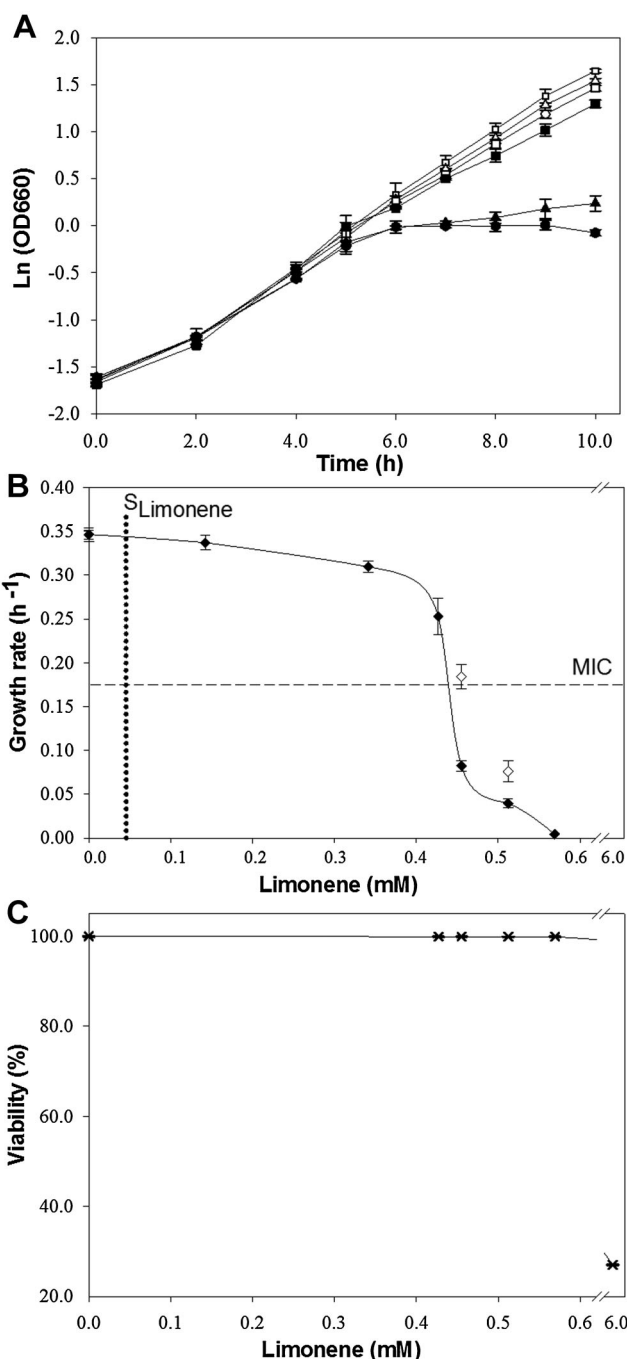
Figure 2. Growth and viability of limonene dosed cultures. **A**: Cultures were grown exponentially and then various amounts of limonene (□ control, △ 0.14 mM, ○ 0.34 mM, ■ 0.43 mM, ▲ 0.46 mM, ● 0.51 mM) were added exogenously at $t = 5$ h. **B**: Growth rate versus increasing limonene concentration (◆ wild-type, ◇ mutant); the aqueous solubility of limonene ($S_{Limonene}$) is 0.045 mM (Schmid et al., 1992). A 50% reduction in growth rate compared to the control without monoterpene is approximately 0.175 h^{-1}, this concentration is defined as the MIC. The mutant represents the limonene challenged chemostat strain after 885 h of continuous cultivation. **C**: Cell viability ✖ was determined for the wild type after 6 h of limonene exposure. Error bars for growth rate and viability represent one standard deviation of biological triplicates (viability deviations were less than 0.02 and therefore are not visible).
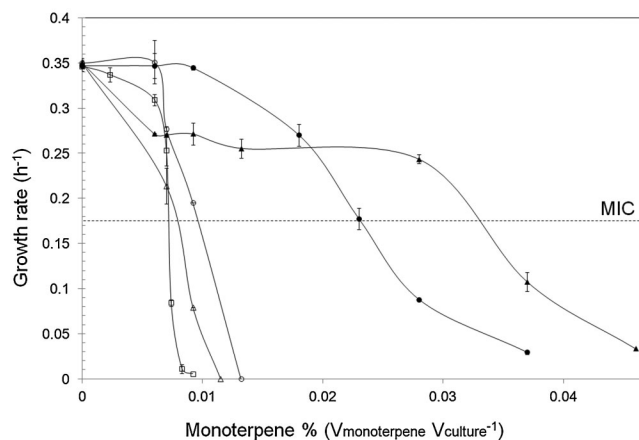
Figure 3. Growth rates of monoterpene dosed cultures (□-Limonene, △-Terpinolene, ○-γ-Terpinene, ●-β-pinene, ▲-Myrcene) versus increasing monoterpene concentration. Growth was monitored as described for limonene in the Figure 2. Error bars represent one standard deviation for biological triplicates.

their $\log P_{ow}$ coefficients, which is defined as the logarithm of the ratio of a compound's equilibrium concentration in the octanol phase to the aqueous phase (Laane et al., 1987; Vermue and Tramper, 1995). Although it is highly dependent on the microorganism, it is generally supported that an organic compound with log $P_{ow} > 5$ should be biocompatible with *S. cerevisiae* (Bruce and Daugulis, 1991). Using a 10% (v v^{-1}) solvent phase, as described previously for similar experiments (Schewe et al., 2009), we confirmed that all 10 solvents met the criterion for biocompatibility with *S. cerevisiae* (μ μ_{max}^{-1} values 0.65–1.0, see Table II). All five monoterpenes partitioned preferentially into the organic phase over the aqueous media (log K_d 1.8–2.7, see Table III). However, corn oil, oleyl alcohol, and dodecanol, caused emulsions that required separation by centrifugation (Table II). These solvents were excluded from the remaining experiments, since interference with biomass quantification could not be ruled out. Considering these characteristics, along with the solvent price, butyl oleate, dioctyl phthalate,

Table I. Monoterpene minimum inhibitory concentrations.

Monoterpene	MIC[a] (mM)	Aqueous solubility[b] (mM, 25°C)	Log P$_{o-w}$[b]
Limonene	0.44	0.045	4.4
Terpinolene	0.53	0.068	4.47
γ-Terpinene	0.70	0.064	4.5
β-Pinene	1.45	0.052	4.42
Myrcene	2.12	0.043	4.5

[a]The MIC is defined as the amount of terpene required to cause a 50% reduction in growth rate compared to the control with no monoterpene present. Although the aqueous solubility is exceeded, concentration units (mM) are used for explanatory reasons.
[b]Aqueous solubilities and log P$_{ow}$ are taken from literature (Schmid et al., 1992).

Table II. Solvent selection criteria.

Solvent	$\mu \, \mu_{max}^{-1} \pm$ SD	Log P_{ow}	Log $K_{d \; limonene} \pm$ SD	Phase separation	Price USD L^{-1}
Corn oil	1.0 ± 0.09	7.4	2.15 ± 0.23	−	7.4
Dodecane	0.65 ± 0.09	6.6	2.20 ± 0.22	+	50.2
Hexadecane	0.90 ± 0.08	8.8	2.57 ± 0.06	+	67.1
Oleyl alcohol	0.90 ± 0.01	5.6	2.50 ± 0.16	−	17.2
Butyl oleate	0.95 ± 0.05	9.8[a]	2.29 ± 0.15	+	6.1
Dibutyl phthalate	0.71 ± 0.12	4.63[b]	1.60 ± 0.01	+	12.0
Dodecanol	0.65 ± 0.09	5.32	2.47 ± 0.15	−	8.5
Dioctyl phthalate	0.73 ± 0.06	7.54[a]	2.53 ± 0.11	+	7.1
Farnesene	0.81 ± 0.08	7.1[c]	ND	+	—
Isopropyl myristate	0.95 ± 0.04	7.4	ND	+	12.8

$\mu \, \mu_{max}^{-1}$ was determined for biocompatibility by comparing the growth rate in the presence of 10% (v/v) solvent addition to cultures with no solvent (μ_{max}); log P_{ow} is the standard partitioning coefficient in an octanol-water system and values are from the previous report (Bruce and Daugulis, 1991); (−) indicates poor phase separation and centrifugation was required, (+) no centrifugation needed; bulk solvent price values were taken from (Spectrum, 2011). Standard deviations ($\pm$SD) are given (n = 3).
[a]Mattiasson and Holst (1991).
[b]Stales et al. (1997).
[c]Kishimoto et al. (2005).

dibutyl phthalate, isopropyl myristate, and farnesene were selected for further analysis.

The five selected solvents were then investigated in a limonene-solvent two-phase system. Limonene was the most inhibitory monoterpene (Fig. 3) and thus was chosen to screen the selected solvents for their ability to reduce toxicity. Based on the relative MICs for all five mono-terpenes, we assumed that solvent candidates that were successful with limonene could be applied as extractants for the other four monoterpene products. The maximum amount of limonene that could be loaded into the solvent mixture before growth was severely inhibited was determined. In Figure 4, at 5% (v v^{-1}) limonene in dibutyl phthalate, growth was reduced by 50% (MIC 308.7 mM) with the amount of limonene present (42.1 g L^{-1} aqueous culture) being 702-fold higher than the MIC for limonene in solvent-free cultures (Table IV). Butyl oleate was the least effective solvent with the growth rate being reduced by 80% in a 1% limonene load (Fig. 4). However, solvents dioctyl phthalate, isopropyl myristate, and farnesene also significantly reduced limonene toxicity with MICs over two-orders

of magnitude higher than the MIC for limonene with no solvent present (Table IV). Cell viability at these critical concentrations for each limonene-solvent system was measured using the PI staining method described above. Viability at each of the reported MICs was over 90% (Table IV).

Modeling Mono and Sesquiterpene Jet Fuel Blends

The fermentation products, limonene and farnesene, require an additional processing step to be used as jet fuels. For example, chemical hydrogenation is used to saturate C–C double bonds that exist in terpene compounds to produce alkane fuel targets such as limonane and farnesane (Ryder, 2009). In order demonstrate that our thermodynamic model accurately predicted fuel properties, we used our model to predict the previously published properties of a 97.1% limonane fuel composition (AMJ-300 in Table V) that was tested using industry standard (ASTM) methods (Renninger et al., 2008). Our predicted properties of AMJ-300 (UNIFAC

Table III. Monoterpene-solvent log K_d values.

Solvent	γ-Terpinene	Terpinolene	Myrcene	β-Pinene	d-Limonene
Corn oil	2.63 ± 0.13	ND	2.18 ± 0.24	1.21 ± 0.18	2.15 ± 0.23
Dodecane	2.64 ± 0.12	ND	2.16 ± 0.20	2.12 ± 0.09	2.20 ± 0.22
Hexadecane	2.73 ± 0.10	ND	2.45 ± 0.03	1.89 ± 0.08	2.57 ± 0.06
Oleyl alcohol	2.71 ± 0.05	ND	1.92 ± 0.30	2.08 ± 0.12	2.50 ± 0.16
Butyl oleate	2.5 ± 0.24	ND	1.84 ± 0.54	2.01 ± 0.18	2.29 ± 0.15
Dibutyl phthalate	2.46 ± 0.18	2.18 ± 0.46	2.06 ± 0.39	1.55 ± 0.14	1.60 ± 0.01
Dodecanol	2.72 ± 0.01	2.14 ± 0.40	2.30 ± 0.14	2.16 ± 0.06	2.47 ± 0.15
Dioctyl phthalate	2.64 ± 0.03	ND	2.33 ± 0.17	1.96 ± 0.26	2.53 ± 0.11
Farnesene	ND	2.85 ± 0.21	2.60 ± 0.26	ND	ND
Isopropyl myristate	ND	ND	ND	ND	ND

K_d is the ratio of monoterpene in the organic solvent phase to the aqueous media phase. Standard deviations are given (n = 3). ND, no monoterpene was detected in the aqueous phase.
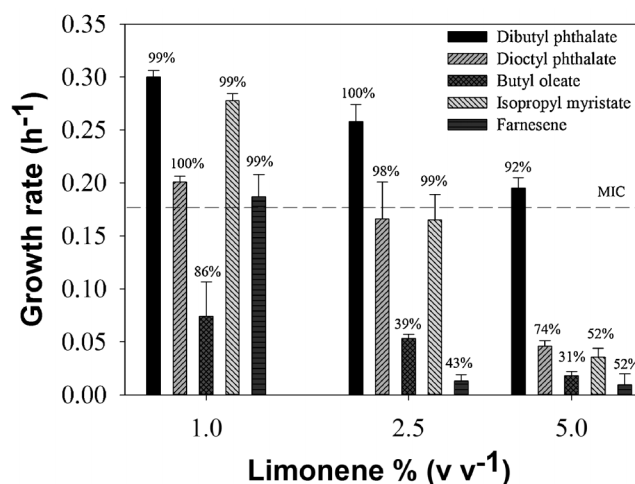
Figure 4. Growth rate versus limonene loading in butyl oleate, dioctyl phthalate, dibutyl phthalate, isopropyl myristate and farnesene. Limonene was loaded at 1, 2.5, 5% ($v_{limonene} v^{-1}_{limonene-solventmix}$) in a limonene-solvent mixture. The % of viable cells is given above each growth rate value. Growth was monitored as described in the Figure 2. Error bars are one standard deviation above the mean for biological triplicates.

AMJ-300 in Table V) were comparable with those previously reported (<10% error). Due to limonene's toxicity, we then used this model to find the minimum limonane load in farnesane that met Jet-A properties. The physicochemical properties of a 10% ($v v^{-1}$) blend of limonane in farnesene are very similar to Jet-A specifications.

Discussion

Monoterpenes are known fungicidal agents, but the exact mechanisms of action are not well understood. For solvent-caused toxicity in microbes, two types of toxicity have been distinguished: Molecular and phase (Bar, 1987). Molecular toxicity has been described as compounds that are soluble in the aqueous phase and due to their hydrophobicity, intercalate within the lipid bilayer and deteriorate membrane function (Sikkema et al., 1995). Increases in membrane fluidity, membrane damage, denaturation of membrane-bound proteins, and loss of energy transduction are some of the consequences of a solvent's impact at the

molecular level (Inoue and Horikoshi, 1991; León et al., 1998; Sikkema et al., 1994b; Vermue et al., 1993). Alternatively, phase toxicity occurs when the amount of solvent present in the culture medium exceeds the compounds solubility point and a distinct second phase exists. The presence of a second phase means that thermodynamically, the aqueous phase is fully saturated as well as the different compartments of the biomass (e.g., cytoplasmic membrane) (León et al., 1998; Osborne et al., 1990; Sikkema et al., 1994b). Phase toxicity could be caused by extraction of outer-cellular components during cell-solvent contact, extraction of nutrients from the media, or cell-coating (Bar, 1987). We observe severe toxicity for all five monoterpenes only well beyond their aqueous solubilities (Table I) and in addition, the most toxic monoterpene found in this work (limonene) caused no growth inhibition when the aqueous media was saturated with limonene (Fig. 2B). It was previously suggested that monoterpene toxicity in microbes occurs at the molecular level causing structural damage to the plasma membrane and interfering with its normal function (Sikkema et al., 1994a; Uribe et al., 1985). In contrast, we observed no loss of viability at the MIC of limonene (Fig. 2B). Only at very high limonene loadings (6.2 mM) was membrane damage observed, resulting in 73% of the total population being no longer viable (Fig. 2B). We did observe significant loss of viability at the MIC of limonene, when added to the culture immediately after inoculation, and this may explain why previous studies (Andrews et al., 1980) have observed molecular toxicity. We conclude that toxicity observed when limonene is added (or slowly accumulating) during *S. cerevisiae* culture must be due to phase effects.

The observation of phase toxicity has implications for strain optimization. We have shown that although growth stops, the cells are still viable. Controlling strains to begin monoterpene production after the initial growth phase is a potential route to address toxicity constraints. For example, the highest production of lactic acid (100 to 154 g L^{-1}), which is also considered a toxic end product, in *Lactobacillus* occurs during the stationary phase of cell growth (Wee et al., 2005). Another important implication of phase toxicity is with respect to engineering tolerance in the biocatalyst. For instance, engineering efflux systems to export compounds from the membrane, as described recently for limonene and the other biofuel targets n-butanol and α-pinene in *E. coli* (Dunlop et al., 2011), should not alleviate monoterpene toxicity in *S. cerevisae* because, as demonstrated here, the

Table IV. Solvent-limonene mixture MICs and cell viability.

Solvent	Limonene MIC (mM)	Limonene (g L^{-1})	Fold increase vs. solvent free system	Cell viability (%)
No solvent	0.44	0.06	—	99
Dibutyl phthalate	308.7	42.1	702	92
Dioctyl phthalate	154.3	21.0	351	98
Isopropyl myristate	154.3	21.0	351	99
Farnesene	61	8.4	140	99

Table V. Predicted jet fuel thermodynamic and physicochemical properties.

Property	Units	Jet A (ASTM)	AMJ-300 (ASTM)	AMJ-300 (UNIFAC)	UQJ-1 (UNIFAC)
Flash point[a]	°C	Min. 38	43	44.37	56.45
Density (at 15°C/288.15 K)	$Kg\,m^{-3}$	775–840	800.9	768.27	778.75
Freezing point[b]	°C	Max −40	< −70	−97.65	−40.36
Viscosity (at −20°C/253.15 K)	$mm^2\,s^{-1}$	Max 8.0	2.849	3.818	7.714
dH° combustion (NET)	$MJ\,kg^{-1}$	Min 42.8	43.4125	43.3341	43.9351

AMJ-300 values are from the previous report (Renninger et al., 2008) and contain limonane 97.1 wt% and p-cymene 1.6 wt%; UQJ-1 contains 10% $v\,v^{-1}$ limonane and 90% $v\,v^{-1}$ farnesane.

[a]Riazi (1986).

[b]Constantinou and Gani (1994).

monoterpene aqueous concentration and consequently, the membrane concentration, is saturated well before we observe any growth inhibition (Table I). Furthermore, we showed that simply evolving the cells over time, which is one of the most straightforward methods for generating improved phenotypes (Kwon et al., 2011), showed negligible improvement in limonene tolerance, MIC increased from 0.44 to 0.45 (see mutant in Fig. 2B).

In contrast to the limited success of cellular engineering, manipulating phase properties by introducing an inert solvent phase shows substantial potential (e.g., MIC for limonene with the solvent dibutyl phthalate is 702-fold higher than the MIC with no solvent). The monoterpene partitioning coefficients (K_d) (Bruce and Daugulis, 1991) for the 10 biocompatible solvents studied are several orders of magnitude higher (log K_d = 2–2.85, see Table III) than those (log K_d = 0.78) reported for an economically feasible extractive ethanol fermentation plant (Maiorella et al., 1984), indicating the commercial potential of such a process. Furthermore, high limonene loads can be achieved in the solvent phase without compromising cell viability. This means that the solvent can act as an effective product sink in situ without negatively impacting the producing organism. As shown in Table IV, cultures with 42.1 g L^{-1} of limonene in dibutyl phthalate can maintain 92% cell viability. Dibutyl phthalate showed the highest limonene load and this may be explained by its similar hydrophobicity to limonene (log P_{ow} is 4.63 in Table II and 4.5 for limonene in Table I) compared to the other solvents tested. To our knowledge this is the highest monoterpene concentration reported during fermentation with baker's yeast.

The use of a solvent that does not require separation from the monoterpene products would simplify this technique. Although Figure 4 suggests that farnesene is not the best solvent option to reduce limonene toxicity, farnesene is of particular interest as an extractive solvent since it can be synthesized by yeast during fermentation (Renninger and McPhee, 2008) and, as shown above, a blend of 10% ($v\,v^{-1}$) limonane in farnesane exhibits physicochemical properties similar to Jet-A (Table V). Using farnesene as an extractant and a co-product will ultimately require careful process engineering that balances both monoterpene toxicity and desired fuel properties. An organism with an ability to produce both the extractant and monoterpene product in situ will positively impact raw-material and downstream processing costs. This is likely to outweigh toxicity advantages of the other solvents tested. By holding the 10% ($v\,v^{-1}$) terpene fuel blend constant, we found that by reducing the ratio of organic to culture volume from 0.05, where we observed no growth and 88% loss in cell viability, to 0.005, both fast cell growth (80% of μ_{max}) and high viability (99%) can be achieved (data not shown). The amount of limonene in the latter system (2.8 mM, 380 mg L^{-1}), is 6.3-fold higher than the MIC without any solvent present.

Conclusion

End product inhibition is a critical problem for the microbial synthesis of monoterpene-dervied fuels and chemicals. We have provided quantitative data for the inhibitory limits of five common monoterpene products and shown that in S. cerevisiae, the mechanism of toxicity is likely to be a phase effect. As an alternative to cellular engineering, we have demonstrated that a biphasic extractive system can significantly enhance fermentation by alleviating monoterpene toxicity in situ. To make this process even more efficient, we have shown that by using farnesene as the extractant, one could obtain a terpene mix that could be directly used for hydrogenation into jet fuel. Depending on the other components of the organic phase this could at the same time reduce the downstream processing cost (e.g., distillation).

References

Amyris. 2009. (Press release) Embraer, General Electric, Azul, and Amyris announce renewable jet fuel evaluation project. (http://www.amyris.com/en/newsroom/83-renewable-jet-fuel-evaluation).

Andrews RE, Parks LW, Spence KD. 1980. Some effects of douglas-fir terpenes on certain microorganisms. Appl Environ Microbiol 40(2): 301–304.

AspenTech. 2000. ASPEN plus user's manual. Cambridge, USA: Aspen Technology Inc.

Bar R. 1987. Phase toxicity in a water-solvent two-liquid phase microbial system. In: Laane C, Tramper J, Lilly MD, editors. Studies in organic chemistry: 29. *Biocatalysis in Organic Media*; International Symposium Wageningen, Netherlands December 7–10, 1986. Amsterdam: Elsevier. p 147–154.

Bar R, Gainer JL. 1987. Acid Fermentation in water-organic solvent two-liquid phase systems. Biotechnol Prog 3(2):109–114.

Bruce LJ, Daugulis AJ. 1991. Solvent selection strategies for extractive biocatalysis. Biotechnol Prog 7(2):116–124.

Carrau FM, Medina K, Boido E, Farina L, Gaggero C, Dellacassa E, Versini G, Henschke PA. 2005. *De novo* synthesis of monoterpenes by *Saccharomyces cerevisiae* wine yeasts. FEMS Microbiol Lett 243(1):107–115.

Carter OA, Peters RJ, Croteau R. 2003. Monoterpene biosynthesis pathway construction in *Escherichia coli*. Phytochemistry 64(2):425–433.

Constantinou L, Gani R. 1994. New group contribution method for estimating properties of pure compounds. AIChE J 40(10):1697–1710.

Daugulis AJ, Swaine DE, Kollerup F, Groom CA. 1987. Extractive fermentation-integrated reaction and product recovery. Biotechnol Lett 9(6):425–430.

Dunlop MJ, Dossani ZY, Szmidt HL, Chu HC, Lee TS, Keasling JD, Hadi MZ, Mukhopadhyay A. 2011. Engineering microbial biofuel tolerance and export using efflux pumps. Mol Syst Biol 7:487.

Fischer MJC, Meyer S, Claudel P, Bergdoll M, Karst F. 2011. Metabolic engineering of monoterpene synthesis in yeast. Biotechnol and Bioeng 108(8):1883–1892.

Fortman JL, Chhabra S, Mukhopadhyay A, Chou H, Lee TS, Steen E, Keasling JD. 2008. Biofuel alternatives to ethanol: Pumping the microbial well. Trends Biotechnol 26(7):375–381.

Fredenslund A, Gmehling J, Rasmussen P. 1977. Vapor-liquid equilibria using UNIFAC. Amsterdam: Elsevier.

Gould MN. 1997. Cancer chemoprevention and therapy by monoterpenes. Environ Health Perspect 105:977–979.

Grohmann K, Baldwin EA, Buslig BS. 1994. Production of ethanol from enzymatically hydrolyzed orange peel by the yeast *Saccharomyces cerevisiae*. Appl Biochem Biotechnol 45/46:315–327.

Harvey BG, Wright ME, Quintana RL. 2009. High-density renewable fuels based on the selective dimerization of pinenes. Energy Fuels 24(1):267–273.

Hull A, Golubkov I, Kronberg B, Marandzheva T, Stam J. 2006. An alternative fuel for spark ignition engines. Int J Engine Res 7(3): 203–214.

Inoue A, Horikoshi K. 1991. Estimation of solvent-tolerance of bacteria by the solvent parameter log P. J Ferment Bioeng 71(3):194–196.

Janusz JM. 2001. Two-phase partitioning bioreactors in fermentation technology. Biotechnol Adv 19(7):525–538.

Keasling JD. 2010. Microbial production of isoprenoids. In: Timmis KN, editor. Handbook of hydrocarbon and lipid microbiology. Berlin: Springer. p. 2951–2966.

Kishimoto T, Wanikawa A, Kagami N, Kawatsura K. 2005. Analysis of hop-derived terpenoids in beer and evaluation of their behavior using the stir bar−sorptive Extraction Method with GC-MS. J Agric Food Chem 53(12):4701–4707.

Kwon Y-D, Kim S, Lee SY, Kim P. 2011. Long-term continuous adaptation of *Escherichia coli* to high succinate stress and transcriptome analysis of the tolerant strain. J Biosci Bioeng 111(1):26–30.

Laane C, Boeren S, Vos K, Veeger C. 1987. Rules for optimization of biocatalysis in organic solvents. Biotechnol Bioeng 30(1):81–87.

Lambert RJW, Skandamis PN, Coote PJ, Nychas GJE. 2001. A study of the minimum inhibitory concentration and mode of action of oregano essential oil, thymol and carvacrol. J Appl Microbiol 91(3): 453–462.

León R, Fernandes P, Pinheiro HM, Cabral JMS. 1998. Whole-cell biocatalysis in organic media. Enzyme Microb Technol 23(7–8):483–500.

Maiorella BL, Blanch HW, Wilke CR. 1984. Economic evaluation of alternative ethanol fermentation processes. Biotechnol Bioeng 26(9): 1003–1025.

Malinowski JJ. 2001. Two-phase partitioning bioreactors in fermentation technology. Biotechnol Adv 19(7):525–538.

Mattiasson B, Holst O. 1991. Extractive bioconversions. New York: Marcel Dekker. p 211.

Murdock DI, Allen WE. 1960. Germicidal effect of orange peel oil and *d*-limonene in water and orange juice. Food Technol 14(9):441–445.

Newman J, Marshall J, Chang M, Nowroozi F, Paradise E, Pitera D, Newman K, Keasling J. 2006. High-level production of amorpha-4,11-diene in a two-phase partitioning bioreactor of metabolically engineered *Escherichia coli*. Biotechnol Bioeng 95:684–691.

Onken U, Rarey-Nies J, Gmehling J. 1989. The Dortmund Data Bank: A computerized system for retrieval, correlation, and prediction of thermodynamic properties of mixtures. Int J Thermophys 10(3): 739–747.

Osborne SJ, Leaver J, Turner MK, Dunnill P. 1990. Correlation of biocatalytic activity in an organic aqueous 2-liquid phase system with solvent concentration in the cell-membrane. Enzyme Microb Technol 12(4): 281–291.

Oswald M, Fischer M, Dirninger N, Karst F. 2007. Monoterpenoid biosynthesis in *Saccharomyces cerevisiae*. FEMS Yeast Res 7(3):413–421.

Peralta-Yahya PP, Ouellet M, Chan R, Mukhopadhyay A, Keasling JD, Lee TS. 2011. Identification and microbial production of a terpene-based advanced biofuel. Nat Commun 2:483.

Pourbafrani M, Talebnia F, Niklasson C, Taherzadeh M. 2007. Protective effect of encapsulation in fermentation of limonene-contained media and orange peel hydrolyzate. Int J Mol Sci 8(8):777–787.

Reiling KK, Yoshikuni Y, Martin VJJ, Newman J, Bohlmann J, Keasling JD. 2004. Mono and diterpene production in *Escherichia coli*. Biotechnol Bioeng 87(2):200–212.

Renninger N, McPhee D. 2008. Fuel compositions including farnesane and farnesene derivatives and methods of making and using same. US Patent: WO2008045555.

Renninger N, Ryder J, Fisher K. 2008. Jet fuel compositions and methods of making and using same. US Patent: WO2008133658.

Renouf MA, Wegener MK, Nielsen LK. 2008. An environmental life cycle assessment comparing Australian sugarcane with US corn and UK sugar beet as producers of sugars for fermentation. Biomass Bioenergy 32(12):1144–1155.

Riazi M. 1986. API databook, 5th edition. procedure 2B7.1.

Roffler SR, Blanch HW, Wilke CR. 1988. In situ extractive fermentation of acetone and butanol. Biotechnol Bioeng 31(2):135–143.

Ryder JA, Amyris Biotechnologies Inc (AMYR-Non-standard), assignee. 2009. Fuel composition, useful to power any equipment such as an emergency generator or internal combustion engine, which requires a fuel such as jet fuels or missile fuels, comprises limonene and farnesane. US Patent: 7589243.

Schewe H, Holtmann D, Schrader J. 2009. P450BM-3-catalyzed whole-cell biotransformation of α-pinene with recombinant *Escherichia coli* in an aqueous–organic two-phase system. Appl Microbiol Biotechnol 83(5): 849–857.

Schmid C, Steinbrecher R, Ziegler H. 1992. Partition-coefficients of plant cuticles for monoterpenes. Trees 6(1):32–36.

Sikkema J, de Bont J, Poolman B. 1995. Mechanisms of membrane toxicity of hydrocarbons. Microbiol Rev 59(2):201–222.

Sikkema J, de Bont JA, Poolman B. 1994a. Interactions of cyclic hydrocarbons with biological membranes. J Biol Chem 269(11):8022–8028.

Sikkema J, Weber FJ, Heipieper HJ, Bont JAMD. 1994b. Cellular toxicity of lipophilic compounds: mechanisms, implications, and adaptations. Biocatalysis 10:113–122.

Spectrum. 2011. Spectrum chemicals and laboratory products. https://www.spectrumchemical.com/OA_HTML/ibeCCtpSctDspRte.jsp?minisite=10020&site=&respid=50577.

Stales CA, Peterson DR, Parkerton TF, Adams WJ. 1997. The environmental fate of phthalate esters: A literature review. Chemosphere 35(4):667–749.

Brennan et al.: Extractive Fermentation of Monoterpenes **2521**

Stark D, von Stockar U. 2003. In situ product removal (ISPR) in whole cell biotechnology during the last twenty years. Process Integration in Biochemical Engineering. In: von Stockar U, van der Wielen L, Bruggink A, Cabral J, Enfors SO, Fernandes P, Jenne M, Mauch K, Prazeres D, Reuss M, editors. Advances in biochemical engineering/ biotechnology. Berlin: Springer. p. 149–175.

Subba MS, Soumithr TC, Rao RS. 1967. Antimicrobial action of cirtrus oils. J Food Sci 32(2):225–229.

Uribe S, Pena A. 1990. Toxicity of allelopathic monoterpene suspensions on yeast dependence on droplet size. J Chem Ecol 16(4):1399–1408.

Uribe S, Ramirez J, Pena A. 1985. Effects of β-pinene on yeast membrane functions. J Bacteriol 161(3):1195–1200.

van der Werf M, de Bont J, Leak D. 1997. Opportunities in microbial biotransformation of monoterpenes. In: Berger R, Babel W, Blanch H, Cooney C, Enfors S, Eriksson K, Fiechter A, Klibanov A, Mattiasson B, Primrose S, editors. Biotechnology of aroma compounds. Berlin: Springer. p 147–177.

Vermue M, Sikkema J, Verheul A, Bakker R, Tramper J. 1993. Toxicity of homologous series of organic solvents for the gram-positive bacteria *Arthrobacter* and *Nocardia* Sp. and the gram-negative bacteria *Acinetobacter* and *Pseudomonas* Sp. Biotechnol Bioeng 42(6):747–758.

Vermue MH, Tramper J. 1995. Interrelations of chemistry and biotechnology. Pure Appl Chem 67:345-373.

Wee Y-J, Kim J-N, Yun J-S, Ryu H-W. 2005. Optimum conditions for the biological production of lactic acid by a newly isolated lactic acid bacterium *Lactobacillus* sp. RKY2. Biotechnol Bioprocess Eng 10(1):23–228.

Wilkins M, Suryawati L, Maness N, Chrz D. 2007. Ethanol production by *Saccharomyces cerevisiae* and *Kluyveromyces marxianus* in the presence of orange-peel oil. World J Microbiol Biotechnol 23(8):1161–1168.

Chapter 3

Physiological and Transcriptional Responses of Saccharomyces cerevisiae to d-Limonene Show Changes to the Cell Wall but Not to the Plasma Membrane

Chapter 3 has been published in the Journal of Applied Environmental Microbiology:

Brennan TCR, Krömer JO, & Nielsen LK (2013) Physiological and Transcriptional Responses of Saccharomyces cerevisiae to d-Limonene Show Changes to the Cell Wall but Not to the Plasma Membrane. *Appl Environ Microbiol* 79(12):3590-3600.

TCRB, JK and LKN designed the experiments. TCRB carried out the experiments and analysis.TCRB, JK and LKN wrote the paper.

Physiological and Transcriptional Responses of Saccharomyces cerevisiae to d-Limonene Show Changes to the Cell Wall but Not to the Plasma Membrane

Timothy C. R. Brennan, Jens O. Krömer and Lars K. Nielsen

Journals.ASM.org

Physiological and Transcriptional Responses of *Saccharomyces cerevisiae* to *d*-Limonene Show Changes to the Cell Wall but Not to the Plasma Membrane

Timothy C. R. Brennan,[a] Jens O. Krömer,[b] Lars K. Nielsen[a]

Australian Institute for Bioengineering and Nanotechnology, University of Queensland, Brisbane, Queensland, Australia[a]; Centre for Microbial Electrosynthesis, Advanced Water Management Centre, University of Queensland, Brisbane, Queensland, Australia[b]

Monoterpenes can, upon hydrogenation, be used as light-fraction components of sustainable aviation fuels. Fermentative production of monoterpenes in engineered microorganisms, such as *Saccharomyces cerevisiae*, has gained attention as a potential route to deliver these next-generation fuels from renewable biomass. However, end product toxicity presents a formidable problem for microbial synthesis. Due to their hydrophobicity, monoterpene inhibition has long been attributed to membrane interference, but the molecular mechanism remains largely unsolved. In order to gain a better understanding of the mode of action, we analyzed the composition and structural integrity of the cell envelope as well as the transcriptional response of yeast cells treated with an inhibitory amount of *d*-limonene (107 mg/liter). We found no alterations in membrane fluidity, structural membrane integrity, or fatty acid composition after the solvent challenge. A 4-fold increase in the mean fluorescence intensity per cell (using calcofluor white stain) and increased sensitivity to cell wall-degrading enzymes demonstrated that limonene disrupts cell wall properties. Global transcript measurements confirmed the membrane integrity observations by showing no upregulation of ergosterol or fatty acid biosynthesis pathways, which are commonly overexpressed in yeast to reinforce membrane rigidity during ethanol exposure. Limonene shock did cause a compensatory response to cell wall damage through overexpression of several genes (*ROM1*, *RLM1*, *PIR3*, *CTT1*, *YGP1*, *MLP1*, *PST1*, and *CWP1*) involved with the cell wall integrity signaling pathway. This is the first report demonstrating that cell wall, rather than plasma membrane, deterioration is the main source of monoterpene inhibition. We show that limonene can alter the structure and function of the cell wall, which has a clear effect on cytokinesis.

Monoterpenes are 10-carbon (C_{10}) olefins composed of two 5-carbon (C_5) isoprene units (1). Monoterpenes, such as limonene, pinene, and cymene, have traditionally been used as flavors and fragrances (2) but recently have gained attention as potential light-component precursors for drop-in jet fuels (3–5). In June 2012, a demonstration flight by Amyris Inc. proved that their biojet fuel, AMJ-700, successfully met engine performance requirements and required no changes to the aircraft (6). AMJ-700 contains 60% monoterpene-derived paraffins, which are critical for meeting strict fuel requirements (5). Although synthesis of monoterpene products in engineered biocatalysts, such as baker's yeast and *Escherichia coli*, is still in the developmental stages (only 30 μg/liter to 1 g/liter of monoterpene product has been achieved so far [7–10]), farnesene (a C_{15} sesquiterpene) uses the same precursors in the cell and is currently produced for diesel markets (11). However, the primary challenge facing microbial monoterpene synthesis is product toxicity, which adversely impacts production parameters such as titer, yield, and rate (12).

The mechanism behind monoterpene inhibition is poorly understood. While solvent stress in microorganisms has been studied extensively over the past 40 years, these reports have focused primarily on short-chain alcohols and organic acids (13), and although monoterpenes are well-known antifungal agents, only a few quantitative studies exist (3, 14–17). Due to their lipophilicity (log P = 4.5), monoterpene inhibition has been attributed to molecular toxicity, i.e., the direct interference of solvent molecules with membrane function (17–19). Consistent with this, increases in membrane fluidity (17) and structural membrane damage (20) were observed in whole yeast cells exposed to pinene.

Solvents partition between the membrane and the aqueous phase. For a sparingly water-soluble solvent in equilibrium, the membrane concentration will be proportional to the solvent's aqueous concentration, and molecular toxicity is typically observed to increase proportionally with the solvent's aqueous concentration (21–23). With the membrane and aqueous phases in equilibrium, molecular toxicity must peak when the aqueous concentration has reached its solubility limit, since both phases are saturated at this point.

Monoterpenes are essential oils; thus, they are sparingly soluble in water (e.g., $S_{limonene}$ = 6 mg/liter) (24). In a recent study, we found that the inhibitory concentrations for five monoterpene products were at least an order of magnitude higher than their aqueous saturation limits (3). The cells were also able to grow at 97% of the maximum growth rate when their cellular compartments (e.g., plasma membrane) were saturated with monoterpene (3). Thus, monoterpene toxicity is per definition not molecular toxicity but rather phase toxicity (25). Phase toxicity has a phenomenological rather than a mechanistic definition: toxicity occurs in the presence of a distinct solvent phase (i.e., after water and membrane saturation) and is a nonequilibrium (kinetic) effect

that increases with interfacial area (e.g., larger solvent phase volume and greater agitation).

Here we investigated the direct impact that limonene has on the yeast cell envelope. Many microorganisms, including yeast, *Pseudomonas putida*, and *E. coli*, respond to solvent stress by altering their lipid bilayers to counteract fluidization effects ([13]). To confirm whether or not molecular toxicity effects were indeed the source of limonene inhibition, membrane fluidity, structural membrane integrity, and membrane composition were measured after limonene exposure. Due to the lack of evidence for molecular toxicity, additional experiments such as cell wall integrity (CWI) staining and cell wall sensitivity assays were used to investigate potential sources of phase toxicity at the surface of the cell. Lastly, analysis of the global transcriptional response was used to support the physiological observations.

MATERIALS AND METHODS

Strain, chemicals, and growth conditions. The *Saccharomyces cerevisiae* strain S288C (*MATα SUC2 gal2 mal mel flo1 flo8-1 hap1*) was provided by the Australian Wine Research Institute (AWRI), Adelaide, South Australia, Australia. Analytical-grade *d*-limonene (93%) was purchased from Sigma-Aldrich. The growth conditions and limonene challenge were as described previously ([3]) with the following modifications. Chemically defined medium (CBS) was used. CBS contained 20 g/liter sucrose, 5 g/liter $(NH_4)_2SO_4$, 3 g/liter KH_2PO_4, 0.5 g/liter $MgSO_4 \cdot 7H_2O$, and the exact components and concentration of vitamins and trace metals described by Brennan et al. ([3]). Overnight precultures (pH 5.0, 30°C) were used to inoculate 25 ml of fresh CBS to an optical density at 660 nm (OD_{660}) of 0.5 against water, and then 2.8 μl of limonene (107 mg/liter) was added exogenously to the medium during mid-exponential growth phase (at ∼5 h; OD_{660} = 2.5). All of the measurements described below were taken 2 h after the limonene challenge for limonene-treated cultures and similarly for control cultures with no limonene present.

Fluorescence anisotropy. The membrane fluidity of limonene-challenged and control cultures was determined using fluorescence anisotropy as described previously ([26], [27]) with the following modifications. After 2 h of limonene exposure, cells were harvested at 13,000 rpm for 1 min, washed twice with 15 mM Tris-HCl buffer, and resuspended to an OD_{660} of 0.2. A 1.0-μl volume of a 12 mM stock solution of diphenyl-hexatriene (DPH) in tetrahydrofuran was then added to the resuspension and incubated at 30°C for 30 min with continuous stirring (200 rpm) to allow the probe to intercalate into the plasma membrane ([27]). The anisotropy was measured with a Spectromax M5 (Sunnyvale, CA) at excitation and emission wavelengths of 358 and 428 nm, respectively, and recorded using Softmax Pro (v 5.3) software. All anisotropy measurements were analyzed in biological triplicate for limonene-treated and control cultures at 30°C. A positive control was used to test for increase fluidity by heat treating cells under the identical conditions described above at 50°C for 50 min. Heat-treated samples had a 16% increase in fluidity compared to the control (anisotropy value $r = 0.138 \pm 0.003$ [$n = 3$]).

Confocal microscopy. Two microliters of calcofluor white (CFW)-stained cells was loaded onto a glass slide. A coverslip was added on top, and a thin layer of nail polish was used to seal the sample between the glass slide and the coverslip. The images were taken throughout the coverslip with a Zeiss 710 confocal laser scanning microscope (CLSM) using a Plan-Apochromat 63×/1.40 oil DIC M27 objective. The 2,048- by 2,048-pixel map images were recorded using a 405-nm wavelength excitation laser, and the data were collected in the 409- to 517-nm window. All the images were analyzed using the ZEN 2011 software (Carl Zeiss Microscopy, Jena, Germany).

Cell wall isolation. Cell walls were isolated and analyzed using the acid (H_2SO_4) treatment method ([28]). Cell wall extractions were performed in biological triplicate for both control and limonene-challenged cultures at

2 h after limonene addition. Cell wall monosaccharide concentrations were normalized using the total dry cell wall mass for individual samples.

Lipid extraction and methylation. Yeast lipids were extracted by using the chloroform-methanol protocol described previously ([26]) with the following modifications. At 2 h after limonene addition, the entire culture volume (22 to 25 ml) was weighed and harvested (4,025 × *g*) for 2 min at 25°C. The cell pellet was washed in phosphate-buffered saline (PBS) (Invitrogen, Life Technologies, Carlsbad, CA), resuspended, and added to a 1:1 solution of methanol and chloroform as described but with 0.27 μg of nonadecanoic acid (Sigma-Aldrich) to a final concentration of 0.018 μg/ml as an internal standard (ISTD). The lower chloroform phase was removed and dried down under nitrogen. Lipid extracts were saponified under reflux (2 h, 80°C) with 1 ml of 2 M NaOH and 2 ml of methanol. After acidification by the addition of 200 μl of 37.5% concentrated HCl, 4 ml (2 aliquots of 2 ml) of chloroform was added and vortexed. Upon phase separation, the chloroform phase (2 ml) was removed, and the second aliquot (2 ml) of chloroform was added and vortexed. Both chloroform aliquotes were then recombined. To recover the lipids, the chloroform was evaporated under nitrogen. For methylation, 200 μl of 2% H_2SO_4 in methanol was added to the extracts and incubated for 2 h at 80°C. Once cooled, 200 μl of 0.9% NaCl was added and vortexed, and then the addition of 300 μl of hexane was used to recover the fatty acid methyl esters (FAME) for gas chromatography-mass spectrometry (GC-MS) analysis. Lipid extraction was carried out in biological triplicate for control and limonene-treated samples.

GC-MS. For GC-MS analysis, 2 μl from the hexane-FAME sample was injected into the GC inlet in splitless mode at 350°C using helium as a carrier gas with a constant flow rate of 1 ml/min. Compounds were separated using a Varian factorFOUR capillary column (VF-5 ms; 0.25-mm inner diameter, 0.25-μm film, 30-m length with a 10-m fused guard column) on an Agilent 7890A gas chromatograph attached to an Agilent 5975C MSD. Initially the oven temperature was set to 70°C, and this was held for 5 min, followed by a temperature ramp of 9°C/min to 320°C and then 30°C/min to 350°C and holding for 6.3 min. Detection was achieved in scan mode at 9.26 scans/s from 30 to 800 amu. Thirty-two individual fatty acid standards (Sigma-Aldrich) were used to build a FAME library using their target ions and retention times. FAME peaks were detected in each sample by matching to compounds within the FAME library, and an alkane (C_{7-30}) standard was used as a retention time index. The relative area for each fatty acid in a sample was calculated by dividing the FAME area by the ISTD area, multiplying by the ratio of actual ISTD to set ISTD mass, and then dividing by grams of dry cell weight (gDCW) of the sample. Biological triplicates were used for each condition.

Fluorochrome staining. Aliquots from control and limonene-treated cultures were taken in mid-exponential phase 2 h after limonene addition. Propidium iodide (PI) was used for determination of cell permeability and membrane integrity ([3]). For cell wall staining, calcofluor white (CFW) (Sigma-Aldrich) was used as described previously ([29]) with the following modifications. One milliliter of culture was quickly harvested at 13,000 rpm for 1 min, washed with sterile Milli-Q water, and resuspended in 200 μl of water containing 100 μg/ml of CFW. The solution was then incubated at 30°C for 2 min, harvested, washed twice with Milli-Q water, and resuspended in 1 ml of water before flow cytometry analysis. All data were produced in biological triplicate.

Flow cytometry. Cell viability was analyzed using PI exactly as described by Brennan et al. ([3]). For calcofluor white staining, cells were analyzed using a BD LSRII flow cytometer with a UV laser at 350 nm. Forward scatter (FSC), side scatter (SSC), and 450/50 band-pass (BP) filter excitation were acquired using BD FACSDiVa software (v 6.1.1). Postacquisition compensation analysis of total fluorescence intensity was carried out using Flow Jo software (v 10.0). All data were analyzed in biological triplicate.

Cell wall sensitivity assay. The sensitivity of cell walls to enzymatic degradation was performed as described by Takahashi et al. ([30]). Briefly, 200 μl of culture was harvested at mid-exponential phase 2 h after limo-

nene addition, washed with sterile water, and diluted to an OD_{660} of 2 in buffer containing NaH_2PO_4 (0.1 M, pH 7.5), 0.04% NaN_3, and 40 μg/ml lyticase enzyme from *Arthrobacter luteus* (Sigma-Aldrich). The samples were placed in an Eppendorf rack at 30°C and 200 rpm, and the cell density was monitored hourly. An identical buffer lacking the enzyme was used as a negative control. The percentage of the original OD was reported for biological triplicates for both control and limonene-challenged cultures.

Transcriptomics. (i) RNA sampling and isolation. RNA was isolated from cultures containing no limonene (control) at mid-exponential phase. For challenged cultures, limonene was added (107 mg/liter) at mid-exponential phase, and RNA was sampled 2 h later. All isolations were done with three biological replicates. For each set of replicates, 10 ml of culture was sampled and harvested for 1 min (4,025 × *g*), the supernatant was discarded, and the total RNA was immediately extracted using the RiboPure-Yeast kit (Ambion, Life Technologies, Carlsbad, CA) according to the manufacturer's protocol except that bead beating (Biospec Products, Bartlesville, OK) was used to fully lyse the cells (3 times for 20 s, followed by 1 min on ice). The total RNA was then digested (twice) using the Turbo DNA-free kit (Invitrogen, Life Technologies, Carlsbad, CA) and then cleaned and concentrated using the RNA Clean & Concentrator-25 kit (Zymo Research, Irvine, CA) according to both manufacturer's instructions. DNA contamination was assessed by quantitative reverse transcription-PCR (qRT-PCR). The total RNA sample quality was then measured using an Agilent 2100 Bioanalyzer and RNA 6000 Nano kit according to manufacturer's methods (Agilent, Santa Clara, CA). Sample labeling and hybridization to Affymetrix yeast genome 2.0 arrays were performed by the Ramaciotti Centre for Gene Function Analysis (University of New South Wales, Sydney, Australia).

(ii) Microarray data analysis. Statistical analysis of the raw microarray data was carried out using GenePattern (31). The six Affymetrix CEL files were imported, normalized, and log transformed using the following software modules within GenePattern: GarvanCaArray2.3.0Importer, NormalizeAffymetrix3prime, and LogTransform. Detection of differentially expressed genes and statistical analysis of the samples were carried out using the limma package (32) within the LimmaGP module. The differentially expressed gene set was then filtered using a cutoff at a Bonferroni-corrected *P* value of ≤0.01. The filtered gene list was then used as input into g:Profiler to asses significantly changed pathways, reactions, and Gene Ontology (GO) terms using a hypergeometric test (33). The results were visualized using the MultiExperiment Viewer software (34). Using the unfiltered gene expression values (log_2), the entire transcriptome data set was viewed using the *Saccharomyces* Genome Database (SGD) pathways tool (http://pathway.yeastgenome.org) for metabolic mapping and identification. The raw microarray data are publically available at http://pwbc.garvan.unsw.edu.au/caarray/project/details.action?project.id=607.

RESULTS

In order to study the response to limonene, the dose added must be sublethal. We have previously observed substantial cell death if inhibitory levels of limonene are added to the inoculum (3). When added in mid-exponential phase, however, cell growth is arrested (Fig. 1a), while viability remains greater than 98% after 2 h of limonene exposure (Fig. 1b). Viability is measured through PI stain exclusion and confirms structural membrane integrity. Further investigation of membrane properties revealed no significant changes in membrane fluidity as measured through fluorescence anisotropy (Fig. 1b), nor were there any significant changes to the fatty acid composition after limonene treatment (Fig. 2b).

While 2 h of limonene treatment caused no significant changes in the cell wall polysaccharide composition (Fig. 2a), it greatly affected cell wall integrity. Limonene-treated cells were hypersensitive to the cell wall binding dye calcofluor white (CFW), exhib-
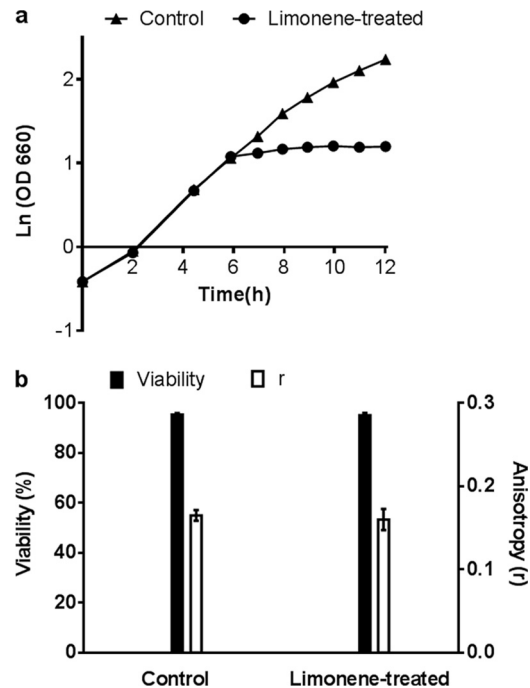
FIG 1 (a) Growth plot for control and limonene-treated (107 mg/liter) cultures. (b) Cell viability and membrane fluidity (anisotropy, r) measurements at 2 h after limonene addition. Error bars represent one standard deviation (SD) above and below the mean for biological replicates.

iting a 4-fold increase in mean fluorescence intensity (MFI) of 5,231 ± 471 compared to that of control cells (MFI = 1,270 ± 45) (Fig. 3a). In confocal microscopy (Fig. 3b and c), the hypersensitivity to CFW appears as enriched fluorescence in the bud neck region of the cells. Limonene-treated cells were also more susceptible to cell wall-degrading enzymes (Fig. 4). A 40% drop in cell density was observed after 1 h for limonene-challenged cells, compared to 20% found in the control.

Global gene expression analysis identified 277 upregulated and 176 downregulated genes (Bonferroni-corrected *P* value of <0.01). Enrichment analysis identified the expected downregulation of biological processes linked to cell growth, e.g., cytokinesis, ribosome biogenesis, nucleotide biosynthesis, and amino acid biosynthesis (see the supplemental material). The only biological process identified as significantly enriched in the upregulated gene set was iron ion homeostasis. Though none of the stress-related biological processes were significantly enriched, several KEGG pathways linked to stress (glutathione metabolism, peroxisome, and autophagy) were identified (see the supplemental material).

While global repression trends in amino acid synthesis, ribosome activity, and protein synthesis were to be expected for arrested cells, we were particularly interested in how the gene expression data related to the physiological observations of the cell envelope. Limonene-treated cells induced expression of seven fatty acid metabolism and six glycerophospholipid metabolism genes (Table 1 and Fig. 5c); however, global metabolic mapping showed no overexpression of either ergosterol or saturated and unsaturated fatty acid biosynthesis pathways (Table 1; see Table S1 in the supplemental material). Limonene treatment also caused the overexpression of carbohydrate, xenobiotic, amino acid, and sulfur transport activity (Table 1 and Fig. 5c), as well as the expres-
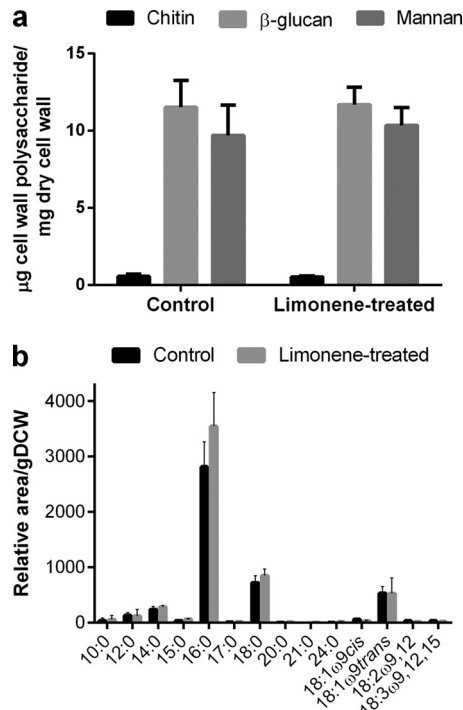
FIG 2 Cell envelope compositional changes due to limonene shock. (a) Cell wall polysaccharide compositions for control and limonene-treated cells. (b) Fatty acid composition at 2 h after limonene challenge. 10:0, decanoic acid; 12:0, dodecanoic acid; 14:0, myristic acid; 15:0, pentadecanoic acid; 16:0, palmitic acid; 17:0, heptadecanoic acid; 18:0, octadecanoic acid; 20:0, eico-sanoic acid; 21:0, docosanoic acid; 24:0, tetracosanoic acid; 18:1ω9cis, oleic acid; 18:1ω9trans, elaidic acid; 18:2ω9,12, linoleic acid; 18:3ω9,12,15 linolenic acid. Error bars represent one SD above the mean ($n = 3$).

FIG 3 (a) Flow cytometry measurements of limonene-treated and control cells using the cell wall binding probe calcofluor white (CFW) at 2 h after limonene addition. Mean fluorescence intensity/cell (arbitrary units, $n = 3$) ± SD. Inset, forward side scatter versus CFW intensity. (b and c) Confocal microscopy images of control cells (b) and limonene-treated cells (c) stained with CFW. Arrows indicate the chitin-enriched bud neck.

sion of several common stress-associated genes (Fig. 5a). Finally, limonene exposure induced a number of genes associated with cell wall organization and biogenesis (Table 1 and Fig. 5b). The observed impact on the structural integrity of the cell wall (Fig. 3 and 4) was further supported by the regulation of the cell wall integrity (CWI) signaling pathway. Several key signaling genes (*MTL1*, *ROM1*, *MPK1*, *BAG7*, and *MLP1*) and the major transcription factor gene *RLM1* were upregulated (Fig. 6). Furthermore, 12 of RLM1's 25 gene targets were overexpressed, most of which encode proteins associated with cell wall organization and/or wall biogenesis (Fig. 6).

DISCUSSION

Monoterpene toxicity is generally assumed to be due to membrane interference, as observed for ethanol (17–19). Yeast cells respond to ethanol exposure by increasing their ergosterol and unsaturated fatty acid composition to increase membrane rigidity (35–37). An early microarray study of α-terpinene toxicity observed global upregulation of genes involved in ergosterol synthesis and sterol uptake (15). In the current study, however, we observed no evidence of membrane interference by limonene. Membrane integrity, fluidity (Fig. 1), and fatty acid composition (Fig. 2b) did not change significantly in response to limonene. Furthermore, no increase in the expression of genes in the ergosterol and fatty acid biosynthesis pathways was observed (Table 1; see Fig. S1 in the supplemental material).

We would have expected results similar to those observed for

α-terpinene (15). Like limonene, terpinenes are cyclic monoterpenes. Terpinene was used at a higher concentration (170 mg/liter rather than 107 mg/liter) but is also slightly less toxic; the terpinene concentration was chosen as the 50% inhibitory concentration (IC$_{50}$) in the previous study (15), while our study used nearly two times the IC$_{50}$ for limonene (3). The monoterpenes were added to cells in mid-exponential phase, i.e., 5 h in culture in our study and overnight in the terpinene study. In both studies, the response was measured at 2 h after monoterpene addition. One significant difference was that complex (YPD) medium was used in the terpinene study, compared to minimal medium in our study. Another major difference was that a number of genes in-

FIG 4 Cell wall sensitivity measurements using lyticase enzyme for limonene-treated cells. All data were carried out in biological triplicate and, error bars represent one SD above and below the mean.

TABLE 1 Differentially expressed genes associated with the plasma membrane and cell wall cellular compartments and functions[a]

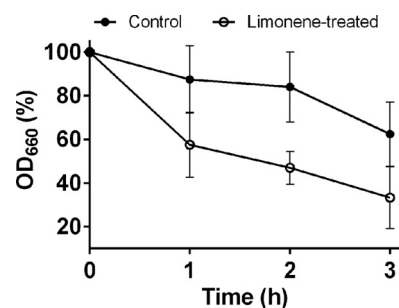| Process (GO term, no. of genes,[b] P value)	Upregulated genes			Downregulated genes		
	Gene	Protein description	Fold change[c]	Gene	Protein description	Fold change
Fatty acid metabolic process (0006631, 7, 3.58E−02)	CAT2	Carnitine acetyl-CoA transferase present in both mitochondria and peroxisomes; transfers activated acetyl groups to carnitine to form acetylcarnitine, which can be shuttled across membranes	1.65	ELO1	Elongase I, medium-chain acyl elongase, catalyzes carboxy-terminal elongation of unsaturated C_{12}–C_{16} fatty acyl-CoAs to C_{16}–C_{18} fatty acids	−2.21
	OLE1	Delta(9) fatty acid desaturase, required for monounsaturated fatty acid synthesis and for normal distribution of mitochondria	1.90			
	POT1	3-Ketoacyl-CoA thiolase with broad chain-length specificity; cleaves 3-ketoacyl-CoA into acyl-CoA and acetyl-CoA during beta-oxidation of fatty acids	2.84			
	HTD2	Mitochondrial 3-hydroxyacyl-thioester dehydratase involved in fatty acid biosynthesis; required for respiratory growth and for normal mitochondrial morphology	0.98			
	EHT1	Acyl-coenzyme A:ethanol O-acyltransferase that plays a minor role in medium-chain fatty acid ethyl ester biosynthesis; possesses short-chain esterase activity; localizes to lipid particles and the mitochondrial outer membrane	0.92			
	FAS2	Alpha subunit of fatty acid synthetase, which catalyzes the synthesis of long-chain saturated fatty acids; contains the acyl-carrier protein domain and beta-ketoacyl reductase, beta-ketoacyl synthase and self-pantetheinylation activities	1.06			
Glycerophospholipid metabolism (0564 [KEGG], 6, 1.42E−02	INO1	Inositol 1-phosphate synthase, involved in synthesis of inositol phosphates and inositol-containing phospholipids; transcription is coregulated with other phospholipid biosynthetic genes by Ino2p and Ino4p, which bind the UASINO DNA element	4.10			
	CLD1	Mitochondrial cardiolipin-specific phospholipase; functions upstream of Taz1p to generate monolyso-cardiolipin; transcription increases upon genotoxic stress; involved in restricting Ty1 transposition; has homology to mammalian CGI-58	1.89			
	CHO1	Phosphatidylserine synthase; functions in phospholipid biosynthesis; catalyzes the reaction CDP-diacylglycerol + L-serine = CMP + L-1-phosphatidylserine; transcriptionally repressed by *myo*-inositol and choline	1.15			
	CKI1	Choline kinase, catalyzing the first step in phosphatidylcholine synthesis via the CDP-choline (Kennedy pathway); exhibits some ethanolamine kinase activity contributing to phosphatidylethanolamine synthesis via the CDP-ethanolamine pathway	1.28			
	CHO2	PEMT, catalyzes the first step in the conversion of phosphatidylethanolamine to phosphatidylcholine during the methylation pathway of phosphatidylcholine biosynthesis	1.13			
	OPI3	Phospholipid methyltransferase (methylene-fatty-acyl-phospholipid synthase); catalyzes the last two steps in phosphatidylcholine biosynthesis	0.95			
Xenobiotic transporter activity (0042910, 3, 2.18E−02)	PDR5	Plasma membrane ABC transporter; multidrug transporter actively regulated by Pdr1p; also involved in steroid transport, cation resistance, and cellular detoxification during exponential growth	2.00	PDR12	Plasma membrane ABC transporter; weak-acid-inducible multidrug transporter required for weak organic acid resistance; induced by sorbate and benzoate and regulated by War1p; mutants exhibit sorbate hypersensitivity	−1.54
	YOR1	Plasma membrane ABC transporter; multidrug transporter mediates export of many different organic anions, including oligomycin; similar to human CFTR	1.65			
	PDR15	Plasma membrane ABC transporter, multidrug transporter, and general stress response factor implicated in cellular detoxification; regulated by Pdr1p, Pdr3p, and Pdr8p; promoter contains a PDR-responsive element	3.19			
Amino acid and sulfur transmembrane transport (0003333 and 0072348, 9, 0.00136–0.01)	AGP3	Low-affinity amino acid permease; may act to supply the cell with amino acids as nitrogen source under nitrogen-poor conditions; transcription is induced under conditions of sulfur limitation; plays a role in regulating Ty1 transposition	5.09			
	MUP1	High-affinity methionine permease; integral membrane protein with 13 putative membrane-spanning regions; also involved in cysteine uptake	4.63			
	MUP3	Low-affinity methionine permease similar to Mup1p	1.87			
	MMP1	High-affinity *S*-methylmethionine permease; required for utilization of S-methylmethionine as a sulfur source; has similarity to S-adenosylmethionine permease Sam3p	2.28			
	SAM3	High-affinity *S*-adenosylmethionine permease; required for utilization of S-adenosylmethionine as a sulfur source; has similarity to S-methylmethionine permease Mmp1p	2.23			

TABLE 1 (Continued)

Process (GO term, no. of genes,[b] P value)	Upregulated genes		Fold change[c]	Downregulated genes		Fold change
	Gene	Protein description		Gene	Protein description	
	ALP1	Arginine transporter; expression is normally very low, and it is unclear what conditions would induce significant expression	1.22			
	YCT1	High-affinity cysteine-specific transporter with similarity to the Dal5p family of transporters; GFP fusion protein localizes to the endoplasmic reticulum; YCT1 is not an essential gene	4.33			
	SUL2	High-affinity sulfate permease; sulfate uptake is mediated by specific sulfate transporters Sul1p and Sul2p, which control the concn of endogenous activated sulfate intermediates	1.47			
	SUL1	High-affinity sulfate permease of the SulP anion transporter family; sulfate uptake is mediated by specific sulfate transporters Sul1p and Sul2p, which control the concn of endogenous activated sulfate intermediates	1.80			
Cell wall organization (0005576, 22, 7.86E−02)	YGP1	Cell wall-related secretory glycoprotein; induced by nutrient deprivation-associated growth arrest and upon entry into stationary phase; may be involved in adaptation prior to stationary-phase entry; has similarity to Sps100p	4.03	HPF1	Haze-protective mannoprotein that reduces the particle size of aggregated proteins in white wines	−2.52
	PIR3	O-glycosylated covalently bound cell wall protein required for cell wall stability; expression is cell cycle regulated, peaking in M/G₁, and also subject to regulation by the cell integrity pathway	4.99	GAS3	Low-abundance, possibly inactive member of the GAS family of GPI-containing proteins; putative 1,3-beta-glucanosyltransferase with similarity to other GAS family members; localizes to the cell wall; mRNA induced during sporulation	−2.27
	FIT2	Mannoprotein that is incorporated into the cell wall via a GPI anchor; involved in the retention of siderophore iron in the cell wall	2.01	UTR2	Chitin transglycosylase that functions in the transfer of chitin to beta(1-6) and beta(1-3) glucans in the cell wall; similar to and functionally redundant with Crh1; GPI-anchored protein localized to bud neck	−2.56
	SUC2	Invertase, sucrose-hydrolyzing enzyme; a secreted, glycosylated form is regulated by glucose repression, and an intracellular, nonglycosylated enzyme is produced constitutively	2.63	SUN4	Cell wall protein related to glucanases; possibly involved in cell wall septation; member of the SUN family	−2.21
	TIP1	Major cell wall mannoprotein with possible lipase activity; transcription is induced by heat and cold shock; member of the Srp1p/Tip1p family of serine-alanine-rich proteins	2.06	DSE4	Daughter cell-specific secreted protein with similarity to glucanases; degrades cell wall from the daughter side, causing daughter to separate from mother	−1.89
	SPI1	GPI-anchored cell wall protein involved in weak acid resistance; basal expression requires Msn2p/Msn4p; expression is induced under conditions of stress and during the diauxic shift; similar to Sed1p	4.74	SCW11	Cell wall protein with similarity to glucanases; may play a role in conjugation during mating based on its regulation by Ste12p	−2.99
	PST1	Cell wall protein that contains a putative GPI attachment site; secreted by regenerating protoplasts; upregulated by activation of the cell integrity pathway, as mediated by Rlm1p; upregulated by cell wall damage via disruption of FKS1	1.88	DSE2	Daughter cell-specific secreted protein with similarity to glucanases; degrades cell wall from the daughter side, causing daughter to separate from mother; expression is repressed by cAMP	−3.16
	FIT3	Mannoprotein that is incorporated into the cell wall via a GPI anchor; involved in the retention of siderophore iron in the cell wall	1.73	CTS1	Endochitinase; required for cell separation after mitosis; transcriptional activation during the G₁ phase of the cell cycle is mediated by transcription factor Ace2p	−2.36
	HSP150	O-mannosylated heat shock protein that is secreted and covalently attached to the cell wall via beta-1,3-glucan and disulfide bridges; required for cell wall stability; induced by heat shock, oxidative stress, and nitrogen limitation	0.97	EGT2	GPI-anchored cell wall endoglucanase required for proper cell separation after cytokinesis; expression is activated by Swi5p and tightly regulated in a cell cycle-dependent manner	−2.09
	CWP1	Cell wall mannoprotein that localizes specifically to birth scars of daughter cells, linked to a beta-1,3- and beta-1,6-glucan heteropolymer through a phosphodiester bond; required for propionic acid resistance	1.07			
	PRB1	Vacuolar proteinase B (yscB), a serine protease of the subtilisin family; involved in protein degradation in the vacuole and required for full protein degradation during sporulation; activity inhibited by Pbi2p	1.30			
	DIA3	Protein of unknown function involved in invasive and pseudohyphal growth	1.35			
	TDH1	Glyceraldehyde-3-phosphate dehydrogenase, isozyme 1, involved in glycolysis and gluconeogenesis; tetramer that catalyzes the reaction of glyceraldehyde-3-phosphate to 1,3-bis-phosphoglycerate; detected in the cytoplasm and cell wall	1.15			

[a] Abbreviations: CoA, coenzyme A; PEMT, phosphatidylethanolamine methyltransferase; ABC, ATP binding cassette; CFTR, cystic fibrosis transmembrane receptor; GFP, green fluorescent protein; GPI, glycosylphosphatidylinositol; cAMP, cyclic AMP.

[b] Number of genes associated with the reported Gene Ontology accession number. The total number of differentially expressed genes was 453.

[c] Log₂ ratio of expression in treated cells to that in control cells.
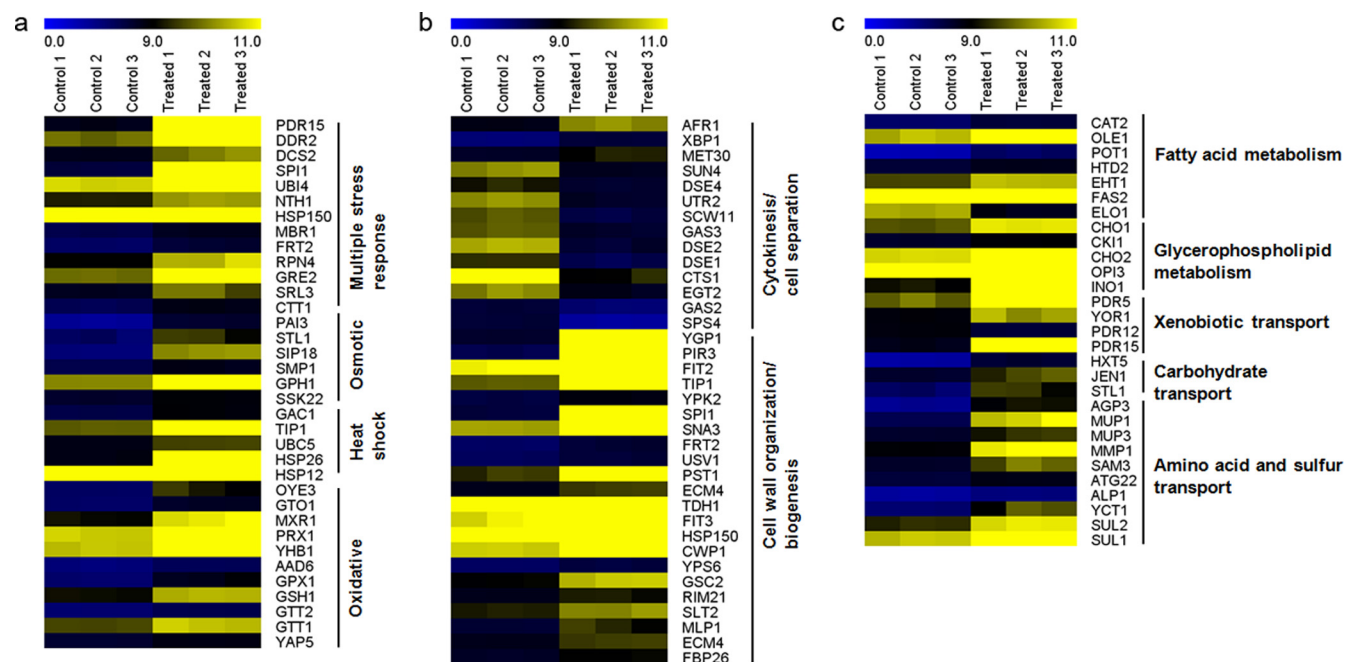
FIG 5 Gene expression values ($\log_2$) for each biological replicate (control versus limonene-treated cells) for genes involved in stress responses (a), cell wall organization and cytokinesis (b), and plasma membrane transport and fatty acid metabolism (c).

volved in redox activity and glutathione metabolism (see the supplemental material) were found for limonene but not for terpinene exposure. Dioxygenase and oxidoreductase genes *JLP1* and *OYE3*, for example, were highly upregulated (6.7- and 3.6-fold changes, respectively [see the supplemental material]) during limonene exposure. Glutathione biosynthesis (*GSH1*, 1.3-fold induced) and peroxide protection *CTT1* and *GPX1* (2.2- and 3-fold induced, respectively) genes (see the supplemental material) were also found in this work but not in the terpinene study. Differences between the two transcriptional responses may stem from culture conditions or monoterpene load, as well as differences in chemical properties between the two compounds and their potential to form epoxides.

Because redox and glutathione metabolism activity was observed, we wanted to exclude oxidative stress as possible source of molecular toxicity. Expression of *GSH1*, *CTT1*, and *GPX1* is a well-characterized response to oxidative stress in *S. cerevisiae* (38). Signature genes involved in antioxidant defense systems, however, were not overexpressed. Genes for key transcriptional regulators (*YAP1* and *SKN7*), thioredoxins (*TRX1*, *TRX2*, *TRR1*, and *TRR2*), glutaredoxins (*GLX1*, *-2*, *3*, *-4*, and *-5*), and superoxide dismutases (*SOD1* and *-2*) as well as for two key stress response element (STRE) regulators (*MSN2* and *MSN4*) were not induced during limonene shock (38, 39). A potential cause of increased redox activity may come from oxygenated limonene compounds such as limonene epoxides, which can form when limonene is exposed to air for long periods of time (40). Epoxide compounds have been reported to cause oxidative damage in yeast (41), and limonene-1,2-epoxide, for example, is 23 times more soluble in water than limonene (137 mg/liter) (42). There may be differences between the toxic effects of monoterpene hydrocarbons and oxy-functionalized monoterpene compounds. For example, 1,8-cineole (an epoxy-monoterpene) was endogenously produced in yeast with no

report of toxicity limitations up to 1 g/liter (10), while a separate study reported that limonene stops growth at 60 mg/liter (3). While limonene itself is toxic at the phase level, limonene epoxides may have caused redox imbalances to cells on the molecular level. In order to rule this out, the experiments were repeated under anaerobic conditions. We found no limonene epoxide formation in GC-MS but observed the same adverse effects on growth (see Fig. S2 in the supplemental material). This means that although limonene epoxides can form in aerobic cultures (see Fig. S3 in the supplemental material), limonene itself remains the primary source of toxicity.

Membrane-bound efflux pumps play a critical role in solvent-tolerance in *P. putida* (43). Expression of the AcrAB-TolC efflux proteins in *E. coli* led to higher tolerance of cyclohexane (44) and increased tolerance and production of pinene and limonene (8). Similar to the bacterial pumping system, cellular detoxification in yeast is driven primarily by pleiotropic drug resistance (PDR) pumps, which are a subfamily of yeast's ABC proteins (45). We found three ABC transporter genes induced under limonene stress (*YOR1*, *PDR15*, and *PDR5*) (Fig. 5c and Table 1). The same three transporters were identified in a recent study, but overexpression failed to improve tolerance for limonene (46), and the pumps may lack affinity to limonene.

Absence of a membrane effect is consistent with limonene toxicity being phase toxicity rather than molecular toxicity. There is no evidence of molecular toxicity, as the system is saturated at a water concentration of 6 mg/liter and the IC_{50} is 10 times greater than the solubility. The solvent phase contacts the cell wall rather than the cell membrane. Having primary roles in protection from turgor pressure and cell division, the cell wall is essential for survival (47). Its latticework is tightly held together by strong hydrogen bonding networks between cellulose and chitin chains as well as covalent glycosidic linkages between all three wall components
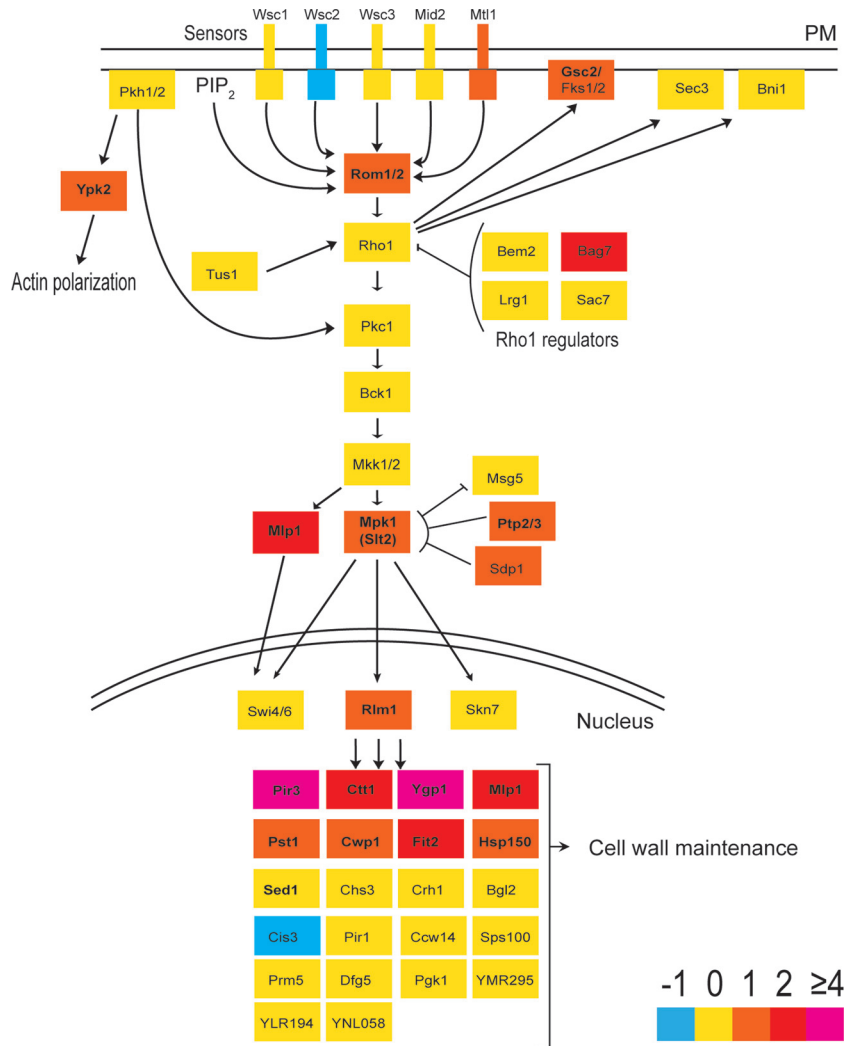
FIG 6 Cell wall integrity (CWI) signaling pathway with transcriptomic expression changes during limonene stress. Colors indicate the fold change (log$_2$) cutoffs. Genes in bold represent genes that were differentially expressed (Bonferroni-corrected P value of <0.01). PM, plasma membrane; PIP$_2$, phosphatidylinositol-4,5-bisphosphate. (Adapted from reference 70 with permission.)

(glucan, mannoprotein, and chitin) (48). Calcofluor white is a fluorochrome that binds to the cell wall by hydrogen bonding with chitin and β-linked polysaccharides (49–51), but in fungi, CFW preferentially binds to the chitin, which is localized in the bud neck (29). In Fig. 3a, a 4-fold increase in the MFI demonstrates that more fluorochrome is bound per cell after limonene treatment. Increased sensitivity to CFW is indicative of cell wall damage in *S. cerevisiae*, *Candida albicans* (52), *Aspergillus niger* (53), and a number of other fungi (54). Disruption of the crystalline lattice of chitin polymers has been shown to weaken the cell wall, causing cell arrest and accumulation of chitin deposits in *S. cerevisiae* (55). Although we did not find higher levels of chitin (Fig. 2a), this mechanism is in concert with our CFW hypersensitivity and growth inhibition results. A decrystallizing effect is also seen in Fig. 4, where the cell walls were found to be more susceptible to glucan-specific degradation with lyticase enzymes after having been treated with limonene. Because we found no changes in the total wall composition after limonene exposure (Fig. 2a), the data suggest that limonene can alter the properties of the cell wall.

Given its pivotal role in the budding process, particularly in septum formation (47, 56), our results indicate that by disrupting the cell wall structure, limonene has a profound effect on cell growth.

The cellular response to limonene further demonstrates cell wall stress. Twelve differentially expressed genes that were found in this study (*CWP1*, *PIR3*, *SED1*, *PST1*, *SLT2*, *MLP1*, *ECM4*, *HSP12*, *DDR2*, *SLR3*, *FBP26*, and *AFR1*) belong to a cluster of 20 well-characterized genes that represent the main transcriptional fingerprint of cell wall stress (57, 58). Furthermore, several genes directly involved in the cell wall integrity (CWI) signaling pathway, the sole purpose of which is to respond to cell wall stress (59), were upregulated in response to limonene exposure (Fig. 6). The guanosine nucleotide exchange factor gene *ROM1*, the cell surface sensor gene *MLT1*, and the genes *SLT2* and *MLP1*, coding for the mitogen-activated protein kinase (MAPK) proteins cascade, were induced (Fig. 6). *RLM1* codes for the transcription factor responsible for the majority of the transcriptional output of CWI (59). *RLM1* was slightly overexpressed (1.2-fold [log$_2$]), while five of its targets (*PST1*, *CWP1*, *PIR3*, *CTT1*, and *YGP1* in Fig. 6) were highly

upregulated. In particular, *PIR3* and *YGP1*, which are required for cell wall organization and stability, were two of the most highly induced genes found, having fold changes of 5 and 4, respectively (Fig. 6 and Table 1). Lastly, the cellular response to limonene caused decreased transcript levels for transcription, ribosomal activity, and purine nucleotide metabolism. These repression trends were also found in two independent studies profiling the global transcriptional response to cell wall damage (57, 58).

The physical interaction between an insoluble limonene phase and a cell is still unclear. We have shown here that limonene dispersions can alter surface properties of yeast cells by disrupting the normal structure of the cell wall, but the relationship between limonene's rheological behavior in an aqueous culture and its apparent toxicity to a microorganism is yet to be determined. In a recent study (3), limonene toxicity was dramatically reduced in the presence of an inert extractant. The extractive solvents dibutyl phthalate (DBP) and isopropyl myristate (IPM), for example, are harmless to yeast cells and are at least an order of magnitude more viscous than limonene ($\mu_{limonene}$ = 0.008 P [60], μ_{DBP} = 0.166 P [61], and μ_{IPM} = 0.043 P [62]). The viscosity of a fluid has a strong influence on droplet size, which affects the dispersion's overall surface area (63). Future work is required to characterize how fluid properties (e.g., viscosity, droplet size, and interfacial tension) affect the interfacial contact between cells and monoterpene dispersions. This information could render more insight into the phase mechanisms responsible for inhibition in biphasic systems.

The impact on cell physiology can change if surfactants are used to solvate monoterpene compounds before they are added. Due to their low aqueous solubility, monoterpenes are commonly administered in biological cultures via emulsifying agents, such as Tween 80 and dimethylformamide (DMF) (8, 17, 64). Because of their amphiphilic nature, surfactants and cosolvents change the interfacial properties at the oil-water interface (65, 66). The result is the formation of micelles, with monoterpene-rich interiors and watery exteriors (65–67). In a recent study, a limonene-Tween 80 solvent mixture caused membrane deterioration and upregulation of ergosterol biosynthesis in yeast (64). These authors found that exogenous ergosterol addition enhanced tolerance (64). In our study, no cosolvent was used; limonene exposure caused no upregulation of ergosterol biosynthesis (see Fig. S4 in the supplemental material) or damage to the membrane (Fig. 1). Furthermore, growth did not improve with ergosterol supplementation in this work (see Fig. S5 in the supplemental material), but we did observe changes in the dose response when Tween 80 was used as a cosolvent compared to limonene alone. At a constant limonene concentration (107 mg/liter), the limonene-Tween 80 mixture caused no growth disturbance, while limonene without Tween 80 caused growth to cease (see Fig. S6 in the supplemental material). While Tween 80 is nontoxic to yeast cells (68), there are clearly multifunctional effects at play when surfactants and toxic solvents are used simultaneously. A detailed mechanism of cosolvent effects on microorganisms is unknown. However, the introduction of cosolvents with hydrophobic compounds, such as monoterpenes, may facilitate more favorable interactions or access of micelle fluid structures with biological membranes, which has been reported for some common detergents (69). Variations in experimental conditions, such as the type of surfactant used and the surfactant concentration, may explain the differences in inhibitory concentrations and mechanistic conclusions found in most monoterpene toxicity studies. Nevertheless, the ultimate goal is to develop yeast strains that produce monoterpenes endogenously in the absence of specialized surfactants. Therefore, understanding the physiological impact of limonene alone was of particular interest in this work.

In conclusion, microbial synthesis of monoterpene products will not be viable unless the toxicity issue is solved. In order to engineer tolerant strains successfully, a greater understanding of the mechanism causing inhibition is first required. While monoterpene inhibition has long been attributed to the disruption of membrane properties (17–19), this is the first study in *S. cerevisiae* demonstrating that monoterpene toxicity is not due to membrane deterioration. Increasing membrane rigidity through changes in fatty acid content or by actively pumping monoterpene compounds from the cell (46) was not found to increase tolerance. Our results underscore the position that monoterpene inhibition is not at the molecular level (e.g., membrane interference effects) (3) and that the mechanism of action must stem from the physical interaction between an insoluble monoterpene phase and the surface of a cell. To this end, we have demonstrated here that limonene can alter the properties of yeast cell walls while triggering a compensatory transcriptional response to cell wall damage. Our data indicate chitin, a critical cell wall component, to be a primary target for limonene action, but the exact mechanism remains unclear. This study reveals that the development of monoterpene-resistant yeast strains will most likely not require alterations to the plasma membrane. Instead, the presented work suggests that strategies that focus on maintaining cell wall integrity and cell surface properties are likely to be more useful targets for strain improvement in the future.

ACKNOWLEDGMENTS

REFERENCES

1. **Keasling JD.** 2010. Microbial production of isoprenoids, p 2951–2966. *In* Timmis KN (ed), Handbook of hydrocarbon and lipid microbiology. Springer, Berlin, Germany.
2. **van der Werf M, de Bont J, Leak D.** 1997. Opportunities in microbial biotransformation of monoterpenes, p 147–177. *In* Berger R, Babel W, Blanch H, Cooney C, Enfors S, Eriksson K, Fiechter A, Klibanov A, Mattiasson B, Primrose S, Rehm H, Rogers P, Sahm H, Schugerl K, Tsao G, Venkat K, Villadsen J, von Stockar U, Wandrey C (ed), Biotechnology of aroma compounds, vol 55. Springer, Berlin, Germany.
3. **Brennan TCR, Turner CD, Krömer JO, Nielsen LK.** 2012. Alleviating monoterpene toxicity using a two-phase extractive fermentation for the bioproduction of jet fuel mixtures in *Saccharomyces cerevisiae*. Biotechnol. Bioeng. **109**:2513–2522.
4. **Harvey BG, Wright ME, Quintana RL.** 2009. High-density renewable fuels based on the selective dimerization of pinenes. Energy Fuels **24**:267–273.
5. **Ryder JA.** February 2009. Fuel composition, useful to power any equipment such as an emergency generator or internal combustion engine, which requires a fuel such as jet fuels or missile fuels, comprises limonene and farnesane. U.S. patent 7589243-B1.

40

6. **Amyris.** 2012. Azul Brazilian airlines makes successful demonstration flight with Amyris renewable jet fuel produced from sugarcane. http://www.amyris.com/NEWS/112/Azul-Brazilian-Airlines-makes-Successful-Demonstration-Flight-with-Amyris-Renewable-Jet-Fuel-Produced-from-Sugarcane.

7. **Carrau FM, Medina K, Boido E, Farina L, Gaggero C, Dellacassa E, Versini G, Henschke PA.** 2005. De novo synthesis of monoterpenes by *Saccharomyces cerevisiae* wine yeasts. FEMS Microbiol. Lett. **243**:107–115.

8. **Dunlop MJ, Dossani ZY, Szmidt HL, Chu HC, Lee TS, Keasling JD, Hadi MZ, Mukhopadhyay A.** 2011. Engineering microbial biofuel tolerance and export using efflux pumps. Mol. Syst. Biol. **7**:487.

9. **Fischer MJC, Meyer S, Claudel P, Bergdoll M, Karst F.** 2011. Metabolic engineering of monoterpene synthesis in yeast. Biotechnol. Bioeng. **108**:1883–1892.

10. **Ignea C, Cvetkovic I, Loupassaki S, Kefalas P, Johnson C, Kampranis S, Makris A.** 2011. Improving yeast strains using recyclable integration cassettes, for the production of plant terpenoids. Microb. Cell Fact. **10**:4.

11. **Renninger N, McPhee D.** April 2008. Fuel compositions including farnesane and farnesene derivatives and methods of making and using same. U.S. patent WO2008045555.

12. **Hill J, Nelson E, Tilman D, Polasky S, Tiffany D.** 2006. Environmental, economic, and energetic costs and benefits of biodiesel and ethanol biofuels. Proc. Natl. Acad. Sci. U. S. A. **103**:11206–11210.

13. **Nicolaou SA, Gaida SM, Papoutsakis ET.** 2010. A comparative view of metabolite and substrate stress and tolerance in microbial bioprocessing: from biofuels and chemicals, to biocatalysis and bioremediation. Metab. Eng. **12**:307–331.

14. **Cristani M, D'Arrigo M, Mandalari G, Castelli F, Sarpietro MG, Micieli D, Venuti V, Bisignano G, Saija A, Trombetta D.** 2007. Interaction of four monoterpenes contained in essential oils with model membranes: implications for their antibacterial activity. J. Agric. Food Chem. **55**:6300–6308.

15. **Parveen M, Hasan MK, Takahashi J, Murata Y, Kitagawa E, Kodama O, Iwahashi H.** 2004. Response of *Saccharomyces cerevisiae* to a monoterpene: evaluation of antifungal potential by DNA microarray analysis. J. Antimicrob. Chemother. **54**:46–55.

16. **Uribe S, Pena A.** 1990. Toxicity of allelopathic monoterpene suspensions on yeast dependence on droplet size. J. Chem. Ecol. **16**:1399–1408.

17. **Uribe S, Ramirez J, Pena A.** 1985. Effects of beta-pinene on yeast membrane functions. J. Bacteriol. **161**:1195–1200.

18. **Schrader J.** 2007. Microbial flavour production, p 507–574. *In* Berger RG (ed), Flavours and fragrances. Springer, Berlin, Germany.

19. **Sikkema J, de Bont J, Poolman B.** 1995. Mechanisms of membrane toxicity of hydrocarbons. Microbiol. Rev. **59**:201–222.

20. **Andrews RE, Parks LW, Spence KD.** 1980. Some effects of douglas-fir terpenes on certain microorganisms. Appl. Environ. Microbiol. **40**:301–304.

21. **León R, Fernandes P, Pinheiro HM, Cabral JMS.** 1998. Whole-cell biocatalysis in organic media. Enzyme Microb. Technol. **23**:483–500.

22. **Osborne SJ, Leaver J, Turner MK, Dunnill P.** 1990. Correlation of biocatalytic activity in an organic aqueous 2-liquid phase seystem with solvent concentration in the cell-membrane. Enzyme Microb. Technol. **12**:281–291.

23. **Sikkema J, de Bont JA, Poolman B.** 1994. Interactions of cyclic hydrocarbons with biological membranes. J. Biol. Chem. **269**:8022–8028.

24. **Schmid C, Steinbrecher R, Ziegler H.** 1992. Partition-coefficients of plant cuticles for monoterpenes. Trees Struct. Funct. **6**:32–36.

25. **Bar R.** 1987. Phase toxicity in a water-solvent two-liquid phase microbial system, p 147–154. *In* Laane C, Tramper J, Lilly MD (ed)., Studies in organic chemistry, vol 29. Biocatalysis in organic media. Elsevier Science Publishers B.V., Amsterdam, Netherlands.

26. **Huffer S, Clark ME, Ning JC, Blanch HW, Clark DS.** 2011. The role of alcohols in growth, lipid composition, and membrane fluidity of yeasts, bacteria, and archaea. Appl. Environ. Microbiol. **77**:6400–6408.

27. **Shinitzky M, Yuli I.** 1982. Lipid fluidity at the submacroscopic level: determination by fluorescence polarization. Chem. Phys. Lipids **30**:261–282.

28. **Francois JM.** 2006. A simple method for quantitative determination of polysaccharides in fungal cell walls. Nat. Protoc. **1**:2995–3000.

29. **Pringle JR.** 1991. Staining of bud scars and other cell wall chitin with Calcofluor. Methods Enzymol. **194**:732–735.

30. **Takahashi TT, Shimoi HS, Ito KI.** 2001. Identification of genes required

31. **Reich M, Liefeld T, Gould J, Lerner J, Tamayo P, Mesirov JP.** 2006. GenePattern 2.0. Nat. Genet. **38**:500–501.

32. **Smyth GK.** 2004. Linear models and empirical Bayes methods for assessing differential expression in microarray experiments. Stat. Appl. Genet. Mol. Biol. **3**:Article3.

33. **Reimand J, Kull M, Peterson H, Hansen J, Vilo J.** 2007. g:Profiler—a web-based toolset for functional profiling of gene lists from large-scale experiments. Nucleic Acids Res. **35**:W193–W200.

34. **Saeed AI, Sharov V, White J, Li J, Liang W, Bhagabati N, Braisted J, Klapa M, Currier T, Thiagarajan M, Sturn A, Snuffin M, Rezantsev A, Popov D, Ryltsov A, Kostukovich E, Borisovsky I, Liu Z, Vinsavich A, Trush V, Quackenbush J.** 2003. TM4: a free, open-source system for microarray data management and analysis. Biotechniques **34**:374–378.

35. **Ding J, Huang X, Zhang L, Zhao N, Yang D, Zhang K.** 2009. Tolerance and stress response to ethanol in the yeast *Saccharomyces cerevisiae*. Appl. Microbiol. Biotechnol. **85**:253–263.

36. **Swan TM, Watson K.** 1998. Stress tolerance in a yeast sterol auxotroph: role of ergosterol, heat shock proteins and trehalose. FEMS Microbiol. Lett. **169**:191–197.

37. **You KM, Rosenfield C-L, Knipple DC.** 2003. Ethanol tolerance in the yeast *Saccharomyces cerevisiae* is dependent on cellular oleic acid content. Appl. Environ. Microbiol. **69**:1499–1503.

38. **Perrone GG, Tan SX, Dawes IW.** 2008. Reactive oxygen species and yeast apoptosis. Biochim. Biophys. Acta Mol. Cell Res. **1783**:1354–1368.

39. **Estruch F.** 2000. Stress-controlled transcription factors, stress-induced genes and stress tolerance in budding yeast. FEMS Microbiol. Rev. **24**:469–486.

40. **Nilsson U, Bergh M, Shao LP, Karlberg AT.** 1996. Analysis of contact allergenic compounds in oxidized d-limonene. Chromatographia **42**:199–205.

41. **Hayes JD, McLellan LI.** 1999. Glutathione and glutathione-dependent enzymes represent a co-ordinately regulated defence against oxidative stress. Free Radical Res. **31**:273–300.

42. **SRC.** 12 October 2012, posting date. Physical property database. http://www.syrres.com/what-we-do/databaseforms.aspx?id=386.

43. **Kieboom J, Dennis JJ, de Bont JAM, Zylstra GJ.** 1998. Identification and molecular characterization of an efflux pump involved in *Pseudomonas putida* S12 solvent tolerance. J. Biol. Chem. **273**:85–91.

44. **Aono R, Tsukagoshi N, Yamamoto M.** 1998. Involvement of outer membrane protein TolC, a possible member of the *mar-sox* regulon, in maintenance and improvement of organic solvent tolerance of *Escherichia coli* K-12. J. Bacteriol. **180**:938–944.

45. **Bauer BE, Wolfger H, Kuchler K.** 1999. Inventory and function of yeast ABC proteins: about sex, stress, pleiotropic drug and heavy metal resistance. Biochim. Biophys. Acta Biomembr. **1461**:217–236.

46. **Hu F, Liu J, Du G, Hua Z, Zhou J, Chen J.** 2012. Key cytomembrane ABC transporters of *Saccharomyces cerevisiae* fail to improve the tolerance to *d*-limonene. Biotechnol. Lett. **34**:1505–1509.

47. **Cabib E, Roh D-H, Schmidt M, Crotti LB, Varma A.** 2001. The yeast cell wall and septum as paradigms of cell growth and morphogenesis. J. Biol. Chem. **276**:19679–19682.

48. **Lipke PN, Ovalle R.** 1998. Cell wall architecture in yeast: new structure and new challenges. J. Bacteriol. **180**:3735–3740.

49. **Haigler C, Brown R, Benziman M.** 1980. Calcofluor white ST alters the in vivo assembly of cellulose microfibrils. Science **210**:903–906.

50. **Klis FM, Boorsma A, De Groot PWJ.** 2006. Cell wall construction in *Saccharomyces cerevisiae*. Yeast **23**:185–202.

51. **Wood PJ.** 1980. Specificity in the interaction of direct dyes with polysaccharides. Carbohydr. Res. **85**:271–287.

52. **Popolo L, Vai M.** 1998. Defects in assembly of the extracellular matrix are responsible for altered morphogenesis of a *Candida albicans* phr1 mutant. J. Bacteriol. **180**:163–166.

53. **Damveld RA, vanKuyk PA, Arentshorst M, Klis FM, van den Hondel CAMJJ, Ram AFJ.** 2005. Expression of *agsA*, one of five 1,3-α-D-glucan synthase-encoding genes in *Aspergillus niger*, is induced in response to cell wall stress. Fungal Genet. Biol. **42**:165–177.

54. **Ram AFJ, Klis FM.** 2006. Identification of fungal cell wall mutants using susceptibility assays based on Calcofluor white and Congo red. Nat. Protoc. **1**:2253–2256.

55. **Elorza MV, Rico H, Sentandreu R.** 1983. Calcofluor white alters the

assembly of chitin fibrils in *Saccharomyces cerevisiae* and *Candida albicans* cells. J. Gen. Microbiol. **129**:1577–1582.

56. **Cabib E.** 2004. The septation apparatus, a chitin-requiring machine in budding yeast. Arch. Biochem. Biophys. **426**:201–207.

57. **Boorsma A, Hd. Nobel Bt. Riet Bargmann B, Brul S, Hellingwerf KJ, Klis FM.** 2004. Characterization of the transcriptional response to cell wall stress in *Saccharomyces cerevisiae*. Yeast **21**:413–427.

58. **García R, Bermejo C, Grau C, Pérez R, Rodríguez-Peña JM, Francois J, Nombela C, Arroyo J.** 2004. The global transcriptional response to transient cell wall damage in *Saccharomyces cerevisiae* and its regulation by the cell integrity signaling pathway. J. Biol. Chem. **279**:15183–15195.

59. **Levin DE.** 2011. Regulation of cell wall biogenesis in *Saccharomyces cerevisiae*: the cell wall integrity signaling pathway. Genetics **189**:1145–1175.

60. **Francesconi R, Castellari C, Comelli F.** 2001. Densities, viscosities, refractive indices, and excess molar enthalpies of methyl tert-butyl ether + components of pine resins and essential oils at 298.15 K. J. Chem. Eng. Data **46**:1520–1525.

61. **French CM, Singer N.** 1956. The conductivity of solutions in which the solvent molecule is "large." I. Solutions of tetraethylammonium picrate in some phthalate esters. J. Chem. Soc. **1956**:1424–1429.

62. **Zhang X, Chen Y, Liu J, Zhao C, Zhang H.** 2012. Investigation on the structure of water/AOT/IPM/alcohols reverse micelles by conductivity, dynamic light scattering, and small angle X-ray scattering. J. Phys. Chem. B **116**:3723–3734.

63. **Stone HA.** 1994. Dynamics of drop deformation and breakup in viscous fluids. Annu. Rev. Fluid Mech. **26**:65–102.

64. **Liu J, Zhu Y, Du G, Zhou J, Chen J.** 2013. Exogenous ergosterol protects *Saccharomyces cerevisiae* from d-limonene stress. J. Appl. Microbiol. **114**:482–491.

65. **Chandler D.** 2005. Interfaces and the driving force of hydrophobic assembly. Nature **437**:640–647.

66. **Narang AS, Delmarre D, Gao D.** 2007. Stable drug encapsulation in micelles and microemulsions. Int. J. Pharm. **345**:9–25.

67. **Garti N, Yaghmur A, Leser ME, Clement V, Watzke HJ.** 2001. Improved oil solubilization in oil/water food grade microemulsions in the presence of polyols and ethanol. J. Agric. Food Chem. **49**:2552–2562.

68. **Wei G, Li Y, Du G, Chen J.** 2003. Effect of surfactants on extracellular accumulation of glutathione by *Saccharomyces cerevisiae*. Process Biochem. **38**:1133–1138.

69. **Schreier S, Malheiros SVP, de Paula E.** 2000. Surface active drugs: self-association and interaction with membranes and surfactants. Physicochemical and biological aspects. Biochim. Biophys. Acta Biomembr. **1508**:210–234.

70. **Levin DE.** 2005. Cell wall integrity signaling in *Saccharomyces cerevisiae*. Microbiol. Mol. Biol. Rev. **69**:262–291.

Chapter 4

Evolutionary engineering improves tolerance towards replacement jet fuels in yeast

Chapter 4 is in final preparation to be submitted to the Proceedings of the National Academy of Sciences of the United States of America.

TCRB, JK and LKN designed the experiments. TCRB carried out the experiments and analysis. TCW designed the molecular engineering experiments and carried the molecular engineering experiments. BS, TCRB designed the cell wall proteomics experiment. TCRB, JK and LKN wrote the paper.

Title: Evolutionary engineering improves tolerance towards jet fuel replacements in yeast

Authors: Timothy C. R. Brennan, Thomas C. Williams, Ben Schulz, Robin Palfreyman, Jens Kromer#, Lars K. Nielsen

Abstract: Monoterpenes are liquid hydrocarbons that can serve as immediate precursors for replacement jet fuels. Microbial production of next-generation fuels, including monoterpenes and other isoprenoids, continues to be a major focus of R&D efforts worldwide. However, monoterpenes are toxic to microorganisms, presenting a major challenge for microbial synthesis. Here we subjected the wild-type (WT) yeast strain (S288C) to approximately 200 generations of limonene-challenged laboratory evolution. Eight strains were isolated across the evolutionary time course and whole-genome resequencing revealed two key loci targets for engineering tolerance (*PDR3, TBC3*). Genomic reconstruction in the ancestral strain recovered the evolved phenotype improving limonene fitness by nine-fold. The data show that the limonene-tolerant phenotype is exclusively caused by a single point mutation in *TCB3*, which results in a truncated version of $Tcb3p^{1-989}$ (tTcb3p). The tTcb3p strain also showed tolerance improvements (11- and 8-fold) towards two other monoterpenes (β-pinene and myrcene) and a 4-fold improvement for the biojet fuel blend AMJ-700t (10% cymene, 50% limonene, 40% farnesene). To date, these are the highest reported concentrations of monoterpenes tolerated by *Saccharomyces cerevisiae*, a major catalyst in the biotech industry. This is a key initial step towards the microbial synthesis of monoterpene-derived jet fuels and towards revealing new biological functions for tricalbin proteins (*TCB1/2/3*). Collectively, elevated tolerance due to tTcb3p can now be used to pursue the microbial production or catalysis of a class of compounds — C_{10} alkenes — that due to their inherent toxicity, have halted research efforts for decades.

Introduction

The first synthetic aviation fuel came from extracting liquid oil from coal. The German chemist Freidrich Bergius, developed this technique in 1913 and it later provided nearly all of Germany's aviation gasoline in World War II [1]. Shortly after WWII, as energy security

concerns escalated in the origins of the Cold War, the U.S. Interior Department called for another Manhattan project to pursue synthetic fuel research based on the Bergius process [2]. After four years of pilot-scale demonstration it was estimated that synthetic fuels from shale would cost nearly three and a half times that of conventional gasoline [2]. In 1953 the program was terminated. In their final report, the National Petroleum Council concluded that further advances in technology were absolutely required in order for synthetic fuels to compete economically with petroleum products [3]. Over half a century later, we find ourselves faced with the same problem: how do we make alternative fuels affordable?

In the last decade, engineering microbial cell factories that convert renewable biomass into replacement liquid transportation fuels has gained global attention as a route to mitigate environmental and energy concerns [4, 5]. Producing more than 60 million tons of beer and 30 million tons of wine annually, *S. cerevisiae* is the industries oldest and most widely used biocatalysts today [6]. The products that can be synthesized by engineered microbes, including baker's yeast, are rapidly changing [7-12]. The revolution in modern synthetic and systems biology has equipped researchers with numerous tools (e.g., omics technologies) to exploit the metabolic capabilities of microorganisms more than ever [13-16]. As a result, new petroleum-compatible hydrocarbons (e.g., farnesane [17], bisbolane [18], limonane [19]) have emerged, as researchers are no longer limited to targeting traditional fermentation products such as bioethanol.

Monoterpenes are a class of isoprenoids that share a common ten-carbon (C_{10}) backbone derived from two five-carbon (C_5) isoprene units [20]. Traditionally used in the flavour and fragrance industry, monoterpenes, such as *d*-limonene, are now being sought after as potential chemopreventive agents [21, 22] and precursors for light end components of "drop-in" jet fuels [23, 24]. Due to their structural complexity, chemical synthesis and extraction of isoprenoids from biological tissues suffer from low yields, impurities and high-cost [25]. Microbial synthesis offers an alternative route [8], with the ability to convert monomeric sugars into a variety of enantiomerically pure monoterpene products [26, 27]. Limonane, is a monocyclic paraffin that matches and has improved physicochemical properties (e.g., < -70°C freezing point) compared to traditional kerosene-based aviation fuel (Jet-A) [28]. In a demonstration flight in June 2012, Amyris, Inc. showed that their biojet fuel (AMJ-700) met engine performance requirements while requiring no aircraft modifications [29]. In addition to meeting engine and fuel specifications, AMJ-700, which contains a mixture of 50% limonane (C_{10} cycloparaffin), 10% cymene (C_{10} aromatic) and 40% farnesane (C_{15}

branched chain paraffin), could also reduce greenhouse-gas emissions by 82% compared to traditional jet fuels [30].

Monocyclic paraffins, such as limonane, are critical for meeting the strict performance requirements for Jet-A aviation fuel [28]. Limonane can be produced directly from a range of biologically-synthesized monoterpene precursors (e.g., limonene, terpinene, terpinolene, pinene) after a single hydrogenation step, which is required to reduce monoterpenes double C-C bonds [28]. Although synthesis of monoterpenes in yeast is still in the developmental stages [28, 31, 32], farnesene (a C_{15} sesquiterpene), uses the same precursors in the cell and is currently produced for diesel markets [17], indicating the potential for commercial-scale jet fuel production. The limitation is, however, that monoterpenes are highly toxic to host engineering platforms (e.g., in *S. cerevisiae*, limonene stops growth at 60 mg/l [19]). Maximizing titers is an absolute requirement for producing biofuels that can compete economically with traditional petrochemicals [33]. End product inhibition negatively impacts production parameters such as yield, titer and rate. Therefore, toxicity is the most critical problem facing microbial monoterpene synthesis.

The antimicrobial action of monoterpenes remains poorly understood. Without detailed knowledge of the specific mechanism(s) responsible for monoterpene inhibition, rational forward engineering approaches are limited [34]. In the last decade, adaptive laboratory evolution (also termed 'reverse engineering') has proven to be a successful technique in the field of microbial biotechnology [35, 36] [reviewed in [37, 38]]. This non-targeted approach builds a desired phenotype from the bottom-up [35], offering advantages over forward engineering in that no extensive knowledge of inhibition, biochemical pathways, gene regulation or complex physiological responses are required in the initial plan [34]. Once a tolerant strain has been isolated, today's high throughput technologies (for example genome resequencing and ome analysis) can then be used to help understand the molecular basis for the improved phenotype [14, 38, 39]. Coupling reverse and foreword engineering methods has been successful in the development and characterization of variety of industrially important microorganisms and products [37, 40, 41]. However, these efforts have primarily focused on alcohol [40, 42, 43] and organic acid [44, 45] tolerance. Unlike these compounds, which have been studied extensively in both bacteria and yeast [46], monoterpenes are an emerging class of products that elicit unknown modes of inhibition and stress to microorganisms. Identifying resistive mechanism(s) is an essential

prerequisite for rationally engineering strains capable of producing monoterpene products beyond their inhibitory limits.

Here we used evolutionary engineering to isolate a superior yeast phenotype, with the objective to gain insight into the mechanism(s) behind monoterpene toxicity and to identify genetic targets for engineering tolerance. The evolved strains are able to withstand several-fold higher concentrations of toxic monoterpenes compared to the un-evolved strain. Whole-genome resequencing identified a set of key mutations and these loci targets (*PDR3* and *TCB3*) were reconstructed in the WT. The evolved tolerant phenotype was successfully recovered upon the introduction of these mutations into the parent strain. These beneficial mutations can now assist strain engineers in the development of robust microorganisms with a greater capacity to tolerate monoterpenes during fermentation or biocatalysis in *S. cerevisiae*

Materials and Methods

Strains, media and chemicals

The *Saccharomyces cerevisiae* strain S288C (*MAT_ SUC2 gal2 mal mel flo1 flo8-1 hap1*) was provided by the Australian Wine Research Institute (AWRI), Adelaide, South Australia, Australia. Analytical-grade quality (e.g., *d*-limonene (93%)) was purchased from Sigma-Aldrich for all solvents tested. Unless otherwise noted, synthetic media (CBS) consisted of 2 g/l sucrose, 5 g/l $(NH_4)_2 SO_4$, 3 g/l KH_2PO_4, 0.5 g/l $MgSO_4 \cdot 7H_2O$, and vitamins and trace metals described in [19]. YPD solid medium consisted of 10 g/l yeast extract, 10 g/l polypeptone and 20 g/l sucrose. LM is YPD medium containing 300 mg/l limonene. Limonene is insoluble in water at the described concentration so a WT plate was used as a control and we assumed the system was well mixed on solid plates.

Evolution by serial batch passages

Adaptive evolution was employed using serial batch passaging during increased limonene exposure. The parent strain (S288C) was transferred from a glycerol stock stored at -80°C and grown on solid YPD medium at 30ºC. A single isolate of the parent strain was used to inoculate 10 ml of CBS media and this pre-culture was grown overnight until the mid-exponential growth phase. The appropriate volume from the pre-culture was used to

inoculate 22 ml of CBS media to a target $OD_{660} = 0.2$. The initial volume of limonene added to the culture at inoculation was 1.0 µl (38 mg/l). Limonene was directly added to the culture aseptically using a 10 µL glass-syringe (Gerstel, Mulheim, Germany) immediately after inoculation. The culture was then incubated at 30°C at 200 rpm (Orbit 25 mm, Multitron, Infors, Bottmingen, Switzerland) in 250 ml Teflon™-lined screw-top baffled shake flasks until the cell density reached mid-exponential phase (OD_{660} ~ 1-2, corresponding to approximately 4 doubling times) before they were transferred. For the next round, the appropriate volume of the previous limonene-challenged culture was used to inoculate fresh medium (22 ml) to a target $OD_{660} = 0.2$. After several transfers (2-4) at a given limonene load, the amount of limonene was increased (between 0.2 – 0.5 µl of additional limonene). After 52 daily sequential passages the final limonene load was 5.8 µl (222 mg/l). After each passage, 0.5 ml of culture was added to 0.5 ml of 40% v/v glycerol solution and the samples were stored at -80°C.

Screening mutants

Mutants were first screened by streaking frozen glycerol stocks out onto solid LM medium plates. The largest single colonies (8-12) were then subjected to a second competitive growth screen in liquid CBS medium containing 95 mg/l of limonene. Isolates were pre-cultured in CBS medium (10 ml) overnight at 30ºC (200 rpm) and the appropriate volume of the pre-culture was used to inoculate 22 ml of CBS to an $OD_{660} = 0.15$ in 250 ml Teflon™-sealed screw-top shake flasks. Then 2.5 µl of limonene was added immediately after inoculation and growth was monitored for 12 h using a Libra S4 spectrophotometer at 660 nm. The mutant with the highest specific growth rate was chosen for tolerance testing.

Tolerance test

The evolved and un-evolved strains were evaluated for resistance to each toxic compound as described in [19]. Briefly, cultures were grown until mid-exponential phase (~ $OD_{660} = 1.0$) and then dosed with varying amounts of solvent. The optical density was evaluated for the ensuing 6 h. The minimum inhibitory concentration (MIC) is defined as the amount of solvent required to inhibit the specific growth rate by approximately 50% compared to that of the control strain with no solvent present. In some cases, 3.6 µl (138 mg/l) of limonene was added to the innoculum (22 ml at $OD_{660} = 0.2$) and growth was monitored as described above. The ratio of the OD_{660} at 12 and 0 h was used as a relative fitness metric

for solvent tolerance as described in [40]. CBS media containing 5 g/l sucrose was used in all tolerance tests. All tolerance tests were performed in biological triplicate for each compound and strain.

Solvent recovery and cell viability

After 12 h of limonene exposure, 1 ml of dodecane was added to the culture, vortexed for 1 min and the mixture was transferred to a sterile 50 ml falcon tube. The suspension was then harvested for 5 min (5,000 rcf) and the top dodecane-solvent layer (1 ml) was transferred to a glass vial and stored at -20°C for later analysis. To calculate recovery, the ratio of the final solvent amount (determined by GC-MS) at the end of 12 h culture, was compared to the solvent amount recovered under identical conditions but in the absence of cells. All data was performed in triplicate.

DNA isolation

All strains were isolated according to [47] with the following modifications. A total of 5 ml of culture was harvested at mid-log (OD ~ 3) (16,000 rcf, 25°C), washed twice with distilled water, pelleted, and resuspended in 800 µl of lysis buffer (1% SDS, 50 mM EDTA, 0.1 M TrisHCl, pH 7.5)). The suspension was then transferred to FastPrep screw cap tubes containing 1 g of 0.5 µm acid washed beads and 100 µl of 5 M NaCl. To lyse the cells, four cycles of 30 s with 1 min on ice in between cycles was carried out in a mechanical bead beater (John Morris Scientific, Pty Ltd.). The suspension was then harvested (16,000 rcf, 4°C) for 15 min, and the resulting clear liquid (roughly 800 µl) was transferred to new 1.5 ml extra-clean tubes (Mo Bio). 777 µl of chloroform isoamylalcohol (24:1) was then added and incubated at 25°C for 30 min with gentle rocking. The mixture was then pelleted for 15 min (16, 000 rcf, 25°C) and the top, aqueous layer was transferred to a new extra-clean tube and mixed with 70% v/v isopropanol and centrifuged (16,000 rcf, 25°C) for 6 min. The isopropanol suspension was decanted and the pellet was resuspended in 70% ethanol. The ethanol suspension was centrifuged (16,000 rcf, 25°C) for 6 min and the pellet was allowed to dry for 45 min. The pellet was then resuspended in 50 µl of DNA and RNA-free water containing 100 µg/ml RNAse A and incubated at room temperature for 30 min.

Genome sequencing

Paired-end (100 bp) genomic DNA libraries were generated using TruSeq DNA Sample Preparation Kits according to the manufactures instructions (Illumina, San Diego, CA, USA). Whole genome re-sequencing was performed by the Queensland Centre for Medical Genomics (Institute for Molecular Bioscience, University of Queensland, Australia) using an illumina HiSEQ 2500 system (HiSEQ Control Software 2.0.5, RTA 1.17.20) following the standard rapid sequencing workflow of cluster generation and sequencing by synthesis. Initially libraries were loaded onto an illumina cBot instrument for template hybridization and initial extension steps using the TruSEQ Rapid Duo cBot Sample Loading Kit (cat# CT-402-4001). Flowcells were then moved to the HiSEQ 2500 instrument to complete cluster generation and sequencing using TruSeq Rapid Cluster Kit - Paired-End (cat# PE-402-4001) and TruSeq Rapid SBS Kits – 200 Cycle (cat# FC-402-4001) following the manufacturer's publications. Samples were loaded at a concentration of 6pM and a total of 209 cycles of sequencing were completed consisting of 2x 101bp reads and a single 7bp index sequence.

For mutation analysis, the default settings in Bowtie2 [48] were used in the alignment. The input paired end reads (101 bp) were trimmed based on quality (3 bases from the start and 23 bases from the end) to produce 75 bp reads for each sample. The results from the mapping were used to identify single nucleotide polymorphisms (SNPs) and insertions and deletions (INDELS) between the mutant and reference strain and alignments were viewed using the Integrative Genomics Viewer (IGV) software [49]. SNPs and INDELS were filtered using a Phred-like consensus quality >30 and for SNPs, the coverage depth was ≥ 10. For INDELS, some INDELS were filtered out if the number of reads with INDELS was less than the number of reads without INDELS. Annotation and prediction of the effects caused by the mutations was carried out using the program SnpEff [50]. The data was run against the ensemble build (EF4.68) of the S288C reference genome and used as input in the SnpEff database.

Genomic reconstruction

Introduction of the mutations, *PDR3* (Q763L) and *TCB3* (frame shift at 989), into the background strain (WT) was carried out using the recyclable dominant marker cassette *amdSYM* described in [51]. The details of the construction and primers used can be found in the supplemental material. A gain-of-function assay was performed for all reconstructed strains. As described above, the relative fitness towards limonene, cymene, β-pinene,

myrcene and AMJ-700t was investigated for the WT, evolved (TB516) and reconstructed strains.

Fluorochrome staining and flow cytometry

For WT and single mutant (*tcb3-989*) strains, cell viability and cell wall damage were assessed using the vital staining dye propidium iodide (PI) and cell wall binding dye calcofluor white (CFW). Briefly, cells were treated with an inhibitory amount of limonene (115 mg/l) during midlog growth phase (20 g/l CBS media). After 2 h of treatment, cell viability (described in [19]) and cell wall staining (described in [52]) were tested in biological triplicate.

Transcriptomics

Total RNA was isolated from single mutant (*tcb3-989*) cultures during mid-exponential growth phase. For control (no limonene) and limonene challenged cultures (107 mg/l) approximately 10 ml of culture was quickly pelleted (17,572 rcf x *g*) for 2 min at 4°C and then immediately resuspended in 2 ml of RNA*later*® solution (Life Technologies, Carlsbad, CA) and stored at 4°C. The RiboPure-Yeast kit (Ambion, Life Technologies, Carlsbad, CA) was used for total RNA extraction according to manufacturer's instructions except bead beating was used to lyse the cells described in [52]. The RNA quality was assessed using an Agilent 2100 Bioanalyzer and RNA 6000 Nano kit according to manufacturer's methods (Agilent, Santa Clara, CA). For the microarrays (Affymetrix yeast genome 2.0), sample labeling and hybridization was performed at the Ramaciotti Centre for Gene Function Analysis (University of New South Wales, Sydney, Australia). Analysis of differentially expressed genes and gene set analysis (GSA) was carried out in R using the default values in Piano [53]. All data was performed in biological triplicate.

Cell wall proteomics

The total cell wall extracts were isolated for WT and single mutant (*tcb3-989*) cultures during mid-exponential growth phase. Cultures were inoculated to a starting $OD_{660} = 0.1$ in 22 ml of CBS (5 g/l sucrose) and allowed to grow until $OD_{660} = 1.0$ in the absence and presence of limonene challenge (107 mg/l). Approximately 20 ml of culture was pelleted (4,025 X g for 5 min at room temperature), washed with sterile water, snap frozen and

stored at -80°C. Cell wall protein extraction followed the method described in [54]. Briefly, yeast cells were lysed with a bead beater, insoluble cell wall material was stringently washed, N-glycans were released with EndoH and deglycosylated proteins covalently linked to the cell wall polysaccharide were digested with trypsin. Peptides were desalted with C18 ZipTips (Millipore) and detected by LC-ESI-MS/MS with a Prominence nanoLC system (Shimadzu) and TripleTof 5600 mass spectrometer with a Nanospray III interface (AB SCIEX). For information dependent acquisition (IDA), analyses were performed as described (Bailey et al 2012 J Prot Res). Identical LC conditions were used for SWATH-MS, with an MS-TOF scan from an *m/z* of 350-1800 for 0.05 s followed by high sensitivity information independent acquisition with 26 *m/z* isolation windows with 1 *m/z* window overlap each for 0.1 s across an *m/z* range of 400-1250. Collision energy was automatically assigned by the Analyst software (AB SCIEX) based on *m/z* window ranges. Proteins were identified from IDA data using ProteinPilot (AB SCIEX) as described (Bailey et al 2012 J Prot Res). False discovery rate analysis using ProteinPilot was performed on all searches. Peptides identified with greater than 99 % confidence and with a local false discovery rate of less than 1 % were included for further analysis. *S. cerevisiae* cell wall proteins identified in this discovery data were used as the spectral library for analysis of SWATH MS/MS data using the SWATH processing script within PeakView 1.2 (AB SCIEX). Fragment ion peak area was used for quantification. The software package MSstats [55] was used for statistical analysis in R. Statistical significance cutoff was set at *p* < 0.05. All data was performed in biological triplicate.

Results

Evolved mutants show improved tolerance towards limonene

Serial batch passaging was used to isolate limonene-tolerant yeast strains. The WT strain, S288C, underwent 52 daily sequential transfers under limonene stress. The limonene load increased from 38 mg/l to 222 mg/l. Tolerant strains were isolated and tested for limonene tolerance at different time points during the adaptive evolution process. Four strains were isolated between 80-190 generations and 4 strains were isolated at 200 generations. Two tests were used to demonstrate the improvement in fitness. The MIC and relative fitness were measured for each strain and compared to the WT [Fig 1 and Table 1 (MIC) and Fig 2 (relative fitness)]. All of the evolved strains showed at least a 1.9-fold improvement in the

MIC (Table 1) and at least a 4-fold improvement in the relative fitness for limonene (Fig 2). The maximum relative fitness score (10.9 ± 1.6) was achieved at 120 generations (strain TB302) and did not significantly improve for later generations (160-200 in Fig 2). For all strains and all tolerance tests, cell viability remained above 95% after 12 h of fermentation (data not shown). These results show that adaptive evolution employing serial batch transfer under constant limonene challenge was successful for isolating limonene-tolerant phenotypes.

In addition, in order to rule out whether or not the evolved strains were metabolizing or converting limonene to undesirable products internally, we recovered limonene after the fermentation and analyzed it via GC-MS. For all of the evolved and WT strains, all of the limonene was recovered and no side products were detected (Table S1). This demonstrates that no significant loss or biocatalytic transformation occurred during fermentation.

Identification of key mutations by whole-genome sequencing

Whole-genome resequencing was used to identify mutations in the eight isolated strains and their genomes were compared with that of the parent strain, S288C. A summary of the sequencing results are listed in Table S1 and the key mutations for each strain are listed in Table 1. Both high quality mapping (≥ 98%) and coverage (≥ 100x) of the genome sequences were achieved for the evolved strains. After filtering, approximately 30-40 total mutations were found per strain (Table S1). Roughly 2-10 SNPs were identified for the evolved mutants and several of them were found in coding regions. The rest of the mutations were INDELs and the majority of these were in non-coding regions (Table S1). The key mutations are listed in Table 1 along with the relative fitness scores in Fig 2. At 84 generations (strain TB21 in Fig 2), a single SNP in the *PDR3* gene showed a 2.7-fold improvement in limonene fitness. A mutation in transcriptional activator of the pleiotropic drug resistance network, *PDR3*, was found in every subsequent strain after 83 generations (Fig 2). Interestingly, the location of the SNP changed across the evolutionary time course. At 84 generations (strain TB21) the SNP was located at Q962F, at 160 (TB 405) it was located at Q763L and at 188 (TB478) the SNP was at G948S and then back to Q763L for all four strains isolated at 200 generations (Table 1). We chose *PDR3* (Q763L) as a target for engineering because this SNP was present in 6/7 mutants that achieved the maximum fitness score (~ 10 in Fig 2).

The second mutation and gene of interest was *TCB3*. Three tricalbin (calcium and lipid binding domains) proteins exist in yeast, which are encoded by genes *TCB1,-2,-3*. Two of these genes (*TCB2, TCB3)* were found to be mutated in this study. *TCB2* was mutated in one strain, along with *PDR3*, at 120 generations. This strain (TB302) achieved the maximum relative fitness (score of ~ 10) harboring only these two mutations (Fig 2). A mutation in *TCB3* (frame shift at amino acid position 989), however, was found in the six subsequent strains, all of which resulted in maximum fitness scores (Fig 2). Therefore *TCB3*, rather than *TCB2*, was chosen as a target for engineering.

Genomic reconstruction of the limonene-tolerant phenotype

We next constructed single- and double- mutations in the WT for *PDR3* (Q763L) and *TCB3* (frame shift 989) genes and investigated their relative fitness in a gain-of-function assay. The single base change in *pdr3-763* showed no significant ($p < 0.05$) improvement in fitness compared to the WT (Fig 3). The frame shift mutation in *tcb3-989*, however, increased limonene fitness by 9-fold and showed no statistical difference in fitness compared to the evolved strain (Fig 3). This data revealed that the mutation *TCB3* was the major contributor to limonene tolerance. The double mutant, *pdr3-763* and *tcb3-989*, resulted in a relative fitness score of 11.5 ± 0.5, which is also statistically ($p < 0.05$) not significant compared to the fitness score achieved by the evolved mutants (Fig 3). In addition, because the mutation in *TCB3* caused a truncated version of Tcb3p, we questioned whether this mutation resulted in a nonfunctional protein. To test this, we used a non-functional version of *TCB3* where the ORF was replaced by the *amdSYM* marker in the single mutant strain *tcb3-989*. The knock-out *TCB3* strain showed no resistance to limonene and matched that of the WT fitness ($\Delta tcb3$ in Fig 3). This clearly demonstrates that the evolved Tcb3p is indeed a functional protein and that the limonene-tolerant phenotype is exclusively caused by this single mutation.

It was recently demonstrated that a truncated version of Tcb3p, containing 491amino acids, can co-localize in the perinuclear endoplasmic reticulum (nER) and the cortical ER (cER), whereas the full Tcb3p protein resides exclusively in the cER [56]. We questioned if limonene resistance was associated with this dual localization property. Shown in Fig 3., a similarly truncated version of Tcb3p$^{1-531}$ resulted in limonene tolerance. While the exact protein length shown here is not the same (531 vs. 491) as described by Manford et al. [56],

this data strongly indicates that limonene resistance is linked to Tcb3p's ability to reside in the perinuclear ER.

Changes to the cell wall transcriptome, proteome and cell wall integrity

A recent study showed that limonene can damage the cell wall [52]. We questioned if the mutated Tcb3p protein caused global regulatory and cell wall protein composition changes during limonene stress. The total number of differentially expressed genes (upregulated = 24, downregulated = 5) was substantially lower for mutant cells compared to the WT during limonene stress (Table S3). This is most likely due to the large number of regulated genes associated with growth defects in the WT [52]. The mutant showed very small perturbations to growth when challenged with limonene and thus the smaller gene list was not surprising (Fig. S2). Roughly 30% of the upregulated gene list (Table S3), however, was associated with cell wall maintenance. Several genes involved in iron ion homeostasis were also upregulated (*SIT1, HMX1, ARN1, FRE5, TIS11*), this response was similarly observed for WT treated cells [52].

We were particularly interested in the impact tTcb3p had on cell wall integrity regulation and cell wall protein abundance during limonene shock. Shown in Fig 4, the CWI signalling pathway, which was highly upregulated in the WT [52], was not induced in mutant cells. Limonene stress induced *ECL1*, *SMP1*, *TIR2*, and *YPL277C* in the mutant but not in the WT and only three upregulated genes were shared between both strains (*YGP1*, *FIT2*, *FIT3*). Differences between the cell wall protein profiles were also observed. For untreated cells, Ygp1p was the only protein induced in the mutant compared to the WT (Table S3). The cell wall proteins Plb1p, Plb2p, Ecm33p, Tos1p, Cis3p and Uth1p were found to be lower in abundance in the mutant vs. the WT (Table S3). During limonene challenge, cell wall proteins Pbl2p, Cis3p, Yps7p, and Ccw14p were induced in the mutant but absent in the WT. Gas3p was the only common regulated cell wall protein found (Fig 4). Taken together, these data demonstrate that both the *TCB3* mutation and limonene affect protein secretion or cell wall biosynthesis, but in different ways. The mechanistic understanding of this, however, is still unresolved.

We next wanted to test if these different regulatory responses resulted in changes in cell wall integrity. CFW was used to test if limonene-treated cells were hypersensitive to the cell wall binding probe. Cells with higher MFI showed higher sensitivity and shift in

fluorescence vs. non-damaged cells (Fig 5). Shown in Fig 5 (b and c), ~ 60% of WT cells showed substantial cell wall damage after limonene treatment. This was a ten-fold increase in number of damaged cells compared to the untreated control (6% in Fig 5b). Alternatively, the mutant cells, harboring the single mutation in Tcb3p, showed a much smaller change in sensitivity to CFW after limonene treatment [approximately two-fold increase in number of cells damaged (24% vs. 11%, Fig 5e and f)]. These results demonstrate that the tTcb3p protein has the ability to preserve cell wall integrity during limonene treatment.

Tolerance towards other terpenes

Finally, we investigated if the improved phenotype could be applied to solvents other than limonene. The single mutation in *TCB3* (*tcb3-989*) resulted in substantial increases in fitness towards β-pinene and myrcene compared to the WT (11- and 8-fold in Fig 6). These data matched or improved the fitness compared to the evolved strain (TB516 in Fig 6). The reconstructed mutant showed no fitness increase for the aromatic monoterpene cymene. In addition, both evolved and reconstructed strains showed at least a 4-fold improvement in fitness towards the biojet fuel blend AMJ-700t (Fig 6). AMJ-700t contains by volume 50% limonene, 10% cymene and 40% farnesene. This fuel blend is different than AMJ-700 in that contains the olefin precursors (cymene, limonene and farnesene) that are produced via yeast fermentation. In order to be used as "drop-in" jet fuels, limonene and farnesene are chemically processed into the paraffins limonane and farnesane (termed AMJ-700) [28]. Taken together, this data demonstrates that by introducing the single mutation in *TCB3* described here, one can achieve increased resistance to a range of monoterpenes and the biojet fuel precursor blend AMJ-700t.

Discussion

Product toxicity is the major limitation for the fermentative production of monoterpenes in yeast. In an effort to alleviate monoterpene toxicity in *S. cerevisiae*, rational forward engineering strategies – involving pumping monoterpene products, such as limonene, out of the cellular membrane – have failed [57]. This result highlights one of the limitations behind forward engineering methods. In order to solve problems successfully, the problem itself needs to be initially well defined. Monoterpene toxicity in microorganisms is poorly understood. Monoterpene inhibition in yeast has long been attributed to membrane

interference due to its lipophilicity (log P = 4.5). However, recent reports demonstrate that limonene has no deleterious effects to membrane integrity or composition and were described to cause defects in the cell wall [52]. These differences may be due to the use of polar aprotic cosolvents (e.g., Tween 80 or dimethyl formamide (DMF)), which are commonly used to solvate monoterpenes before administering them into cultures [52]. Nevertheless, alternative strategies—that do not rely on an initial mechanistic understanding of inhibition—are required for strain improvement.

In this study, we used evolutionary engineering to isolate resistant yeast phenotypes. Adaptive evolution employing serial batch passaging resulted in strains with improved fitness towards limonene (Fig 2). Genome resequencing across the evolutionary time course allowed for a spatiotemporal representation of the environmentally selected mutations. The mutations in the transcription factor *PDR3* were in every evolved strain (Fig 2). Interestingly, the SNP location changed during evolution (Table 1). The fact that *PDR3* was mutated in three separate locations during evolution lends the suggestion that this activator was important to resistance. However, given the evidence that overexpression of ABC transports failed to improve limonene tolerance [57], we did not expect *PDR3* to be a major player. This was indeed the case, genomic reconstruction of the Q763L mutation in the WT showed no fitness improvement (Fig. 3).

TCB3 was mutated in all of the evolved strains with maximum fitness scores (Fig 2). A mutation in *TCB2* was also found early on (120 generations, strain TB302 in Fig 2.). By exclusion, the fact that the mutation in *PDR3* (Q763L) resulted in no fitness improvement means that the *TCB2* mutation was the sole contributor to tolerance in strain TB302, which achieved the maximum fitness score (Fig. 2). This suggests that the tricalbin [TRI (three) CA (calcium) L (lipid) BIN (binding)] [58] proteins Tcb1/2/3p play an important role in limonene resistance. We chose the mutation in *TCB3*, rather than *TCB2*, because it was found in the majority of the maximum evolved strains. Genomic reconstruction of *tcb3-989* in the WT revealed that the limonene resistant phenotype was exclusively caused by this single point mutation. The correlation of a genotype to phenotype is a complex problem [59]. In budding yeast, no other report has ever described a single point mutation that confers tolerance towards next-generation biofuels.

The question that remained was simple. How did tTcb3p relieve toxicity during limonene treatment and what else could we learn about the native Tcb3p function? We postulated

that limonene was interfering with ER inheritance at the bud site through chitin decrystallization and that the unique ability of tTcb3p to reside in the nER enabled cells to overcome this. Inheritance of the nER and cER have drastically different fates during the budding process [60]. For the cER to be successfully inherited into the daughter cell, yeast use actin to move cER tublars along the major axis of the mother-bud axis [60, 61]. The tricalbins (Tcb1/2/3) and other tether proteins (Ist2p) that exclusively localize to cER, are unable to diffuse naturally across the diffusion barrier caused by the septum ring at the mother-bud neck [56, 62]. Therefore, mRNAs encoding for Tcb1/2/3 and Ist2 have to be transported as cargo via actin cables by myosin motor proteins such as Myo4p and She3p [60, 61]. Alternatively, inheritance of the nER takes place during mitosis and does not require actin but relies on the mitotic spindle to push the nER into the bud [60]. Because the mutation at *tcb3-989* enables tTcb3p to reside in the nuclear ER, pre-existing tTcb3p can be inherited directly from the mother cell. This allows tTcb3p to initially establish the cER in the newly formed bud without having to be transplanted by actin via cER inheritance. This mechanism would be in concert with a similar ER-PM tethering protein Scs2p, which resides in both the nER and cER, and is able to establish the cER in the newly formed bud in absence of the two other ER-PM tethering proteins (double mutant Δist2, Δtcb1/2/3) [56]. While we do show that limonene can disrupt cell wall chitin, future work is required to show the tTcb3p changes ER morphology and inheritance during limonene stress.

Conclusion

Solving the toxicity issue is key to the viable production of monoterpene-derived bioaviation fuels. Limonene toxicity in yeast is poorly understood and previous forward engineering approaches (e.g., transporters) have failed to improve resistance. This work used evolution engineering to identify genetic targets for engineering limonene tolerance in yeast. This study revealed a novel genetic mutation to confer limonene resistance in the truncation of the tricalbin protein Tcb3p. We showed that this mutation can rescue cells from cell wall damage during limonene challenge but the exact mechanism remains unclear. This may be due to the ability of tTcb3p to colocalize to the nER and the cER may be important in ER inheritance during limonene exposure. This is a key step towards the development of solvenogenic yeast strains with a greater capacity to tolerate toxic olefins. This study will hopefully aid biofuel strain engineers and molecular biologists in revealing new funcitons of tricalbins in the future.

Tables

Table 1. Summary of limonene MICs and mutations for evolved strains

Strain	Gen	MIC[a] (mg/l)	FC[b]	Mutation	Gene	Function
WT	0	69	-	-	-	-
TB21	84	130	1.9	SNP (L962F)	*PDR3*	Transcriptional activator of the pleiotropic drug resistance network
TB302	120	130	1.9	SNP (Q763L)	*PDR3*	See above
				INDEL (frame shift 316)	*TCB2*	ER protein located in the mother and daughter bud, involved in ER-plasma membrane tethering
TB405	160	122	1.8	SNP (Q763L)	*PDR3*	See above
				INDEL (frame shift 989)	*TCB3*	ER protein located in the mother and daughter bud, involved in ER-plasma membrane tethering
				INDEL (frame shift 192) SNP (Q192G)	*TSA1*	Thioredoxin peroxidase
				SNP (D380H)	*UBP11*	Ubiquitin-specific protease
TB478	188	150	2.1	SNP (G948S)	*PDR3*	See above

				SNP (nonsense Q1197*)	TCB3	See above
				SNP (P790T)	ARO80	Zinc finger transcriptional activator of aromatic amino acid catabolic genes
				SNP (E718D)	CPA2	Large subunit of carbamoyl phosphate synthetase, which catalyzes a step in the synthesis of citrulline, an arginine precursor
				SNP (P195L)	DID4	Protein of the ESCRT-III complex, required for sorting of integral membrane proteins into lumenal vesicles of multivesicular bodies, and for delivery of newly synthesized vacuolar enzymes to the vacuole, involved in endocytosis
TB51 1	200	138	2.0	SNP (Q763L)	PDR3	See above
				INDEL (frame shift 989)	TCB3	See above
				INDEL (frame shift 192), SNP (Q192G)	TSA1	See above
				SNP (W580S)	KSP1	Serine/threonine protein kinase
				SNP (nonsense Q1014*)	PSE1	Karyopherin/importin that interacts with the nuclear pore complex
				SNP (L84S)	RPL30	Ribosomal 60S subunit protein
TB51 6	200	138	2.0	SNP (Q763L)	PDR3	See above
				INDEL (frame	TCB3	See above

				shift 989)		
				INDEL, SNP (Q192G)	*TSA1*	See above
				SNP (R159T)	*CDC34*	Ubiquitin-conjugating enzyme, regulates cell cycle progression by targeting key substrates for degradation
TB517	200	145	2.1	SNP (Q763L)	*PDR3*	See above
				INDEL (frame shift 989)	*TCB3*	See above
				SNP (nonsense Q1014*)	*PSE1*	See above
				SNP (L84S)	*RPL30*	See above
TB519	200	138	2.0	SNP (Q763L)	*PDR3*	See above
				INDEL (frame shift 989)	*TCB3*	See above
				SNP (G826R)	*SIP3*	Transcription cofactor, acts through interaction with DNA-bound Snf1p
				SNP (L127F)	*YMR102C*	Protein of unknown function

[a] The minimum inhibitory concentration (MIC) is defined as the amount of limonene required to inhibit the specific growth rate by approximately 50% compared to growth rate with no solvent present for each strain.

[b] Fold change (FC) is the ratio of the MIC for the evolved and WT strain.

Figures
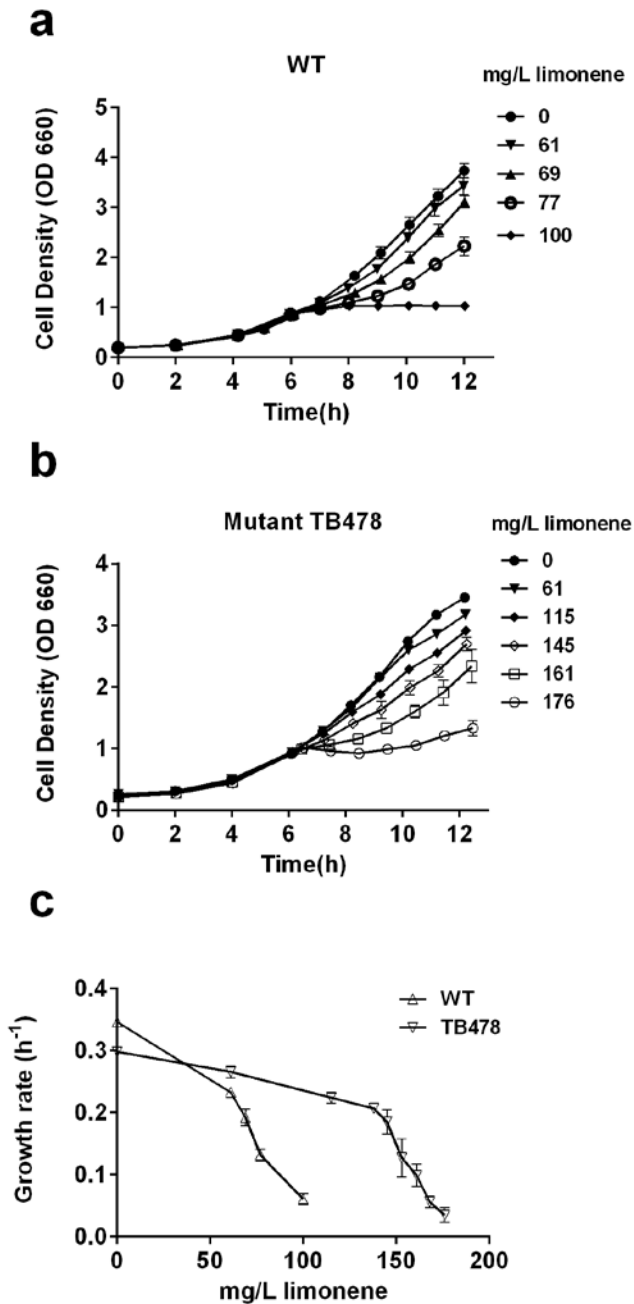
Figure 1. Growth of WT and evolved strain TB478 during limonene challenge. (a) Wild-type (WT), (b) mutant TB478 challenged with various amounts of limonene during mid-exponential growth. (c) Growth rate of WT and TB478 against increasing limonene load. Error bars represent one SD above and below the mean from biological replicates ($n = 3$).
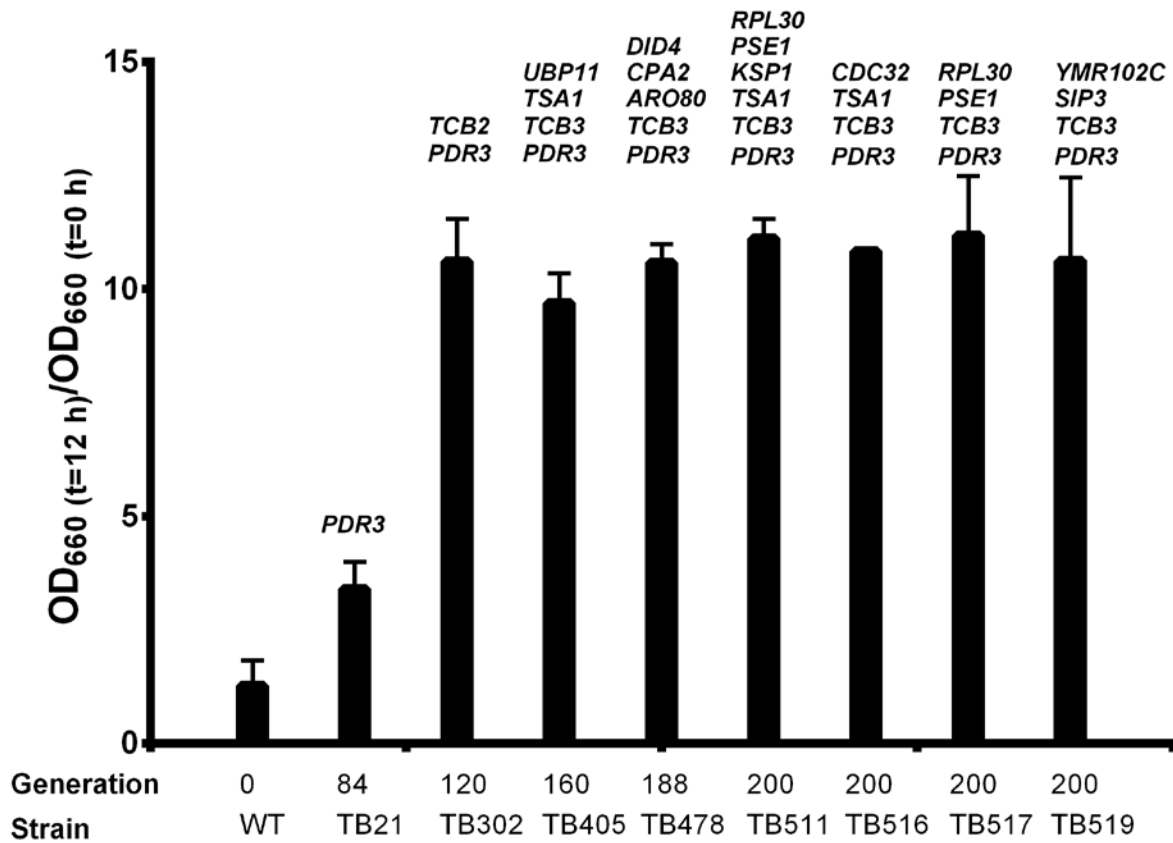
Figure 2. Summary of the evolved strains' relative fitness and genetic mutations. Each strain is a single isolate and the mutation in that strain are listed above. ReFlative fitness is defined as the ratio of the cell density (OD_{660}) at 12 and 0 h during limonene exposure (138 mg/l). Error bars represent one SD above the mean for biological replicates ($n = 3$).
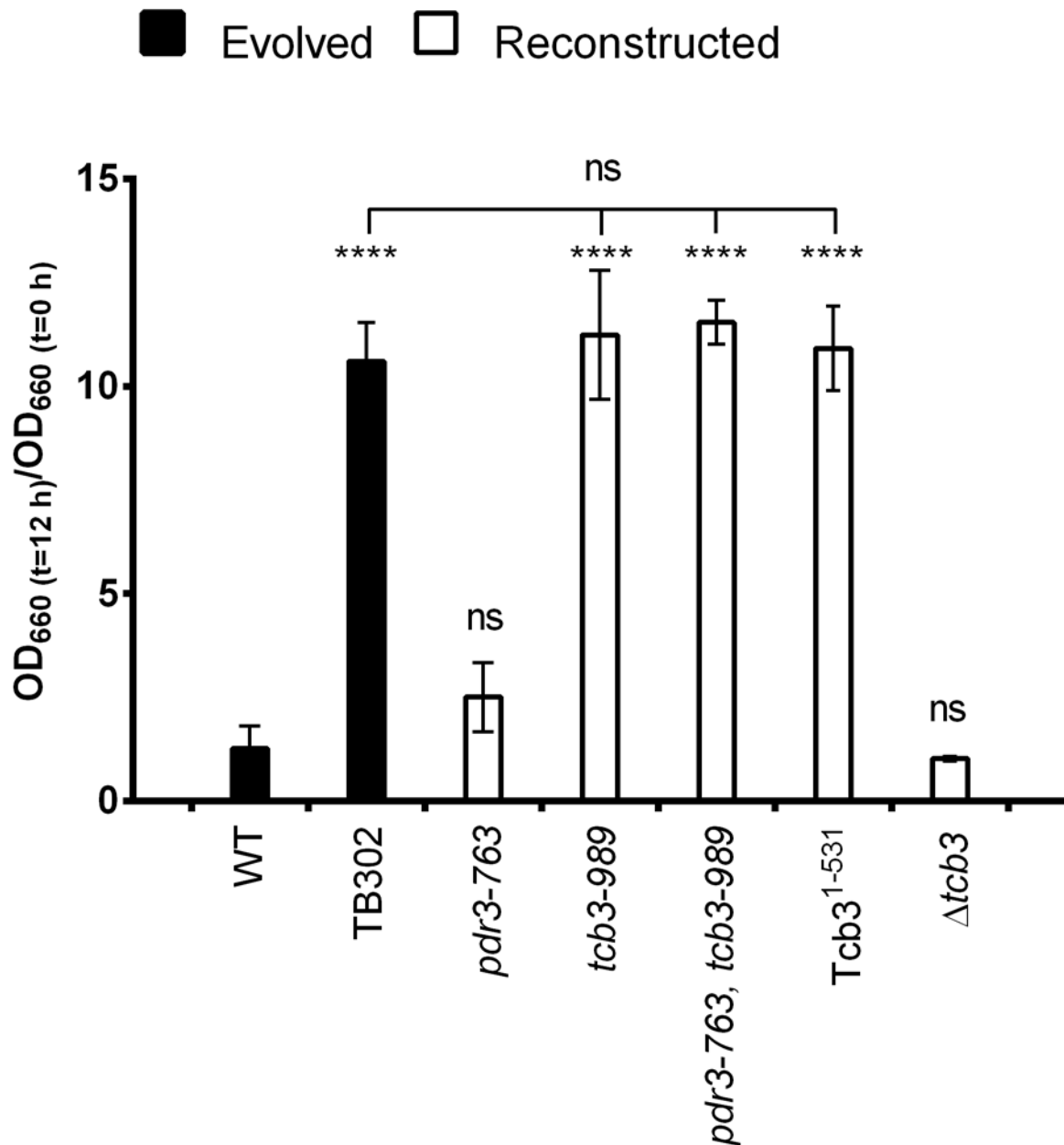
Figure 3. Relative fitness towards limonene for reconstructed mutations. Beneficial mutations in *PDR3* and *TCB3* were constructed in the parent strain (WT). Relative fitness is defined in Fig 2. Error bars represent one SD above the mean for biological replicates (n = 3). Significance was determined by one-way ANOVA to correct for multiple comparisons relative to the WT (****$p < 0.001$, ns, not significant; $p < 0.05$).
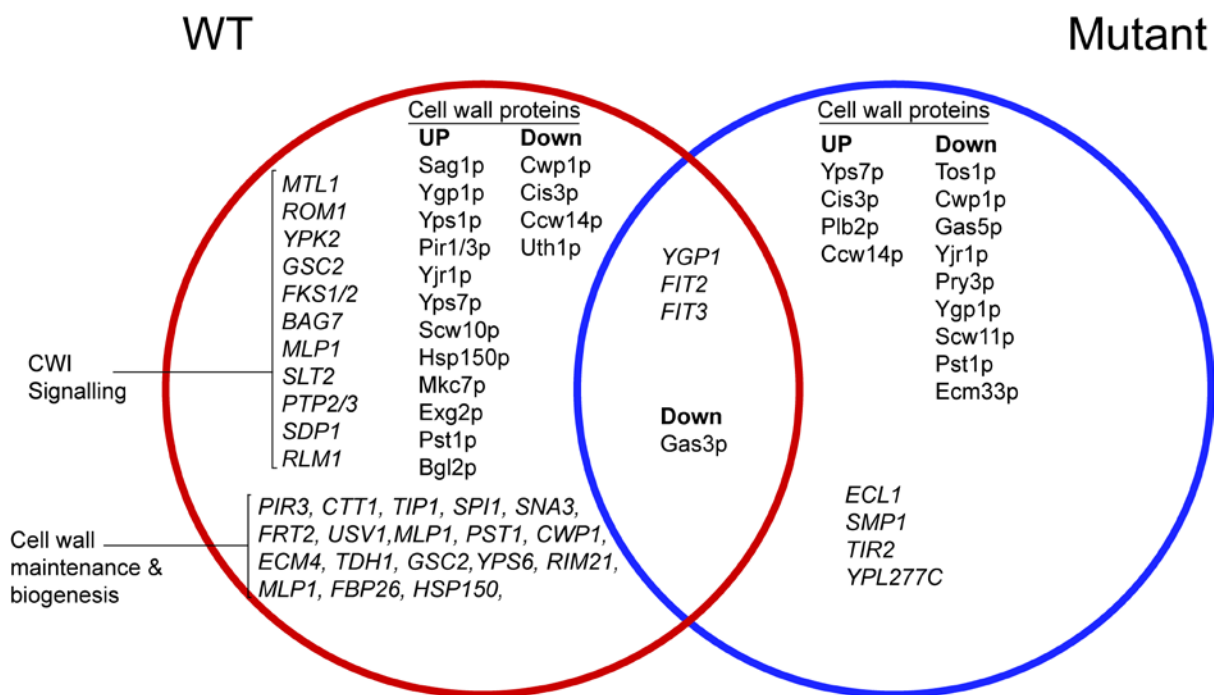
Figure 4. Cell wall transcriptome and proteome response during limonene stress (+/-limonene treatment). Venn diagram representing overlap and differences in cell wall gene expression (upregulated genes only) and protein abundance for WT and single mutant (*tcb3-989*) cells. Upregulated cell wall genes from the WT were used from Brennan et al. [52]. Upregulated genes (mutant) and cell wall proteins (WT and mutant) were analyzed in this study.
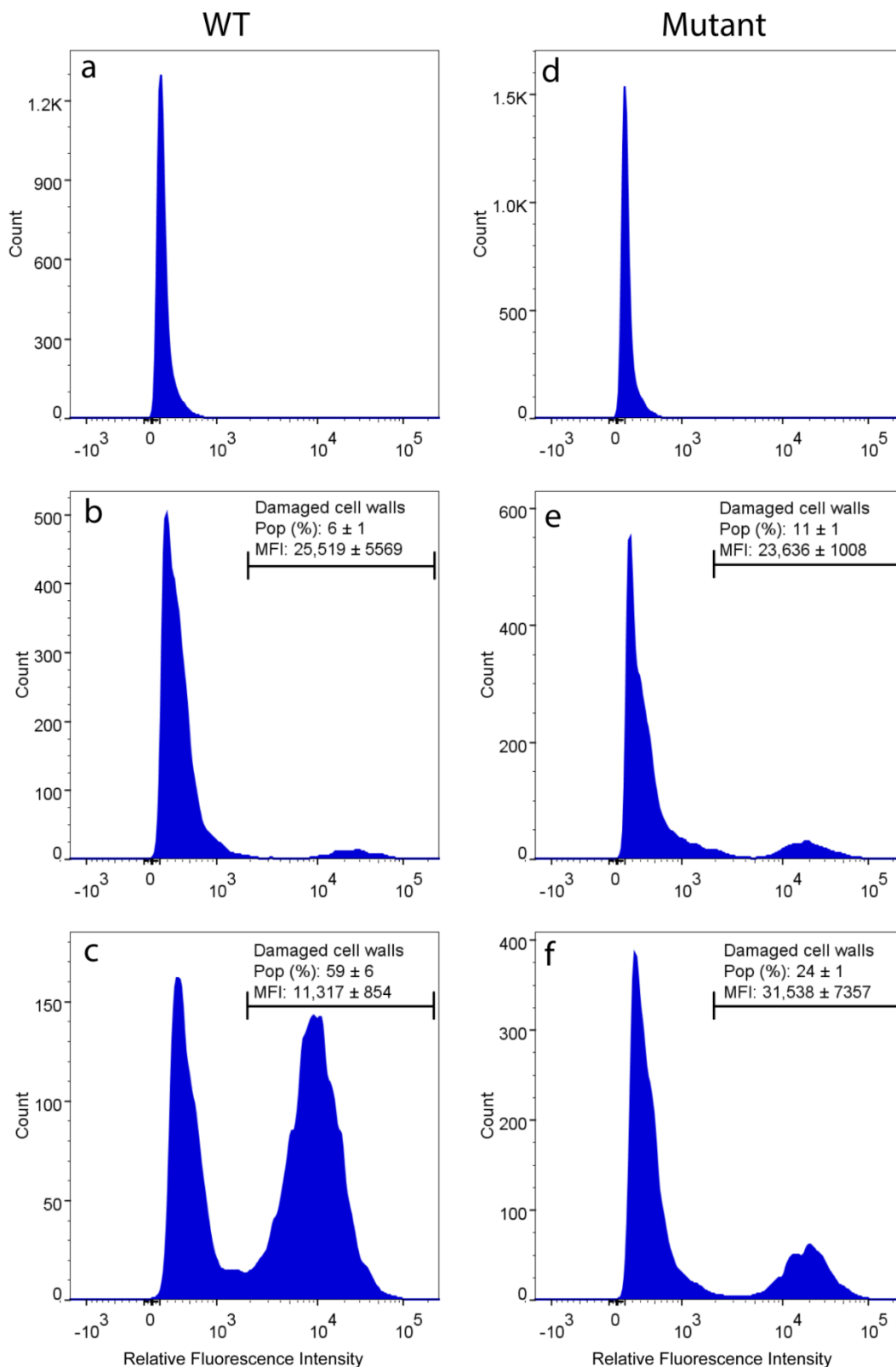
Figure 5. Histograms representing the variation in fluorescence emitted from WT and single mutant (*tcb3-989*) cells. (**a** and **d**) nonstained cells; (**b** and **e**) untreated control cells stained with CFW; (**c** and **f**) cells stained with CFW after 2 h of limonene treatment. Cells with damaged cell walls show an increase in sensitivity and fluorescence towards CFW.

The mean fluorescence intensity (MFI) and percentage of damaged cells (Pop %) are reported for biological replicates ($n = 3$, ± SD).
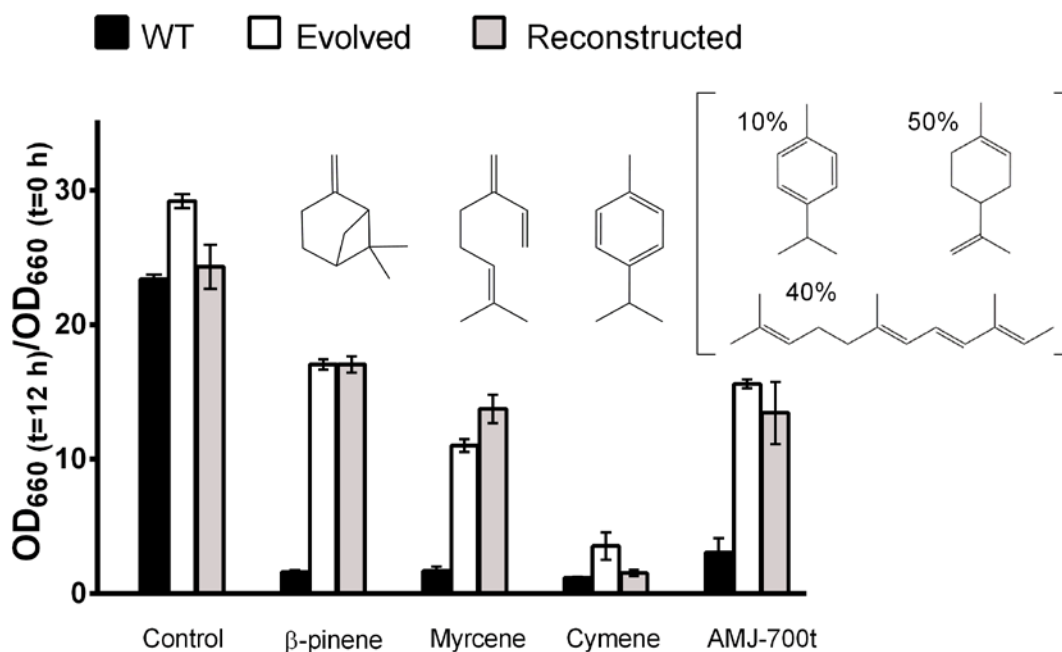
Figure 6. Relative fitness towards other terpenes. WT, evolved (TB516), and the reconstructed WT (single mutant: *tcb3-989*) strains were subjected to relative fitness assays for β-pinene (198 mg/l), myrcene (361 mg/l), cymene (140 mg/l) and AMJ-700t (225 mg/l). AMJ-700t contains by volume (10% cymene, 50% limonene, 40% farnesene). Controls represent no treatment. Relative fitness is defined in Fig 2. Error bars represent one SD from the mean for biological replicates ($n = 3$).

Chapter 4 References:

1.   Stranges, A.N. Friedrich Bergius and the Rise of the German Synthetic Fuel Industry. *Isis* **75**, 643-667 (1984).

2.   Yergin, D. The prize: the epic quest for oil, money, and power. (Simon & Schuster, New York; 1991).

3.   Vietor, R.H.K. The Synthetic Liquid Fuels Program: Energy Politics in the Truman Era. *The Business History Review* **54**, 1-34 (1980).

4.   Lee, S.K., Chou, H., Ham, T.S., Lee, T.S. & Keasling, J.D. Metabolic engineering of microorganisms for biofuels production: from bugs to synthetic biology to fuels. *Current Opinion in Biotechnology* **19**, 556-563 (2008).

5.	Rude, M.A. & Schirmer, A. New microbial fuels: a biotech perspective. *Current Opinion in Microbiology* **12**, 274-281 (2009).

6.	Demain, A.L. REVIEWS: The business of biotechnology. *Industrial Biotechnology* **3**, 269-283 (2007).

7.	Siddiqui, M.S., Thodey, K., Trenchard, I. & Smolke, C.D. Advancing secondary metabolite biosynthesis in yeast with synthetic biology tools. *FEMS Yeast Research* **12**, 144-170 (2012).

8.	Khosla, C. & Keasling, J.D. Timeline - Metabolic engineering for drug discovery and development. *Nature Reviews Drug Discovery* **2**, 1019-1025 (2003).

9.	de Jong, B., Siewers, V. & Nielsen, J. Systems biology of yeast: enabling technology for development of cell factories for production of advanced biofuels. *Current Opinion in Biotechnology*.

10.	Nielsen, J., Larsson, C., van Maris, A. & Pronk, J. Metabolic engineering of yeast for production of fuels and chemicals. *Current Opinion in Biotechnology* **24**, 398-404 (2013).

11.	Hong, K.-K. & Nielsen, J. Metabolic engineering of Saccharomyces cerevisiae: a key cell factory platform for future biorefineries. *Cell. Mol. Life Sci.* **69**, 2671-2690 (2012).

12.	Liu, L., Redden, H. & Alper, H.S. Frontiers of yeast metabolic engineering: diversifying beyond ethanol and Saccharomyces. *Current Opinion in Biotechnology* **24**, 1023-1030 (2013).

13.	Joyce, A.R. & Palsson, B.O. The model organism as a system: integrating 'omics' data sets. *Nat Rev Mol Cell Biol* **7**, 198-210 (2006).

14.	Bro, C. & Nielsen, J. Impact of 'ome' analyses on inverse metabolic engineering. *Metabolic Engineering* **6**, 204-211 (2004).

15.	Bordel, S., Agren, R. & Nielsen, J. Sampling the Solution Space in Genome-Scale Metabolic Networks Reveals Transcriptional Regulation in Key Enzymes. *PLoS Comput Biol* **6**, e1000859 (2010).

16.	Lee, J.W. et al. Systems metabolic engineering of microorganisms for natural and non-natural chemicals. *Nat Chem Biol* **8**, 536-546 (2012).

17.	Renninger, N. & McPhee, D. (USA; 2008).

18.	Peralta-Yahya, P.P. et al. Identification and microbial production of a terpene-based advanced biofuel. *Nat Commun* **2**, 483 (2011).

19.	Brennan, T.C.R., Turner, C.D., Krömer, J.O. & Nielsen, L.K. Alleviating monoterpene toxicity using a two-phase extractive fermentation for the

bioproduction of jet fuel mixtures in Saccharomyces cerevisiae. *Biotechnology and Bioengineering*, n/a-n/a (2012).

20. Keasling, J. Synthetic biology for synthetic chemistry. *ACS Chem Biol* **3**, 64 - 76 (2008).

21. Miller, J., Thompson, P., Hakim, I., Chow, H.H.S. & Thomson, C. d-Limonene: a bioactive food component from citrus and evidence for a potential role in breast cancer prevention and treatment. *Oncol Rev* **5**, 31-42 (2011).

22. Miller, J.A. et al. Human breast tissue disposition and bioactivity of limonene in women with early stage breast cancer. *Cancer Prevention Research* (2013).

23. Fortman, J.L. et al. Biofuel alternatives to ethanol: pumping the microbial well. *Trends in Biotechnology* **26**, 375-381 (2008).

24. Harvey, B.G., Wright, M.E. & Quintana, R.L. High-density renewable fuels based on the selective dimerization of pinenes. *Energy & Fuels* **24**, 267-273 (2009).

25. Chang, M. & Keasling, J. Production of isoprenoid pharmaceuticals by engineered microbes. *Nat Chem Biol* **2**, 674 - 681 (2006).

26. Lücker, J. et al. Monoterpene biosynthesis in lemon (Citrus limon). *European Journal of Biochemistry* **269**, 3160-3171 (2002).

27. Rico, J., Pardo, E. & Orejas, M. Enhanced Production of a Plant Monoterpene by Overexpression of the 3-Hydroxy-3-Methylglutaryl Coenzyme A Reductase Catalytic Domain in Saccharomyces cerevisiae. *Appl Environ Microbiol* **76**, 6449-6454 (2010).

28. Ryder, J.A. (Amyris Biotechnologies Inc (AMYR-Non-standard), 2009).

29. Amyris (Press release) Azul brazilian airlines makes successful demonstration flight with amyris renewable jet fuel produced from sugarcane. *http://www.amyris.com/en/newsroom/225-photo-release-azul-brazilian-airlines-makes-successful-demonstration-flight-with-amyris-renewable-jet-fuel-produced-from-sugarcane* (2012).

30. Nassar, A. et al. Sustainability of sugarcane-derived renewable jet fuel: life cycle GHG emissions and benchmark of major sustainability standards. *http://www.iconebrasil.org.br/arquivos/noticia/2482.pdf* (June 14, 2012).

31. Fischer, M.J.C., Meyer, S., Claudel, P., Bergdoll, M. & Karst, F. Metabolic engineering of monoterpene synthesis in yeast. *Biotechnology and Bioengineering*, n/a-n/a (2011).

32. Ignea, C. et al. Improving yeast strains using recyclable integration cassettes, for the production of plant terpenoids. *Microbial Cell Factories* **10**, 4 (2011).

33. Hill, J., Nelson, E., Tilman, D., Polasky, S. & Tiffany, D. Environmental, economic, and energetic costs and benefits of biodiesel and ethanol biofuels. *Proceedings of the National Academy of Sciences* **103**, 11206-11210 (2006).

34. Oud, B., van Maris, A.J.A., Daran, J.-M. & Pronk, J.T. Genome-wide analytical approaches for reverse metabolic engineering of industrially relevant phenotypes in yeast. *FEMS Yeast Research* **12**, 183-196 (2012).

35. Bailey, J.E. et al. Inverse metabolic engineering: A strategy for directed genetic engineering of useful phenotypes. *Biotechnol Bioeng* **52**, 109-121 (1996).

36. Patnaik, R. et al. Genome shuffling of *Lactobacillus* for improved acid tolerance. *Nat Biotech* **20**, 707-712 (2002).

37. Portnoy, V.A., Bezdan, D. & Zengler, K. Adaptive laboratory evolution -- harnessing the power of biology for metabolic engineering. *Current Opinion in Biotechnology* **22**, 590-594 (2011).

38. Çakar, Z.P., Turanlı-Yıldız, B., Alkım, C. & Yılmaz, Ü. Evolutionary engineering of Saccharomyces cerevisiae for improved industrially important properties. *FEMS Yeast Research* **12**, 171-182 (2012).

39. Jarboe, L.R., Liu, P. & Royce, L.A. Engineering inhibitor tolerance for the production of biorenewable fuels and chemicals. *Current Opinion in Chemical Engineering* **1**, 38-42 (2011).

40. Atsumi, S. et al. Evolution, genomic analysis, and reconstruction of isobutanol tolerance in Escherichia coli. *Mol Syst Biol* **6** (2010).

41. Çakar, Z.P., Seker, U.O.S., Tamerler, C., Sonderegger, M. & Sauer, U. Evolutionary engineering of multiple-stress resistant Saccharomyces cerevisiae. *FEMS Yeast Research* **5**, 569-578 (2005).

42. Brown, S.D. et al. Mutant alcohol dehydrogenase leads to improved ethanol tolerance in Clostridium thermocellum. *Proceedings of the National Academy of Sciences* **108**, 13752-13757 (2011).

43. Reyes, L.H., Almario, M.P., Winkler, J., Orozco, M.M. & Kao, K.C. Visualizing evolution in real time to determine the molecular mechanisms of n-butanol tolerance in Escherichia coli. *Metabolic Engineering*.

44. Wright, J. et al. Batch and continuous culture-based selection strategies for acetic acid tolerance in xylose-fermenting *Saccharomyces cerevisiae*. *FEMS Yeast Research* **11**, 299-306 (2011).

45.   Jantama, K. et al. Combining metabolic engineering and metabolic evolution to develop nonrecombinant strains of Escherichia coli C that produce succinate and malate. *Biotechnol Bioeng* **99**, 1140-1153 (2008).

46.   Nicolaou, S.A., Gaida, S.M. & Papoutsakis, E.T. A comparative view of metabolite and substrate stress and tolerance in microbial bioprocessing: From biofuels and chemicals, to biocatalysis and bioremediation. *Metabolic Engineering* **12**, 307-331 (2010).

47.   Otero, J.M. et al. Whole genome sequencing of Saccharomyces cerevisiae: from genotype to phenotype for improved metabolic engineering applications. *Bmc Genomics* **11** (2010).

48.   Langmead, B. & Salzberg, S.L. Fast gapped-read alignment with Bowtie 2. *Nature Methods* **9**, 357-U354 (2012).

49.   Robinson, J.T. et al. Integrative genomics viewer. *Nature Biotechnology* **29**, 24-26 (2011).

50.   Cingolani, P. et al. A program for annotating and predicting the effects of single nucleotide polymorphisms, SnpEff: SNPs in the genome of Drosophila melanogaster strain w(1118); iso-2; iso-3. *Fly* **6**, 80-92 (2012).

51.   Solis-Escalante, D. et al. amdSYM, a new dominant recyclable marker cassette for Saccharomyces cerevisiae. *FEMS Yeast Research* **13**, 126-139 (2013).

52.   Brennan, T.C.R., Krömer, J.O. & Nielsen, L.K. Physiological and Transcriptional Responses of Saccharomyces cerevisiae to d-Limonene Show Changes to the Cell Wall but Not to the Plasma Membrane. *Appl Environ Microbiol* **79**, 3590-3600 (2013).

53.   Väremo, L., Nielsen, J. & Nookaew, I. Enriching the gene set analysis of genome-wide data by incorporating directionality of gene expression and combining statistical hypotheses and methods. *Nucleic Acids Research* **41**, 4378-4391 (2013).

54.   Schulz, B.L. & Aebi, M. Analysis of Glycosylation Site Occupancy Reveals a Role for Ost3p and Ost6p in Site-specific N-Glycosylation Efficiency. *Molecular & Cellular Proteomics* **8**, 357-364 (2009).

55.   Choi, M., Chang, C.-Y. & Olga, V. Protein significance analysis in LC-MS, SRM and DIA for label-free or label-based proteomics experiments; http://www.bioconductor.org/packages/2.13/bioc/manuals/MSstats/man/MSstats.pdf . (2013).

56. Manford, Andrew G., Stefan, Christopher J., Yuan, Helen L., MacGurn, Jason A. & Emr, Scott D. ER-to-Plasma Membrane Tethering Proteins Regulate Cell Signaling and ER Morphology. *Developmental Cell* **23**, 1129-1140 (2012).

57. Hu, F. et al. Key cytomembrane ABC transporters of *Saccharomyces cerevisiae* fail to improve the tolerance to *d*-limonene. *Biotechnology Letters* **34**, 1505-1509 (2012).

58. Creutz, C.E., Snyder, S.L. & Schulz, T.A. Characterization of the yeast tricalbins: membrane-bound multi-C2-domain proteins that form complexes involved in membrane trafficking. *CMLS, Cell. Mol. Life Sci.* **61**, 1208-1220 (2004).

59. Dowell, R.D. et al. Genotype to Phenotype: A Complex Problem. *Science* **328**, 469-469 (2010).

60. Lowe, M. & Barr, F.A. Inheritance and biogenesis of organelles in the secretory pathway. *Nature Reviews Molecular Cell Biology* **8**, 429-439 (2007).

61. Estrada, P. et al. Myo4p and She3p are required for cortical ER inheritance in Saccharomyces cerevisiae. *The Journal of Cell Biology* **163**, 1255-1266 (2003).

62. Shepard, K.A. et al. Widespread cytoplasmic mRNA transport in yeast: Identification of 22 bud-localized transcripts using DNA microarray analysis. *Proceedings of the National Academy of Sciences* **100**, 11429-11434 (2003).

Chapter 5: Discussion

Product toxicity is the limiting factor facing microbial monoterpene production. This thesis used multiple angles to address this issue. First, a better understanding of the actual mechanism(s) of action were required in order to begin developing viable strategies to overcome toxicity. Chapter 2 quantified exactly how much monoterpene was required to inhibit cell growth and provided a biochemical route to address toxicity in situ. This work led to the key distinction between phase and molecular toxicity, which was then further investigated using systems biology tools (e.g., transcriptomics) in Chapter 3. Chapter 4 then described ALE as a tool to further understand toxicity mechanism(s) and provide gene targets for engineering tolerance in the future.

To be a viable substitute for a petroleum fuel, alternative fuels need to be produced in sufficient quantities. Currently, the endogenous production of monoterpenes in *S. cerevisiae* (1 g/l)[1] are well below the titers required to be economically competitive in the transportation industry (~ 100 g/l). Monoterpenes are produced primarily via the mevalonate pathway, which has been studied extensively and are reviewed elsewhere [2-4] (Fig 5.1). The success of monoterpene production will rely on the careful balance of pathway intermediates, redox cofactors and the control of the FPP synthase (controlled by the *ERG20* gene) [2]. FPPS is responsible for adding one C_5 IPP unit to the growing C_{10} GPP chain to make C_{15} FPP. The availability of GPP, the precursor for monoterpenes, for synthesis seems to be a key parameter for production because with the exception of a few wine strains, yeast does not produce GPP *de novo* [5, 6]. GPP is not released from the FPPS active site and is primarily used for the formation of FPP. Tight control over the amount of GPP and FPP available for monoterpene production and cellular development is important. Monoterpene synthase (MTS) activity, which acts to cyclize the GPP to form the C_{10} monoterpene product, may also be critical area to focus on for strain improvement [2]. The addition of a chaperone heat-shock protein (*HSP90*) improved production of cineole by 60%, suggesting that protein-protein interactions could augment MTS catalytic activity and productivity [1].

Several groups have reported much higher titers for monoterpene alcohols (monoterpenoids), such as geraniol (36 mg/l) [7] and cineole (1 g/l) [1], compared to monoterpene olefins such as limonene (1.5 mg/l) [8]. Oxyfunctionalized monoterpenes, which contain epoxy or hydroxyl groups, most likely have very different physiological effects in baker's yeast compared to monoterpene olefins. Differences in physio-chemical

properties (e.g., solubility) can drastically change the resulting impact a solvent has towards a microorganism [9]. A clear distinction should be made between monoterpene olefins and monoterpene alcohols when discussing production constraints. Due to the oxygen moieties, the energy densities are lower for monoterpene alcohols compared to their olefin counterparts (e.g., $\Delta_cH°_{limonane}$ = 44 MJ/kg and $\Delta_cH°_{cineole}$ = 39 MJ/kg) [10, 11]. Given the strict engine performance requirements for jet fuels [12], a product's energy content should also be highly considered in the design of microbial biocatalysts.

Comparing the minimum inhibitory concentration for each monoterpene product across species is an important parameter when choosing a host platform for engineering. Production of monoterpenes in *E. coli* has been reported to be substantially higher than yeast. Alonso-Gutierrez et al. reported titers of around 400 mg/l for limonene [13]. Although a strict experimental interrogation of the inhibitory limits of monoterpenes in *E. coli* has yet to be determined, there are clearly differences in mechanisms of inhibition between the two organisms. This most likely has to do with the differences in the cellular envelope organization. *E. coli* has two membranes separated by a periplasmic space [14] whereas yeast have a single membrane adjacent to a rigid and thick cell wall [15]. The mass transfer rate of a limonene droplet from inside a cell, across the cellular envelope, and into the extracellular medium (or vice versa) will depend on the droplets membrane and cell wall partitioning behaviour. A rigorous, quantitative *in vivo* analysis of this phenomenon has yet to be completed for *E. coli* and yeast. Mass transport of monoterpenes in yeast is assumed to has be a passive diffusion process [16] and Ciamponi et al. demonstrated that the cell wall, rather than the plasma membrane, was the main determinate for limonene mass transfer [17]. This was the first study highlighting that transport resistance may depend more on cell wall partitioning than membrane partitioning.

Even if the metabolic engineering community can overcome the various pathway and transport issues, product toxicity remains the primary limitation for monoterpene production. In order to find solutions to this problem, it is important to first know what the mechanism of toxicity is. This is the rationale of this thesis: if we can understand the precise mechanism(s) of toxicity, we can build better solutions.

In 1987, Rahael Bar published a seminal paper describing two classes of solvent toxicity for microorganisms: molecular and phase. Molecular toxicity is cellular inhibition caused by dissolved solvent molecules (e.g., interchelating into membranes and disrupting membrane function), whereas phase toxicity is inhibition caused by the presence of separate organic phase [18]. Bar concluded that in order to systematically study the

fundamental impact solvents exert on microorganisms, the two effects must be clearly distinguished from the beginning [18]. Before Chapter 2 was published, no distinction between phase and molecular toxicity had ever been made for monoterpenes. The literature ascribed monoterpene toxicity to molecular effects, namely interference with membrane properties and membrane function [19-22]. However, monoterpenes, such as limonene, are sparingly soluble in water ($S_{limonene}$ = 6 mg/l) and the inhibitory concentrations reported were well in excess of solubility. How then could limonene be toxic at the molecular level if it existed as a separate organic phase? This was the key question that initiated the investigation.

In Chapter 2, we quantified how much monoterpene solvent it took to decrease cell growth. The MICs for limonene and other monoterpenes were an order of magnitude larger than their aqueous solubility, meaning that (1) monoterpene toxicity is a phase effect and (2) structural membrane damage (using vital PI stain) did not occur. We then examined a biochemical engineering strategy to address toxicity using two-phase fermentation. Extractive fermentation demonstrated that the MIC for limonene in a two-phase system could be increased 700-fold. However, further investigations for strain engineering techniques were necessary as there are two main drawbacks when using two-phase systems during fermentation: energy required for higher mixing rates and energy intensive recovery processing such as distillation.

Chapter 3 investigated if other hallmarks of membrane interference are present when cells are treated with limonene. The model for molecular toxicity and membrane interference is the impact of ethanol on yeast [23, 24]. Ethanol's mode of action in yeast is through the fluidization of the plasma membrane [23]. Physical membrane damage, increase in membrane fluidity, upregulation of monounsaturated fatty acids, ergosterol biosynthesis are common physiological responses to ethanol [23]. Logically, if membrane fluidization is the mechanism, we should observe these same effects with limonene. We did not. Chapter 3 showed that structural membrane damage, membrane fluidity, membrane composition and key transcriptional responses (e.g., fatty acid and ergosterol synthesis) did not change during limonene stress. This work is the first body of data demonstrating that the membrane is not the target of toxicity for limonene in yeast.

Three distinctions should be noted between previous studies [19, 22, 25] and this thesis in terms of the experimental approaches used to investigate monoterpene toxicity. Firstly, we added monoterpenes in mid-exponential phase (5 hours post inoculation) rather than upon inoculation. When added at inoculation, limonene caused overt cell death (assessed

using vital PI stain), while viability remained high when the same amount was added in mid-exponential phase. Evidently, the combination of inoculation and limonene stress exceeded the cells ability to cope. The membrane failure observed in previous studies could be the result of cell death as opposed to the cause of cell death. Secondly, we did not use surfactants to aid in the aqueous solvation of monoterpenes. It is possible that molecular toxicity does occur in the ternary water-limonene-surfactants, where far higher limonene concentrations are reached in the continuous phase. The experimental approach used in this thesis resembles a production environment far better than previous studies; monoterpenes will accumulate later in the culture and surfactants are not added to increase solubility. Chapter 3 demonstrated that growth in the presence of a limonene-solvent system is very different than limonene alone (Appendix). Lastly, all tests in this thesis were performed using exogenous addition of monoterpene in non-producing strains. This choice was made due to the lack of access and resources to monoterpene-producing strains. Unfortunately Amyris Inc. was unable to provide producing strains due to legal issues and our own group (as well as other groups) could not provide engineered strains with titers beyond inhibitory limits.

If limonene was not disrupting the membrane, then how was it inhibiting cell growth? A description of the mechanism(s) of phase toxicity is only partially answered here. Described in Chapter 3, the cell wall was found to be damaged after limonene exposure. This was an interesting finding because the cell wall is the first line of defence and the first cellular component to come in contact with extracellular species (i.e., emulsion droplets). The data showed that limonene droplets interfere with the normal organization of cell wall structures. Chitin is considered the hydrophobic core of the cell wall [26] and is central in providing the cell wall's mechanical strength [15]. Limonene dispersions may have a higher affinity for hydrophobic chitin structures compared to other glucose or mannan sugar polymers found in the cell wall. Given its pivotal role in cell separation and cytokinesis the disruption of cell wall integrity must be one of the key modes of action of limonene toxicity.

The cell wall is a highly dynamic organelle that can change quickly in response to environmental cues and future studies probing the nanomechanical properties of yeast cell walls could be very enlightening. Atomic force microscopy (AFM) can provide precise real-time mechanical measurements at the cell surface [27]. It has already been used, *in vivo*, to reveal that the cell wall has strict characteristic motion frequencies that are dependent on temperature and metabolic processes [28]. Here, AFM analysis was attempted to study cell

surface effects of limonene but the experiment failed due to the inability to immobilize the cells properly within porous membranes (immobilization is a requirement for AFM studies). However, if the cell stabilization step can be achieved AFM studies could be critical in the evaluation of phase toxicity within microbial biphasic emulsion systems in the future. Silicon microwell arrays with etched wells roughly size of cells (~5 um) could also be potentially method to immobilize cells for AFM as well.

What is still unclear is how limonene dispersions disrupt cell wall architecture. The data in Chapter 3 shows that chitin and cell wall microfibrils are somewhat decrystallized after limonene treatment. Given that the cell wall content and thickness did not change after limonene exposure (Chapter 3) this means that limonene causes structural damage to the cell wall lattice structure. If limonene droplets are indeed localizing within the cell wall and interfering with microfibril packing (e.g., swelling effect), then their droplet size must be within the limits of the thickness of the cell wall (100-200 nm) [29]. Determining the droplet size distribution (DSD) for organic solvents would be useful data to relate how dispersions compare to cell size. Monoterpene DSD has not been reported in fermentation systems. However, a cell wall loosening effect would be supported by a recent study discussed earlier where limonene was found to swell cell walls more readily than the monoterpenoids linalool and carvone during flavour encapsulation [17]. Another proposed phase toxicity effect is that of cell-coating, where the solvent coats the cell surface blocking nutrient transport. This is highly unlikely given that the sugar uptake rate was the same for treated and non-treated cells during fermentation (data not shown). Cell wall swelling and/or structural damage during solvent-cell contact are likely mechanisms of phase toxicity but these still require an analysis of the DSD (It should be noted that measurements for farnesene and limonene's DSD was attempted but failed due to experimental instrument issues).

The phase toxicity phenomenon must have a key kinetic component, but this space is not well described. If we assume that an oil droplet negatively impacts a cell during cell-oil contact then phase toxicity would be proportional to this interfacial area. Mixing rate, DSD and total droplet surface area are important properties in emulsion systems. For example, the total interfacial area (TIA) of a yeast culture at $OD_{600nm} = 1$ is roughly $1x10^{11}$ μm^2 (given a cell is perfectly round with diameter of 5 μm). If a toxic amount of limonene is added (3 μl) the TIA of limonene would be approximately three orders of magnitude smaller than that of the cells ($4x10^8$ μm^2) if the radius was 25 μm. If the average radius of a limonene droplet shrunk to 25 nm then the TIA would roughly match that of the cell TIA

(4×10^{11} μm^2). Thus, DSD is a key property in determining the interfacial contact area between cells and oil dispersions.

The average radius of a limonene-water dispersion system would also be useful in studying the phenomena of hydrophobicity and its potential role in phase toxicity. The hydrophobic effect, which is the tendency for oil and water to segregate, is qualitatively well understood but rigorous quantitative descriptions are lacking [30]. In 1959, Walter Kauzman noted that water's interaction with hydrophobic species seemed to cause particles to cluster forming hydrophobic units [31]. Hydrophobicity is a complex phenomenon that depends on whether small molecular units or large clusters, or a combination of both are involved in the system. The radius of a hydrophobic particle, or its length, is important because it impacts the solvation energy (ΔG free energy required to solvate a species in water). Depending on the length, when hydrophobic particles cluster together the overall volume to surface area is much larger than that of an individual particle. This larger ratio lowers the energy requirement for solvation and is the main driving force for cluster assembly.

ΔG is a useful quantity in describing hydrophobicity and can also be used to estimate other important properties such as oil-water surface tension, γ ($\Delta G \approx 4\pi r^2 \gamma$) [30, 32]. Because phase toxicity involves the interfacial interactions between water, the surface of cells and solvent clusters, surface behaviour must be important. Surface tension is proportional to a fluid's viscosity: $\gamma = Ae^{-B/\eta}$, where η is viscosity and A and B are temperature and fluid dependent constants [33]. Chapter 3 highlights that limonene is an order of magnitude less viscous than IPM and IPM is not harmful to cells at all. Given viscosity's role in determining fluid behaviour, differences in surface tension and droplet size clearly change hydrophobic effects at the water-particle interphase [30, 34] and thus must impact the way solvents interact with cells. This means that fluid rheology impacts phase toxicity.

Ideally, we would have one quantity that describes a solvent's relevant fluid mechanical behaviour during fermentation and its phase toxicity effect on an organism. Log P_{ow} works for molecular toxicity at the membrane level but cannot be used for phase toxicity because membrane-water partitioning is irrelevant once the cells and the water phases are saturated (i.e., beyond the solvent's solubility). Chemical engineers use dimensionless numbers to describe and predict patterns (e.g., Reynolds number (Re) for fluid flow in a pipe). Presented here is a theoretical dimensionless quantity called the

Brennan number (Br). Br contains the necessary biochemical parameters encountered during fermentation in a bioreactor involving water-immiscible non-Newtonian fluids:

$$Br = \frac{Pk_bT\phi}{\gamma\eta V_p}$$

Where power (from impeller) is $P \propto \rho_l N^3 D_i^5$ in [J/s] [35] with N = impeller speed [rev/s], D_i diameter of impeller [cm], ρ_l is density of liquid [g/cm^3]. Interfacial tension γ [J/s^2], viscosity η [kg/m•s], temperature T [K], average particle volume [m^3], Boltzmann's constant [m^{2}kg/s^{2}K] and volume fraction of the oil phase ϕ.

The idea would be to plot Br as a function of the microbes specific growth rate, μ_{max}, for various solvents (see below). Similar to the cut off for laminar and turbulent flow regimes using the Re number (~ 2300) the goal would be to identify patterns between rheology and toxicity. Could there similarly be a transition from non-toxic to toxic regimes corresponding to one Brennan number for all solvents?
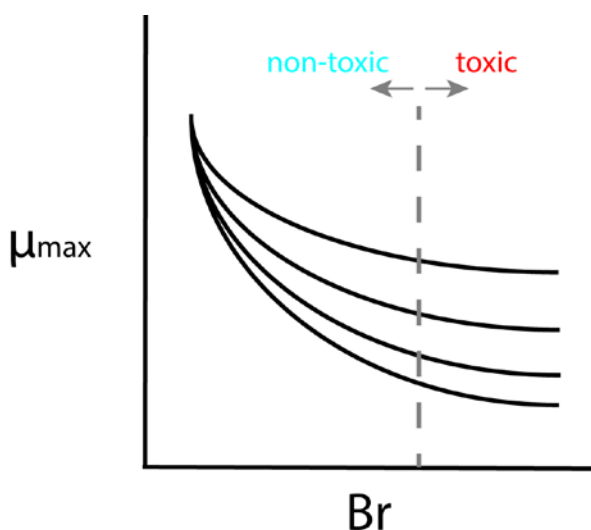
Figure 5.2. Theoretical plot of specific growth rate versus Br number for various solvents.

The characterization of a solvent's rheological properties within a microbial fermentation system requires more attention. This is of particular interest because the types of products that are being targeted today via metabolic engineering and microbial fermentation are petroleum-compatible fuels (e.g., farnesene, bisbolene, pinene), which are essentially water-immiscible oils that exist as a separate phase in culture. Linking fluid rheology, such as γ or DSD, to microbial toxicity is an untouched space. These studies would add to the fundamental knowledge of both phase toxicity and important phenomena such as hydrophobicity within microbial systems.

Although our efforts were only partially realized in revealing the cellular mechanism(s) of inhibition, a solution to the toxicity problem was still required. In Chapter 2 we took advantage the immiscibility physio-chemical property and established a biochemical engineering route to alleviate toxicity *in situ*. The initial idea was based on the observation that inhibition only occurred in a biphasic system. If an inert hydrophobic solvent could act as a reservoir, then we suspected that the monoterpene particles would thermodynamically prefer the solvent phase rather than water. In situ product removal (ISPR) is a well-studied field with numerous successful examples of two-phase liquid-liquid extraction designs [36]. However, most biphasic extraction techniques require further processing to recover the desired product [36]. The use of a solvent that could serve as an extractant and a coproduct would eliminate energy intensive downstream processing operations (e.g., distillation) associated with common ISPR techniques. Chapter 2 proved that farnesene is a suitable solvent for this purpose, being that it can be blended with C_{10} monoterpene products to generate jet fuels and that it can also serve as an excellent extractant.

The final chapter (Chapter 4) focused on generating a cellular engineering strategy to address toxicity. Adaptive laboratory evolution (ALE) is a technique that does not depend on prior knowledge of inhibition. It builds a desired phenotype from the bottom up [37]. ALE is a fascinating and powerful technique. Researchers now have the ability to interrogate adaptive evolution on the molecular level. This strategy was of particular interest in addressing limonene toxicity because of the uncertainties around the mechanism(s) at play. Chapter 4 demonstrated that ALE was successful at generating limonene-resistant phenotypes. When coupled with genome resequencing and genomic reconstruction, the precise beneficial mutation (tTcb3p) was identified. This result successfully linked the genotype to phenotype, which is a nontrivial and complex problem [38]. Interestingly, in Chapter 2 ALE was used in a CSTR design vs. batch passaging for approximately the same duration (200 generations in Chapter 4). The CSTR design may have failed to produce resistant isolates due to the lack of experimental sensitivity in controlling limonene concentration, which is more accurate to control and measure in batch mode. In addition, in Chapter 3 there were no differences found in expression of Tcb3/2 when dosed with limonene highlighting that these targets would not have been found using dose response coupled with transcriptomics analysis. Nevertheless, extractive fermentation and tTcb3p now serve as useful tools to the scientific community. The success of Chapter 4, however, generated another intriguing

question: how does tTcb3p relieve limonene toxicity and what greater mechanistic understanding can we gain from it?

There are three pieces of data that are important to solving this puzzle: (1) cells stop dividing but they are still viable, (2) limonene causes cell wall damage only in WT cells, and (3) the truncation in Tcb3p causes it to co-localize in the nER and the cER. The working hypothesis is that limonene interferes with ER inheritance during cytokinesis through the disruption of cell wall chitin at the bud neck. This doesn't kill cells, but stops proliferation (initially observed in Chapter 2).

Recent literature would support this mechanism. As discussed in Chapter 4, the nER and cER are inherited into daughter cells via different processes [39]. Because tTcb3p can localize to both ER domains, pre-existing nER-bound tTcb3p may be inherited directly from the mother cell; circumventing cER inheritance altogether. cER inheritance is more sensitive to the structural integrity of the septum apparatus, required for actin stabilization, than nER inheritance [40-42]. It has been shown that a similar ER-PM tethering protein, Scs2p, which resides in both the nER and cER, is able to establish the cER in daughter cells in absence of the two other ER-PM tethering protein families (double mutant Δist2, Δtcb1/2/3) [43]. Suggesting that if cER inheritance is blocked, nER-inherited tTcb3p and Scs2p, could establish the ER in daughter cells without assistance.

In addition, recent evidence showed that during ER stress, the nucleus and nER were transmitted to the daughter cell but the cER delivery was inhibited, suggesting that nER is free of ER stress [44]. This means that nER tTcb3p may initially establish the cER in the newly formed bud during stress. In mutant cells, establishment of the cER in the daughter cell may result in formation cell wall maintenance, proper septum degradation and other cellular processes required to finalize cytokinesis. Alternatively, WT daughter cells would lack the ER and all of the biological functions that depend on it. However, ER inheritance in WT cells still needs to be demonstrated during limonene shock.

Internal cellular signalling may also play a role. It was recently shown that when ER stress is detected, the ER stress surveillance (ERSU) pathway activates Slt2p. Activation of *SLT2* delays ER inheritance and cytokinesis [44]. Chapter 3 showed that limonene treatment causes cell wall damage and activation of *SLT2* in WT cells. *SLT2* is not activated for mutant cells (Chapter 4, Fig. 5). *SLT2* activation may be serving as an additional regulatory signalling mechanism that aids in ER inheritance and cytokinesis delays during limonene stress.

Regardless of whether limonene blocks ER inheritance or not, Chapter 4 revealed that Tcb3/2p are important proteins that may have physiological functions beyond ER-

membrane tethering. It may serve as a starting point for more defined studies on nER and cER inheritance and the role of the cER in daughter-mother cell separation (an area that is still not fully understood [39]). In addition, the data also suggests that there could be a clear behavioural distinction between the nER and cER during cellular stress. This has been described for particular ER stresses [44] but further investigations to test for functional differences between the two domains would be impactful in the future.

Finally, this thesis highlights some key insights in terms of the strategies to be used for strain improvement in the future. The production of renewable biofuels and chemicals requires the development of solventogenic organisms [24, 45]. Engineering tolerance in yeast and *E. coli* for this purpose has received increased attention in recent years [45]. The ultimate goal of tolerance engineering is to identify straightforward genetic modifications that result in increased resistance towards a particular compound. To this end, this work showed that evolution engineering techniques trumped dose response strategies coupled with transcriptomics, such as those experiments presented in Chapter 3. In general, numerous reports use a dose response experimental design with the goal of isolating resistant gene targets for further engineering [24]. The limitation of this approach is that it almost always relies on global gene expression data with the assumption that higher gene expression will result in improved fitness in a constructed strain. When growth is severely impaired by a solvent, the resulting transcriptomic data is often complex and unclear. For example in Chapter 3, the microarray data showed upregulation of several general stress response related genes, exporters, cell wall repair enzymes and a few fatty acid metabolism genes. With around 300 differentially upregulated genes it was uncertain how the transcriptome data could be successfully translated into a viable genetic engineering strategy for strain development. Chapter 3 did not result in the identification of concrete tolerant gene targets. This demonstrates that dose response techniques followed by microarray or RNAseq analysis suffer because gene lists are often too big and ascertaining precise gene targets for further analysis is difficult and resource intensive.

Evolution engineering offers a more effective way to generate genetic leads for strain improvement. Due to the surge in next-generation sequencing adaptive laboratory evolution (ALE) has become a very active research area in the last decade [46]. In yeast, this technique is attractive for several reasons: (1) short doubling times (~ 2 h) (2) well established genome resources (http://www.yeastgenome.org) and (3) low mutation rates. *S. cerevisiae* generates roughly one adaptive mutation per 10^{11} cell divisions [47]. Thus, the resulting mutation list (i.e., target list) from the ALE method is substantially smaller

compared to the dose response gene list. In Chapter 4 for example, the total number of gene targets was 14 compared to 300 from transcription analysis in Chapter 3. Another advantage is that ALE results in the precise genetic information for further investigation whereas transcriptomic results assume that overexpression of a particular gene(s) will confer tolerance. This is not always the case. For example, ABC transporters (*PDR5*, *YOR1*, *PDR15*) were induced when yeast cells were treated with limonene [48] (similar to our observations in Chapter 3). However, overexpression of these genes failed to improve tolerance to limonene [48].

In terms of future production, both the plasma membrane and cell wall results will have implications for producing yeast strains. Efflux will likely negatively impact yields due to its high energy use; whereas cell wall remodelling due to mutated Tcb3p does not require additional ATP. Thus, the single mutation in *TCB3* or two-phase extractive fermentation are more likely to be successful and generalizable in a producing strains to improve toxicity limitations. Nevertheless, because of the clear differences in makeup of the cellular envelope yeast and bacteria may have different strategies to deal with toxicity; as efflux pumps have been shown to improve production and tolerance in industrially relevant hosts such as *E. coli* [25] and *P. putida* [34] but not yeast [48].

In conclusion, this thesis set out to answer two questions: (1) what is the precise mechanism of monoterpene toxicity in *S. cerevisiae* and (2) what are the strategies to overcome inhibition? Outlined here are two strategies to overcome monoterpene toxicity: biphasic extraction and truncating Tcb3p. Moreover, this thesis has contributed to the fundamental understanding of monoterpene inhibition in yeast. Before this body of work, monoterpene toxicity was considered to be molecular toxicity caused by membrane damage. This work demonstrates that this is not the case and monoterpene toxicity is in fact, phase toxicity, which can cause cell wall damage. We describe key areas of further investigation (e.g., rheological properties, mass transfer kinetics) that will hopefully guide researchers in fruitful directions in the future. Lastly, this work serves as a starting point for biological studies of ER morphology and inheritance with an emphasis on the discovery of additional biological functions for tricalbin proteins.
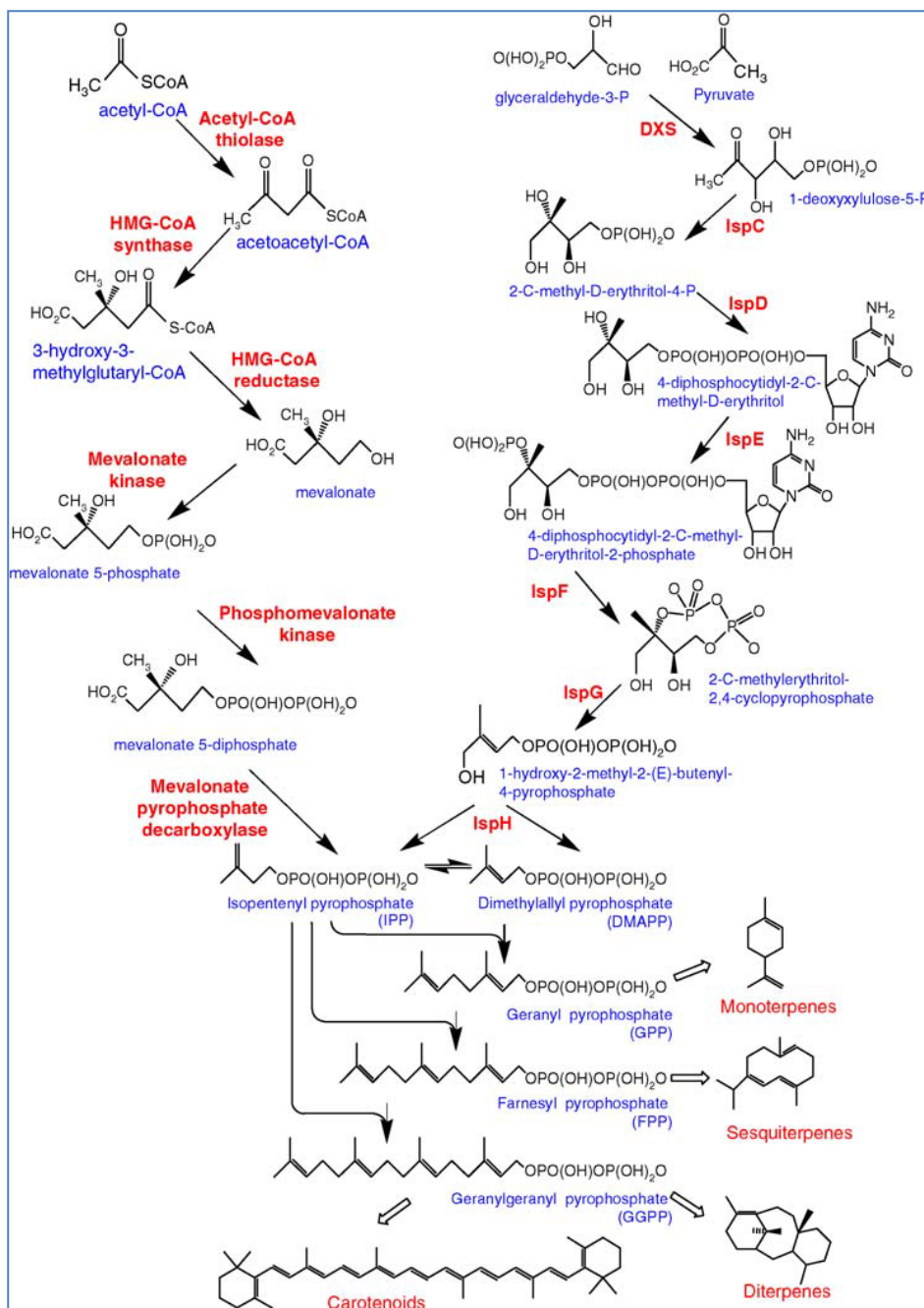
Figure 5.1. Terpene biosynthetic pathways. Right: DXP pathway. Left: Mevalonate pathway. Image used with permission from [3].

Chapter 5 Reference List:

1.   Ignea, C. et al. Improving yeast strains using recyclable integration cassettes, for the production of plant terpenoids. *Microbial Cell Factories* **10**, 4 (2011).

2.   Fischer, M., Meyer, S., Oswald, M., Claudel, P. & Karst, F. in Isoprenoid Synthesis in Plants and Microorganisms. (eds. T.J. Bach & M. Rohmer) 65-71 (Springer New York, 2013).

3.   Keasling, J.D. in Handbook of hydrocarbon and lipid microbiology. (ed. K.N. Timmis) 2951-2966 (Springer Berlin Heidelberg, 2010).

4. Sarria, S., Wong, B., Martín, H.G., Keasling, J.D. & Peralta-Yahya, P. Microbial synthesis of pinene. *ACS Synthetic Biology* (2014).

5. Oswald, M., Fischer, M., Dirninger, N. & Karst, F. Monoterpenoid biosynthesis in *Saccharomyces cerevisiae. FEMS Yeast Research* **7**, 413-421 (2007).

6. Fischer, M.J.C., Meyer, S., Claudel, P., Bergdoll, M. & Karst, F. Metabolic engineering of monoterpene synthesis in yeast. *Biotechnol Bioeng* **108**, 1883-1892 (2011).

7. Liu, J., Zhang, W., Du, G., Chen, J. & Zhou, J. Overproduction of geraniol by enhanced precursor supply in Saccharomyces cerevisiae. *Journal of Biotechnology* **168**, 446-451 (2013).

8. Behrendorff, J., Vickers, C., Chrysanthopoulos, P. & Nielsen, L. 2,2-Diphenyl-1-picrylhydrazyl as a screening tool for recombinant monoterpene biosynthesis. *Microbial Cell Factories* **12**, 76 (2013).

9. Sikkema, J., de Bont, J. & Poolman, B. Mechanisms of membrane toxicity of hydrocarbons. *Microbiological reviews* **59**, 201-222 (1995).

10. Renninger, N., Ryder, J. & Fisher, K. in WO 2008/133658 A2. (ed. W.i.p. organization) 87 (USA; 2008).

11. Matsuda, S.P.T., Wilson, W.K. & Xiong, Q.B. Mechanistic insights into triterpene synthesis from quantum mechanical calculations. Detection of systematic errors in B3LYP cyclization energies. *Organic & Biomolecular Chemistry* **4**, 530-543 (2006).

12. Ryder, J.A. Fuel composition, useful to power any equipment such as an emergency generator or internal combustion engine, which requires a fuel such as jet fuels or missile fuels, comprises limonene and farnesane. US patent 7589243-B1. (2009).

13. Alonso-Gutierrez, J. et al. Metabolic engineering of Escherichia coli for limonene and perillyl alcohol production. *Metabolic Engineering*.

14. Silhavy, T.J., Kahne, D. & Walker, S. The Bacterial Cell Envelope. *Cold Spring Harbor Perspectives in Biology* **2** (2010).

15. Bowman, S.M. & Free, S.J. The structure and synthesis of the fungal cell wall. *BioEssays* **28**, 799-808 (2006).

16. Bishop, J.R.P., Nelson, G. & Lamb, J. Microencapsulation in yeast cells. *Journal of Microencapsulation* **15**, 761-773 (1998).

17. Ciamponi, F., Duckham, C. & Tirelli, N. Yeast cells as microcapsules. Analytical tools and process variables in the encapsulation of hydrophobes in *S. cerevisiae. Applied Microbiology and Biotechnology* **95**, 1445-1456 (2012).

18. Bar, R. in Laane, C., J. Tramper and M. D. Lilly (Ed.). Studies in Organic Chemistry, 29. Biocatalysis in Organic Media; International Symposium, Wageningen, Netherlands, December 7-10, 1986. Xii+426p. Elsevier Science Publishers B.V.: Amsterdam, Netherlands (Dist. In the USA and Canada by Elsevier Science Publishing Co., Inc.: New York, N.Y., USA). Illus 147-154 (1987).

19. Uribe, S., Ramirez, J. & Pena, A. Effects of beta-pinene on yeast membrane functions. *Journal of Bacteriology* **161**, 1195-1200 (1985).

20. Andrews, R.E., Parks, L.W. & Spence, K.D. Some effects of douglas-fir terpenes on certain microorganisms. *Appl Environ Microbiol* **40**, 301-304 (1980).

21. Prashar, A., Hili, P., Veness, R.G. & Evans, C.S. Antimicrobial action of palmarosa oil (Cymbopogon martinii) on Saccharomyces cerevisiae. *Phytochemistry* **63**, 569-575 (2003).

22. Liu, J., Zhu, Y., Du, G., Zhou, J. & Chen, J. Exogenous ergosterol protects *Saccharomyces cerevisiae* from d-limonene stress. *J Appl Microbiol* **114**, 482-491 (2013).

23. Ding, J. et al. Tolerance and stress response to ethanol in the yeast *Saccharomyces cerevisiae. Applied Microbiology and Biotechnology* **85**, 253-263 (2009).

24. Nicolaou, S.A., Gaida, S.M. & Papoutsakis, E.T. A comparative view of metabolite and substrate stress and tolerance in microbial bioprocessing: From biofuels and chemicals, to biocatalysis and bioremediation. *Metabolic Engineering* **12**, 307-331 (2010).

25. Dunlop, M.J. et al. Engineering microbial biofuel tolerance and export using efflux pumps. *Molecular Systems Biology* **7**, 487 (2011).

26. Cabib, E., Blanco, N., Grau, C., Rodríguez-Peña, J.M. & Arroyo, J. Crh1p and Crh2p are required for the cross-linking of chitin to β(1-6)glucan in the Saccharomyces cerevisiae cell wall. *Molecular Microbiology* **63**, 921-935 (2007).

27. Dufrêne, Y.F. Atomic Force Microscopy, a Powerful Tool in Microbiology. *Journal of Bacteriology* **184**, 5205-5213 (2002).

28. Pelling, A.E., Sehati, S., Gralla, E.B., Valentine, J.S. & Gimzewski, J.K. Local Nanomechanical Motion of the Cell Wall of Saccharomyces cerevisiae. *Science* **305**, 1147-1150 (2004).

29. Klis, F.M., Mol, P., Hellingwerf, K. & Brul, S. Dynamics of cell wall structure in Saccharomyces cerevisiae. *FEMS Microbiology Reviews* **26**, 239-256 (2002).

30. Chandler, D. Interfaces and the driving force of hydrophobic assembly. *Nature* **437**, 640-647 (2005).

31. Kauzmann, W. Some factors in the interpretation of protein denaturation. *Advances in protein chemistry* **14**, 1-63 (1959).

32. Huang, D.M. & Chandler, D. The Hydrophobic Effect and the Influence of Solute−Solvent Attractions. *The Journal of Physical Chemistry B* **106**, 2047-2053 (2002).

33. Schonhorn, H. Surface Tension-Viscosity Relationship for Liquids. *J. Chem. Eng. Data* **12**, 524-525 (1967).

34. Smith, R. & Tanford, C. Hydrophobicity of Long Chain n-Alkyl Carboxylic Acids, as Measured by Their Distribution Between Heptane and Aqueous Solutions. *Proc Natl Acad Sci U S A* **70**, 289-293 (1973).

35. Blanch, H.W. & Clark, D.S. Biochemical Engineering. (Marcel Dekker, Inc., New York, New York 1997).

36.   Stark, D. & von Stockar, U., Vol. 80. (eds. U. von Stockar et al.) 149-175 (Springer Berlin / Heidelberg, 2003).

37.   Bailey, J.E. et al. Inverse metabolic engineering: A strategy for directed genetic engineering of useful phenotypes. *Biotechnol Bioeng* **52**, 109-121 (1996).

38.   Dowell, R.D. et al. Genotype to Phenotype: A Complex Problem. *Science* **328**, 469-469 (2010).

39.   Lowe, M. & Barr, F.A. Inheritance and biogenesis of organelles in the secretory pathway. *Nature Reviews Molecular Cell Biology* **8**, 429-439 (2007).

40.   Sagot, I., Klee, S.K. & Pellman, D. Yeast formins regulate cell polarity by controlling the assembly of actin cables. *Nature Cell Biology* **4**, 42-50 (2002).

41.   Moore, J.K., Stuchell-Brereton, M.D. & Cooper, J.A. Function of Dynein in Budding Yeast: Mitotic Spindle Positioning in a Polarized Cell. *Cell Motility and the Cytoskeleton* **66**, 546-555 (2009).

42.   Fehrenbacher, K.L., Davis, D., Wu, M., Boldogh, I. & Pon, L.A. Endoplasmic reticulum dynamics, inheritance, and cytoskeletal interactions in budding yeast. *Molecular Biology of the Cell* **13**, 854-865 (2002).

43.   Manford, Andrew G., Stefan, Christopher J., Yuan, Helen L., MacGurn, Jason A. & Emr, Scott D. ER-to-Plasma membrane tethering proteins regulate cell signaling and ER morphology. *Developmental Cell* **23**, 1129-1140 (2012).

44.   Babour, A., Bicknell, A.A., Tourtellotte, J. & Niwa, M. A Surveillance Pathway Monitors the Fitness of the Endoplasmic Reticulum to Control Its Inheritance. *Cell* **142**, 256-269 (2010).

45.   Dunlop, M.J. Engineering microbes for tolerance to next-generation biofuels. *Biotechnology for Biofuels* **4** (2011).

46.   Portnoy, V.A., Bezdan, D. & Zengler, K. Adaptive laboratory evolution -- harnessing the power of biology for metabolic engineering. *Current Opinion in Biotechnology* **22**, 590-594 (2011).

47.   Zeyl, C. Capturing the adaptive mutation in yeast. *Research in Microbiology* **155**, 217-223 (2004).

48.   Hu, F. et al. Key cytomembrane ABC transporters of *Saccharomyces cerevisiae* fail to improve the tolerance to *d*-limonene. *Biotechnology Letters* **34**, 1505-1509 (2012).

Appendix

The Appendix contains supplementary information for Chapter 3 and 4.

Supplementary information File 1 (SI File 1)

Title: Physiological and transcriptional response to *d*-limonene in *Saccharomyces cerevisiae* shows changes to the cell wall, not the plasma membrane

Authors: Timothy C. R. Brennan[1], Jens O. Krömer[2]#, Lars K. Nielsen[1]
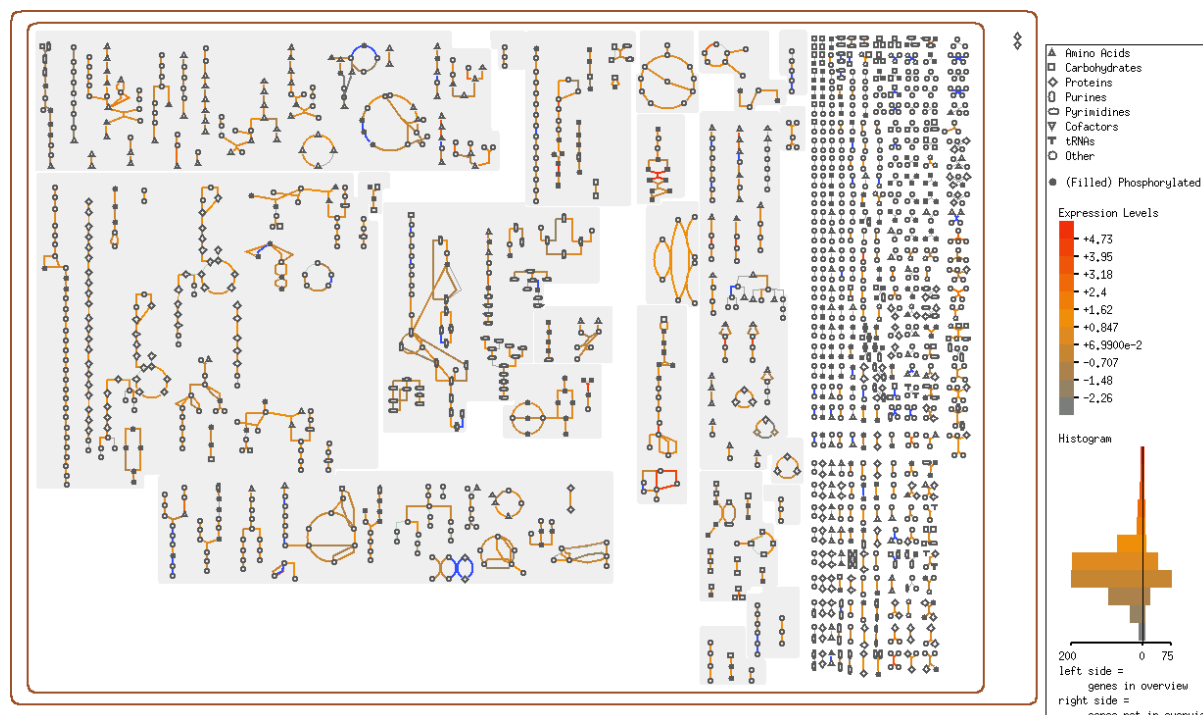
SI Fig 1. Metabolic map of entire transcriptome dataset.

Total number of data rows (not including comment lines): 10563
Number of rows for which the gene could not be found: 9804
Number of rows for which the gene name was ambiguous: 0
Number of rows for which the gene is valid, but for which a data value was missing or malformed: 0

The table below shows statistics for the selected column/column ratio for all genes and for those genes that appear in the Overview (or in any of the selected overviews, if multiple were selected).

Data Statistics	All Genes	Overview Genes
Number of values:	759	619
Minimum value:	-3.037	-3.037

Maximum value: 5.5071   5.5071

Median: -0.0144   0.032449998

Mean: -0.0021671697 0.019628845

Standard deviation: 0.9757149   1.027266

SI Table 1. Metabolic pathway analysis of exposure to limonene. Values are $\log_2$ treatment/control ratio and only pathways exceeding threshold value of ±2 are shown.

Pathway	Pathway Diagram	Enzymes, Genes, and Enzyme Cellular Locations
lysine biosynthesis		homocitrate synthase — LYS20 homocitrate synthase — LYS21 homoaconitase — LYS4 homo-isocitrate dehydrogenase — LYS12 alpha aminoadipate reductase — LYS2 saccharopine dehydrogenase (NADP+, L-glutamate-forming) — LYS9 saccharopine dehydrogenase (NAD+, L-lysine-forming) — LYS1
arginine biosynthesis		ornithine carbamoyltransferase — ARG3 acetylornithine aminotransferase — ARG8 acetylglutamate kinase / N-acetyl-gamma-glutamyl-phosphate reductase — ARG5,6 carbamoyl phosphate synthetase — CPA1 CPA2 acetylglutamate synthase — ARG2 acetylornithine acetyltransferase — ARG7 arginosuccinate synthetase — ARG1 argininosuccinate lyase — ARG4
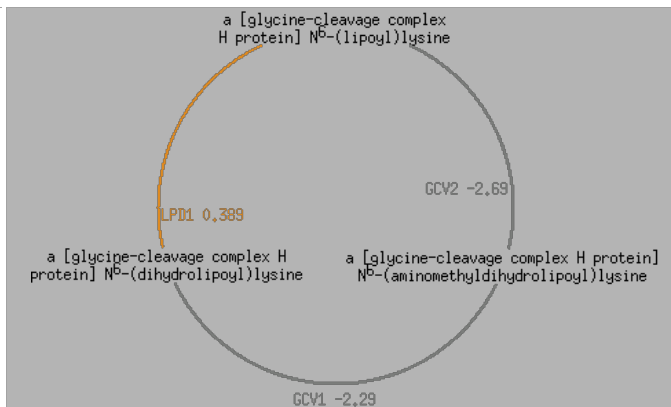
glycine cleavage complex		glycine decarboxylase complex P subunit	GCV2
		GCV1	GCV1
		dihydrolipoamide dehydrogenase	LPD1
folate interconversions		C1-tetrahydrofolate synthase	ADE3
		mitochondrial C1-tetrahydrofolate synthase	MIS1
		Serine hydroxymethyltransferase, mitochondrial	SHM1
		serine hydroxymethyltransferase	SHM2
		thymidylate synthase	CDC21
		dihydrofolate reductase	DFR1
		glycine cleavage complex	GCV1 GCV2 LPD1
		MTHFR	MET13
		MTHFR	MET12
		NAD-dependent 5,10-methylenetetrahydrafolate dehydrogenase	MTD1
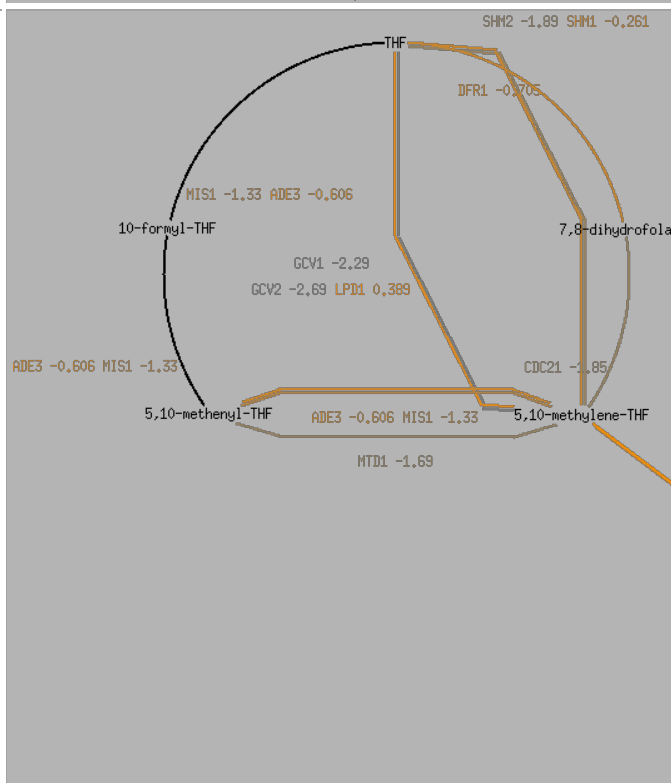
folate biosynthesis

GTP
FOL2 0.067
dihydroneopterin triphosphate
dihydroneopterin phosphate
dihydroneopterin
FOL1 0.356
2-amino-4-hydroxy-6-hydroxymethyl-7,8-dihydropteridine
chorismate
ABZ1 0.0114
FOL1 0.356
4-amino-4-deoxychorismate
2-amino-4-hydroxy-6-hydroxymethyl-7,8-dihydropteridine diphosphate
ABZ2 0.0606
p-aminobenzoate
FOL1 0.356
7,8-dihydropteroate
FOL3 -0.403
7,8-dihydrofolate
DFR1 -0.705   CDC21 -1.85
SHM2 -1.89 SHM1 -0.261
MET12 -0.0735
MET13 0.924 5-methyl-THF
THF
GCV1 -2.29   5,10-methylene-THF
GCV2 -2.69 LPD1 0.389
MIS1 -1.33 ADE3 -0.606
ADE3 -0.606 MIS1 -1.33   MTD1 -1.69
10-formyl-THF
5,10-methenyl-THF
ADE3 -0.606 MIS1 -1.33

aminodeoxychorismate synthase	ABZ1
GTP-cyclohydrolase I	FOL2
aminodeoxychorismate lyase	ABZ2
2-amino-4-hydroxy-6-hydroxymethyldihydropteridine pyrophosphokinase [multifunctional]	FOL1
dihydrofolate synthase	FOL3
dihydrofolate reductase	DFR1
glycine cleavage complex	GCV1 GCV2 LPD1
Serine hydroxymethyltransferase, mitochondrial	SHM1
serine hydroxymethyltransferase	SHM2
thymidylate synthase	CDC21
MTHFR	MET13
MTHFR	MET12
NAD-dependent 5,10-methylenetetrahydrofolate dehydrogenase	MTD1
C1-tetrahydrofolate synthase	ADE3
mitochondrial C1-tetrahydrofolate synthase	MIS1

de novo biosynthesis of purine nucleotides		phosphoribosylpyrophosphate amidotransferase	ADE4
		glycinamide ribotide transformylase	ADE8
		5'-phosphoribosylformyl glycinamidine synthetase	ADE6
		phosphoribosylglycinamidine synthetase / phopshoribosylaminoimidazole synthetase	ADE5,7
		phosphoribosylaminoimidazole-carboxylase	ADE2
		phosphoribosyl amino imidazolesuccinocarbozamide synthetase	ADE1
		inosine monophosphate cyclohydrolase [multifunctional]	ADE16
		inosine monophosphate cyclohydrolase [multifunctional]	ADE17
		IMP dehydrogenase	IMD2
		IMP dehydrogenase	IMD3
		IMP dehydrogenase	IMD4
		GMP synthase	GUA1
		guanylate kinase	GUK1
		adenylosuccinate synthetase	ADE12
		adenylosuccinate lyase	ADE13
		adenylate kinase	ADK1
		mitochondrial GTP:AMP phosphotransferase	ADK2
		ribonucleotide reductase	RNR1 RNR2 RNR3RNR4
		nucleoside diphosphate kinase	YNK1
folate transformations		Serine hydroxymethyltransferase, mitochondrial	SHM1
		serine hydroxymethyltransferase	SHM2
		MTHFR	MET13
		MTHFR	MET12
		glycine cleavage	GCV1 GCV2 L
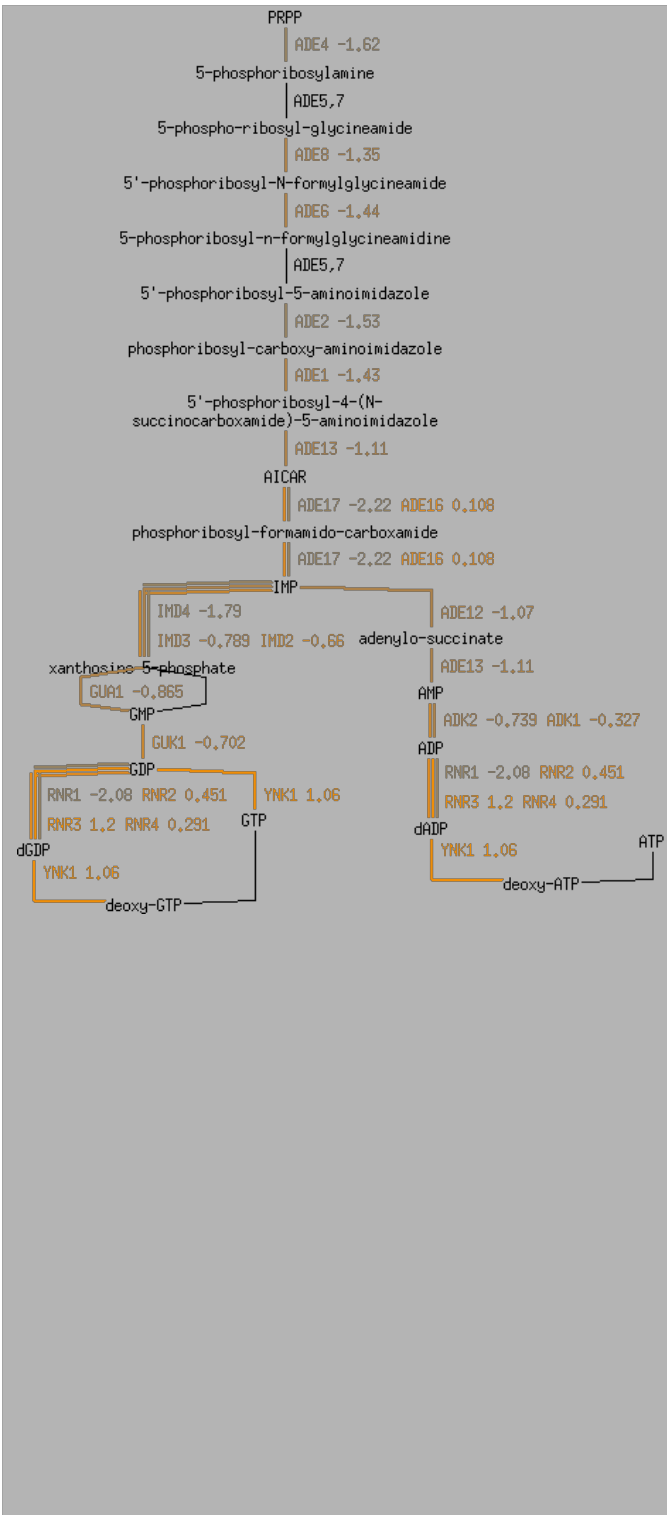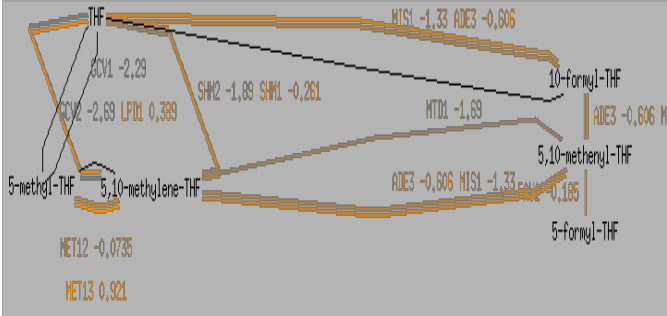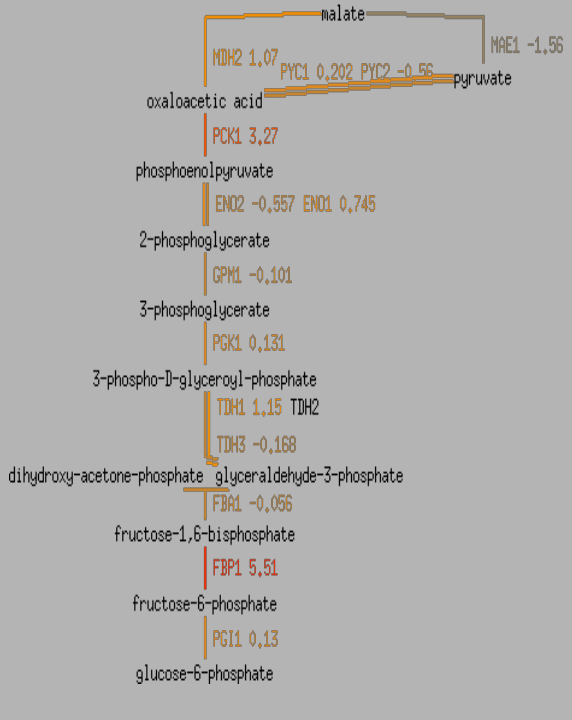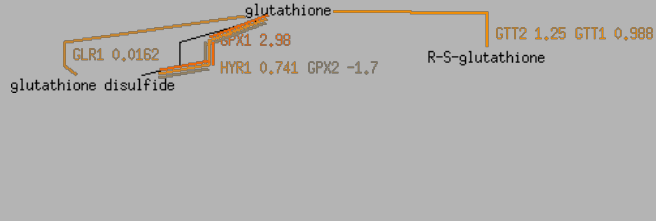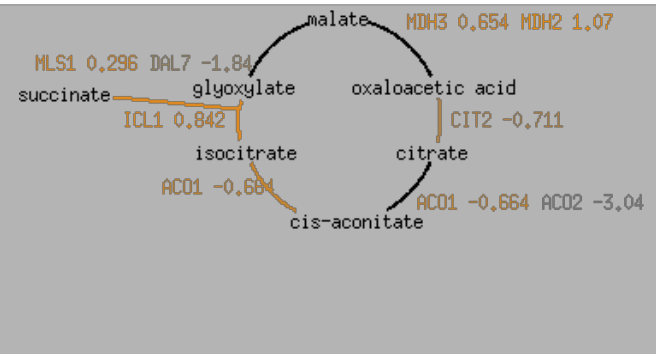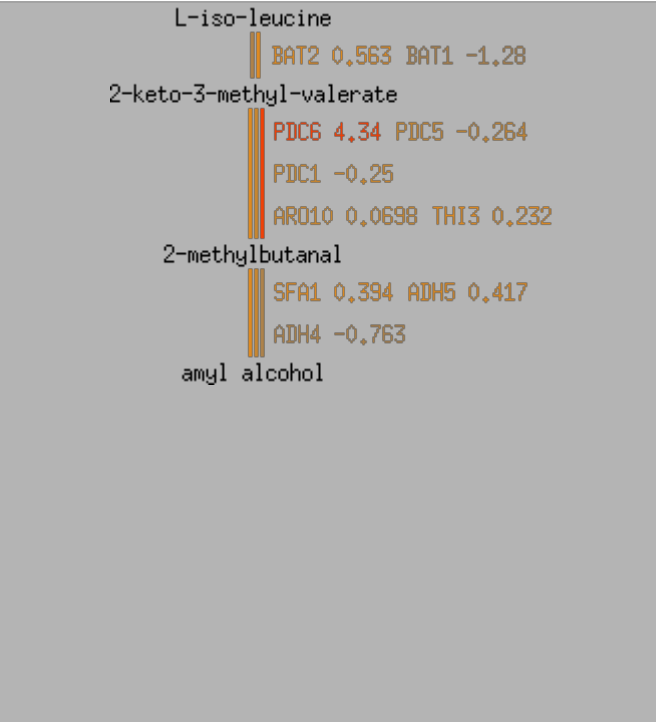
	complex	PD1
	NAD-dependent 5,10-methylenetetrahydrafolate dehydrogenase	MTD1
	mitochondrial C1-tetrahydrofolate synthase	MIS1
	C1-tetrahydrofolate synthase	ADE3
	5,10-methenyltetrahydrofolate synthetase	FAU1
gluconeogenesis		malic enzyme — MAE1
		pyruvate carboxylase — PYC2
		pyruvate carboxylase — PYC1
		cytosolic malate dehydrogenase — MDH2
		phosphoenolpyruvate carboxylkinase — PCK1
		enolase I — ENO1
		enolase — ENO2
		phosphoglycerate mutase — GPM1
		3-phosphoglycerate kinase — PGK1
		glyceraldehyde-3-phosphate dehydrogenase — TDH3
		glyceraldehyde 3-phosphate dehydrogenase — TDH2
		glyceraldehyde-3-phosphate dehydrogenase — TDH1
		aldolase — FBA1
		fructose-1,6-bisphosphatase — FBP1
		glucose-6-phosphate isomerase — PGI1
arginine degradation (anaerobic)		arginase — CAR1
		ornithine aminotransferase — CAR2
		delta 1-pyrroline-5-carboxylate reductase — PRO3

allantoin degradation	allantoin 　DAL1 -2.15 allantoate 　DAL2 -0.431 (S)-Ureidoglycolate 　DAL3 -1.03 urea 　DUR1,2 Urea-1-carboxylate 　DUR1,2 CO_2	allantoinase　DAL1 allantoicase　DAL2 ureidoglycolate hydrolase　DAL3 urea carboxylase / allophanate hydrolase　DUR1,2
leucine biosynthesis	2-keto-isovalerate 　LEU9 -2.54 LEU4 -0.419 2-isopropylmalate 　LEU1 -0.926 3-isopropylmalate 　LEU2 -0.886 a-ketoisocaproate 　BAT2 0.563 BAT1 -1.28 L-leucine	alpha-isopropylmalate synthase　LEU4 alpha-isopropylmalate synthase, minor isozyme　LEU9 isopropylmalate isomerase　LEU1 beta-IPM dehydrogenase　LEU2 branched-chain amino acid aminotransferase　BAT1 branched-chain amino acid transaminase　BAT2
valine degradation	L-valine 　BAT2 0.563 BAT1 -1.28 2-keto-isovalerate 　PDC6 4.34 PDC5 -0.264 　PDC1 -0.25 isobutanal 　SFA1 0.394 ADH5 0.417 　ADH4 -0.763 isobutyl alcohol	branched-chain amino acid aminotransferase　BAT1 branched-chain amino acid transaminase　BAT2 pyruvate decarboxylase / decarboxylase　PDC1 pyruvate decarboxylase / decarboxylase　PDC5 pyruvate decarboxylase / decarboxylase　PDC6 alcohol dehydrogenase　ADH1 alcohol dehydrogenase　ADH2 alcohol dehydrogenase　ADH3 alcohol dehydrogenase　ADH4 alcohol dehydrogenase　ADH5 formaldehyde dehydrogenase / alcohol dehydrogenase　SFA1
citrulline biosynthesis	L-glutamine 　CPA1 -0.846 CPA2 -1.31 carbamoyl-phosphate 　ARG3 -3.02 citrulline	carbamoyl phosphate synthetase　CPA1 CPA2 ornithine carbamoyltransferase　ARG3
serine biosynthesis from 3-phosphoglycerate	3-phosphoglycerate 　SER33 0.522 SER3 -2.11 3-phospho-hydroxypyruvate 　SER1 -0.612 3-phospho-serine 　SER2 -1.25 L-serine	3-phosphoglycerate dehydrogenase　SER3 3-phosphoglycerate dehydrogenase　SER33 phosphoserine transaminase　SER1 phosphoserine phosphatase　SER2

glutathione-glutaredoxin redox reactions		glutathione oxidoreductase	GLR1
		glutathione transferase	GTT1
		glutathione transferase	GTT2
		Glutathione peroxidase	GPX2
		glutathione-peroxidase	HYR1
		Glutathione peroxidase	GPX1
glyoxylate cycle		cytosolic malate dehydrogenase	MDH2
		peroxisome malate dehydrogenase	MDH3
		citrate synthase	CIT2
		aconitate hydratase	ACO2
		aconitase	ACO1
		isocitrate lyase	ICL1
		malate synthase 2	DAL7
		malate synthase	MLS1
isoleucine degradation		branched-chain amino acid aminotransferase	BAT1
		branched-chain amino acid transaminase	BAT2
		ketoisocaproate decarboxylase / decarboxylase	THI3
		decarboxylase	ARO10
		pyruvate decarboxylase / decarboxylase	PDC1
		pyruvate decarboxylase / decarboxylase	PDC5
		pyruvate decarboxylase / decarboxylase	PDC6
		alcohol dehydrogenase	ADH1
		alcohol dehydrogenase	ADH2
		alcohol dehydrogenase	ADH3
		alcohol dehydrogenase	ADH4
		alcohol dehydrogenase	ADH5
		formaldehyde dehydrogenase / alcohol dehydrogenase	SFA1

de novo biosynthesis of pyrimidine ribonucleotides		carbamyl phosphate synthase / aspartate transcarbamylase	URA2
		dihydrooratase	URA4
		dihydroorotate dehydrogenase	URA1
		orotate phosphoribosyltransferase	URA10
		orotate phosphoribosyltransferase	URA5
		orotidine-5'-phosphate decarboxylase	URA3
		uridylate kinase	URA6
		CTP synthase	URA7
		CTP synthase	URA8
acetoin biosynthesis II		pyruvate decarboxylase / decarboxylase	PDC1
		pyruvate decarboxylase / decarboxylase	PDC5
		pyruvate decarboxylase / decarboxylase	PDC6
sucrose degradation		invertase	SUC2
glycine biosynthesis from glyoxylate		alanine:glyoxylate aminotransferase	AGX1
phenylalanine degradation		aromatic amino acid aminotransferase I	ARO8
		aromatic amino acid aminotransferase II	ARO9
		pyruvate decarboxylase / decarboxylase	PDC1
		pyruvate decarboxylase / decarboxylase	PDC5
		pyruvate decarboxylase / decarboxylase	PDC6
		decarboxylase	ARO10
		alcohol dehydrogenase	ADH1
		alcohol dehydrogenase	ADH2
		alcohol dehydrogenase	ADH3
		alcohol dehydrogenase	ADH4
		alcohol dehydrogenase	ADH5
		formaldehyde dehydrogenase / alcohol dehydrogenase	SFA1

beta-alanine biosynthesis	spermine FMS1 0.784 3-aminopropanal ALD3 2.75 ALD2 0.717 b-alanine	amine oxidase	FMS1
		aldehyde dehydrogenase (stress inducible cytoplasmic)	ALD2
		aldehyde dehydrogenase (stress inducible cytoplasmic)	ALD3
fatty acid oxidation pathway	acyl$_n$-2-CoA FAA1 -0.115 FAA4 0.472 FAA3 -1.31 FAA2 0.376 FAT1 ... a fatty acid POT1 2.84 an acyl-CoA a 3-oxoacyl-CoA POX1 0.428 FOX2 0.946 a (3S)-3-hydroxyacyl-CoA trans-2-enoyl-CoA FOX2 0.946 DCI1 -0.451 ECI1 0.475 a cis-3-enoyl-CoA	fatty acid transporter	FAT1
		acyl-CoA synthetase	FAA2
		acyl-CoA synthase	FAA3
		long chain fatty acyl:CoA synthetase	FAA4
		long chain fatty acyl:CoA synthetase	FAA1
		d3,d2-Enoyl-CoA Isomerase	ECI1
		delta(3,5)-delta(2,4)-dienoyl-CoA isomerase	DCI1
		fatty-acyl coenzyme A oxidase	POX1
		3-hydroxyacyl-CoA dehydrogenase	FOX2
		3-oxoacyl CoA thiolase	POT1
superpathway of glutamate biosynthesis	isocitrate IDP3 0.987 IDP2 3.06 NH$_3$ IDP1 -0.617 GLN1 0.231 2-oxoglutarate —— L-glutamine GLT1 -1.2 NH$_3$ 2-oxoglutarate GDH1 -0.797 GDH3 1.83 L-glutamate	NADP-dependent isocitrate dehydrogenase	IDP1
		NADP-dependent isocitrate dehydrogenase	IDP2
		NADP-dependent isocitrate dehydrogenase	IDP3
		glutamine synthetase	GLN1
		NADP-dependent glutamate dehydrogenase	GDH3
		NADP-dependent glutamate dehydrogenase	GDH1
		glutamate synthase (NADH)	GLT1
oxidative branch of the pentose phosphate pathway	glucose-6-phosphate ZWF1 1.13 D-6-phospho-glucono-d-lactone SOL4 1.28 SOL3 -1.26 6-phospho-D-gluconate GND1 -0.67 GND2 2.09 ribulose-5-phosphate	glucose-6-phosphate dehydrogenase	ZWF1
		6-phosphogluconolactonase	SOL3
		6-phosphogluconolactonase	SOL4
		6-phosphogluconate dehydrogenase	GND2
		6-phosphogluconate dehydrogenase, decarboxylating	GND1

superpathway of glucose fermentation		hexokinase II	HXK2
		hexokinase I	HXK1
		glucokinase	GLK1
		glucose-6-phosphate isomerase	PGI1
		phosphofructokinase	PFK1 PFK2
		aldolase	FBA1
		triosephosphate isomerase	TPI1
		glyceraldehyde-3-phosphate dehydrogenase	TDH3
		glyceraldehyde 3-phosphate dehydrogenase	TDH2
		glyceraldehyde-3-phosphate dehydrogenase	TDH1
		3-phosphoglycerate kinase	PGK1
		phosphoglycerate mutase	GPM1
		enolase I	ENO1
		enolase	ENO2
		pyruvate kinase	CDC19
		pyruvate kinase	PYK2
		pyruvate decarboxylase / decarboxylase	PDC1
		pyruvate decarboxylase / decarboxylase	PDC5
		pyruvate decarboxylase / decarboxylase	PDC6
		aldehyde dehydrogenase (stress inducible cytoplasmic)	ALD2
		aldehyde dehydrogenase (major mitochondrial)	ALD4
		aldehyde dehydrogenase (minor mitochondrial)	ALD5
		aldehyde dehydrogenase (major cytoplasmic)	ALD6
		alcohol dehydrogenase	ADH1
		alcohol dehydrogenase	ADH2
		alcohol dehydrogenase	ADH3
		alcohol dehydrogenase	ADH4
		alcohol dehydrogenase	ADH5
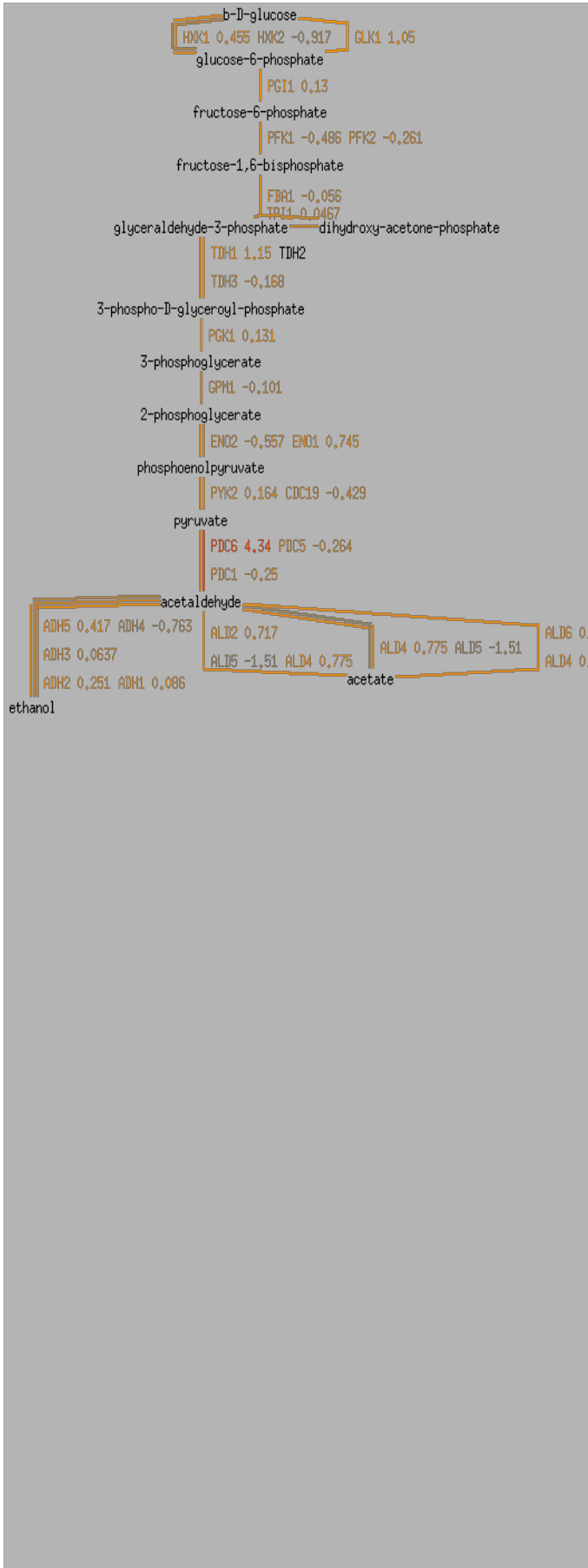
tryptophan degradation		aromatic amino acid aminotransferase I	ARO8
		aromatic amino acid aminotransferase II	ARO9
		pyruvate decarboxylase / decarboxylase	PDC1
		pyruvate decarboxylase / decarboxylase	PDC5
		pyruvate decarboxylase / decarboxylase	PDC6
		decarboxylase	ARO10
		alcohol dehydrogenase	ADH1
		alcohol dehydrogenase	ADH2
		alcohol dehydrogenase	ADH3
		alcohol dehydrogenase	ADH4
		alcohol dehydrogenase	ADH5
		formaldehyde dehydrogenase / alcohol dehydrogenase	SFA1
salvage pathways of pyrimidine ribonucleotides		cytidine deaminase	CDD1
		deoxycytidine kinase / cytidine kinase / uridine kinase	URK1
		nicotinic acid riboside hydrolase [multifunctional]	URH1
		cytosine deaminase	FCY1
		UPRTase	FUR1
		nucleoside diphosphate kinase	YNK1
removal of superoxide radicals		cytoplasmic superoxide dismutase	SOD1
		mitochondrial superoxide dismutase	SOD2
		catalase A	CTA1
		catalase T	CTT1

de novo biosynthesis of pyrimidine deoxyribonucleotides		ribonucleotide reductase	RNR1 RNR2 RNR3 RNR4
		dUTP pyrophosphatase	DUT1
		thymidylate synthase	CDC21
		uridylate kinase / thymidylate kinase	CDC8
		nucleoside diphosphate kinase	YNK1

non-oxidative branch of the pentose phosphate pathway		D-ribulose-5-Phosphate 3-epimerase	RPE1
		ribose-5-phosphate ketol-isomerase	RKI1
		transketolase	TKL2
		transaldolase	TAL1
		transketolase	TKL1
TCA cycle, aerobic respiration		pyruvate carboxylase	PYC2
		pyruvate carboxylase	PYC1
		mitochondrial malate dehydrogenase	MDH1
		citrate synthase	CIT1
		citrate synthase	CIT3
		aconitate hydratase	ACO2
		aconitase	ACO1
		NAD-dependent isocitrate dehydrogenase	IDH1 IDH2
		2-ketoglutarate dehydrogenase complex	LPD1 KGD1 KGD2
		succinyl-CoA ligase	LSC1 LSC2
		succinate dehydrogenase (ubiquinone)	SDH4 SDH3 SDH2 SDH1
		minor succinate dehydrogenase (ubiquinone)	SDH4 SDH3 SDH2 YJL045W
		fumarate hydralase	FUM1
myo-inositol biosynthesis		L-myo-inositol-1-phosphate synthase	INO1
		inositol monophosphatase	INM1
		inositol monophosphate	INM2
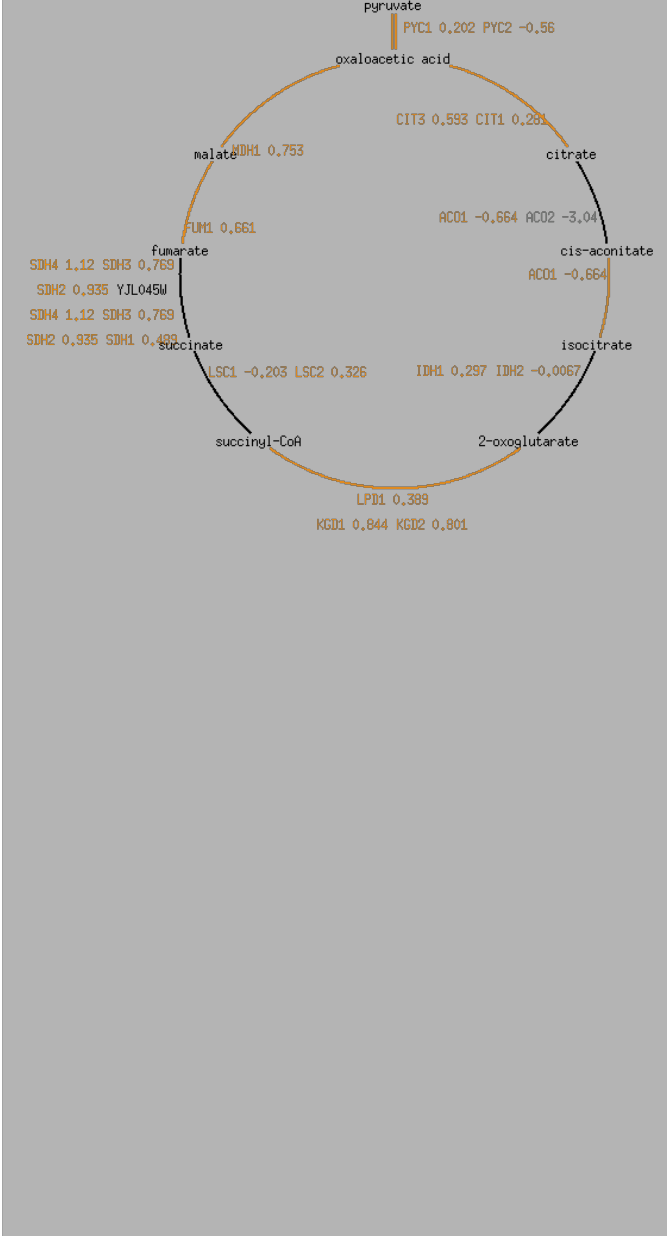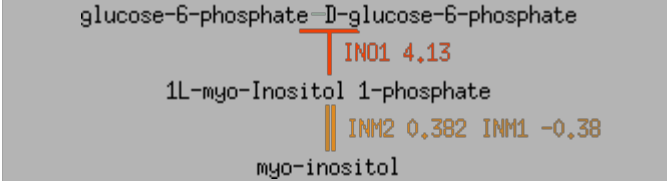
SI Table 2. Differentially expressed genes 2 h after limonene exposure. Genes are categorized based on either cellular compartments and/or biological processes.

Gene	Description	FC [a]	P value [b]
Cell wall cellular compartment			
Cytokinesis			
XBP1	Transcriptional repressor that binds to promoter sequences of the cyclin genes, CYS3, and SMF2; expression is induced by stress or starvation during mitosis, and late in meiosis; member of the Swi4p/Mbp1p family; potential Cdc28p substrate, XBP1	2.1	2.58E-05
AFR1	Alpha-factor pheromone receptor regulator, negatively regulates pheromone receptor signaling; required for normal mating projection (shmoo) formation; required for Spa2p to recruit Mpk1p to shmoo tip during mating; interacts with Cdc12p, AFR1	1.9	1.81E-04
MET30	F-box protein containing five copies of the WD40 motif, controls cell cycle function, sulfur metabolism, and methionine biosynthesis as part of the ubiquitin ligase complex; interacts with and regulates Met4p, localizes within the nucleus, MET30	1.6	2.18E-03
DSE4	Daughter cell-specific secreted protein with similarity to glucanases, degrades cell wall from the daughter side causing daughter to separate from mother, DSE4	-1.9	2.50E-04
GAS2	1,3-beta-glucanosyltransferase, involved with Gas4p in spore wall assembly; has similarity to Gas1p, GAS2	-2.0	8.47E-04
EGT2	Glycosylphosphatidylinositol (GPI)-anchored cell wall endoglucanase required for proper cell separation after cytokinesis, expression is activated by Swi5p and tightly regulated in a cell cycle-dependent manner, EGT2	-2.1	7.20E-03
SUN4	Cell wall protein related to glucanases, possibly involved in cell wall septation; member of the SUN family, SUN4	-2.2	1.47E-04
GAS3	Putative 1,3-beta-glucanosyltransferase, has similarity to Gas1p; localizes to the cell wall, GAS3	-2.3	6.04E-04
CTS1	Endochitinase, required for cell separation after mitosis; transcriptional activation during late G and early M cell cycle phases is mediated by transcription factor Ace2p, CTS1	-2.4	9.10E-04
UTR2	Cell wall protein that functions in the transfer of chitin to beta(1-6)glucan; putative chitin transglycosidase; glycosylphosphatidylinositol (GPI)-anchored protein localized to the bud neck; has a role in cell wall maintenance, UTR2	-2.6	3.22E-04
SCW11	Cell wall protein with similarity to glucanases; may play a role in conjugation during mating based on its regulation by Ste12p, SCW11	-3.0	3.29E-04
DSE1	Daughter cell-specific protein, may participate in	-3.1	1.03E-

	pathways regulating cell wall metabolism; deletion affects cell separation after division and sensitivity to drugs targeted against the cell wall, DSE1		03
DSE2	Daughter cell-specific secreted protein with similarity to glucanases, degrades cell wall from the daughter side causing daughter to separate from mother; expression is repressed by cAMP, DSE2	-3.2	7.35E-04
SPS4	Protein whose expression is induced during sporulation; not required for sporulation; heterologous expression in E. coli induces the SOS response that senses DNA damage, SPS4	-3.7	3.24E-06
Cell wall organization			
YGP1	Cell wall-related secretory glycoprotein; induced by nutrient deprivation-associated growth arrest and upon entry into stationary phase; may be involved in adaptation prior to stationary phase entry; has similarity to Sps100p, YGP1	4.0	1.13E-07
PIR3	O-glycosylated covalently-bound cell wall protein required for cell wall stability; expression is cell cycle regulated, peaking in M/G1 and also subject to regulation by the cell integrity pathway, PIR3	5.0	9.39E-07
FIT2	Mannoprotein that is incorporated into the cell wall via a glycosylphosphatidylinositol (GPI) anchor, involved in the retention of siderophore-iron in the cell wall, FIT2	2.0	6.39E-05
TIP1	Major cell wall mannoprotein with possible lipase activity; transcription is induced by heat- and cold-shock; member of the Srp1p/Tip1p family of serine-alanine-rich proteins, TIP1	2.1	1.44E-04
YPK2	Protein kinase with similarityto serine/threonine protein kinase Ypk1p; functionally redundant with YPK1 at the genetic level; participates in a signaling pathway required for optimal cell wall integrity; homolog of mammalian kinase SGK, YPK2	1.8	5.36E-04
SPI1	GPI-anchored cell wall protein involved in weak acid resistance; basal expression requires Msn2p/Msn4p; expression is induced under conditions of stress and during the diauxic shift; similar to Sed1p, SPI1	4.7	8.17E-04
SNA3	Integral membrane protein localized to vacuolar intralumenal vesicles, computational analysis of large-scale protein-protein interaction data suggests a possible role in either cell wall synthesis or protein-vacuolar targeting, SNA3	1.2	8.98E-04
FRT2	Tail-anchored endoplasmic reticulum membrane protein, interacts with homolog Frt1p but is not a substrate of calcineurin (unlike Frt1p), promotes growth in conditions of high Na+, alkaline pH, or cell wall stress; potential Cdc28p substrate, FRT2	1.7	3.36E-03
USV1	Putative transcription factor containing a C2H2 zinc finger; mutation affects transcriptional regulation of genes	1.2	4.26E-03

	involved in protein folding, ATP binding, and cell wall biosynthesis, USV1		
PST1	Cell wall protein that contains a putative GPI-attachment site; secreted by regenerating protoplasts; up-regulated by activation of the cell integrity pathway, as mediated by Rlm1p; upregulated by cell wall damage via disruption of FKS1, PST1	1.9	4.73E-03
ECM4	Omega class glutathione transferase; not essential; similar to Ygr154cp; green fluorescent protein (GFP)-fusion protein localizes to the cytoplasm, ECM4	1.4	2.94E-04
TDH1	Glyceraldehyde-3-phosphate dehydrogenase, isozyme 1, involved in glycolysis and gluconeogenesis; tetramer that catalyzes the reaction of glyceraldehyde-3-phosphate to 1,3 bis-phosphoglycerate; detected in the cytoplasm and cell wall [Source:SGD;Acc:S000003588]	1.1	5.38E-03
FIT3	Mannoprotein that is incorporated into the cell wall via a glycosylphosphatidylinositol (GPI) anchor, involved in the retention of siderophore-iron in the cell wall, FIT3	1.7	5.54E-03
Hsp150	O-mannosylated heat shock protein that is secreted and covalently attached to the cell wall via beta-1,3-glucan and disulfide bridges; required for cell wall stability; induced by heat shock, oxidative stress, and nitrogen limitation, HSP150	1.0	6.70E-03
CWP1	Cell wall mannoprotein, linked to a beta-1,3- and beta-1,6-glucan heteropolymer through a phosphodiester bond; involved in cell wall organization, CWP1	1.1	7.41E-03
YPS6	Putative GPI-anchored aspartic protease, YPS6	1.2	8.35E-03
GSC2	Catalytic subunit of 1,3-beta-glucan synthase, involved in formation of the inner layer of the spore wall; activity positively regulated by Rho1p and negatively by Smk1p; has similarity to an alternate catalytic subunit, Fks1p (Gsc1p), GSC2	1.6	1.04E-03
RIM21	Component of the RIM101 pathway, has a role in cell wall construction and alkaline pH response; has similarity to A. nidulans PalH, RIM21	1.1	5.03E-03
SLT2	Serine/threonine MAP kinase involved in regulating the maintenance of cell wall integrity and progression through the cell cycle; regulated by the PKC1-mediated signaling pathway,	0.9	0.057308
MLP1	Protein kinase implicated in the Slt2p mitogen-activated (MAP) kinase signaling pathway; associates with Rlm1p, ---	2.1	1.38E-03
ECM4	Omega class glutathione transferase; not essential; similar to Ygr154cp; green fluorescent protein (GFP)-fusion protein localizes to the cytoplasm, ECM4	1.4	2.94E-04
FBP26	Fructose-2,6-bisphosphatase, required for glucose metabolism	1.4	7.85E-04
Transmembrane transport			

AGP3	Low-affinity amino acid permease, may act to supply the cell with amino acids as nitrogen source in nitrogen-poor conditions; transcription is induced under conditions of sulfur limitation, AGP3	5.1	3.92E-06
MUP1	High affinity methionine permease, integral membrane protein with 13 putative membrane-spanning regions; also involved in cysteine uptake, MUP1	4.6	1.75E-04
YCT1	High-affinity cysteine-specific transporter with similarity to the Dal5p family of transporters; green fluorescent protein (GFP)-fusion protein localizes to the endoplasmic reticulum; YCT1 is not an essential gene, YCT1	4.3	3.25E-04
HXT5	Hexose transporter with moderate affinity for glucose, induced in the presence of non-fermentable carbon sources, induced by a decrease in growth rate, contains an extended N-terminal domain relative to other HXTs,	3.9	8.32E-06
STL1	Glycerol proton symporter of the plasma membrane, subject to glucose-induced inactivation, strongly but transiently induced when cells are subjected to osmotic shock, STL1	3.9	2.35E-03
PDR15	Plasma membrane ATP binding cassette (ABC) transporter, multidrug transporter and general stress response factor implicated in cellular detoxification; regulated by Pdr1p, Pdr3p and Pdr8p; promoter contains a PDR responsive element, PDR15	3.2	4.08E-04
MMP1	High-affinity S-methylmethionine permease, required for utilization of S-methylmethionine as a sulfur source; has similarity to S-adenosylmethionine permease Sam3p, MMP1	2.3	1.05E-03
SAM3	High-affinity S-adenosylmethionine permease, required for utilization of S-adenosylmethionine as a sulfur source; has similarity to S-methylmethionine permease Mmp1p, SAM3	2.2	1.71E-03
JEN1	Lactate transporter, required for uptake of lactate and pyruvate; phosphorylated; expression is derepressed by transcriptional activator Cat8p during respiratory growth, and repressed in the presence of glucose, fructose, and mannose, JEN1	2.2	2.20E-03
JEN1	Lactate transporter, required for uptake of lactate and pyruvate; phosphorylated; expression is derepressed by transcriptional activator Cat8p during respiratory growth, and repressed in the presence of glucose, fructose, and mannose, JEN1	2.2	2.20E-03
CSR2	Nuclear protein with a potential regulatory role in utilization of galactose and nonfermentable carbon sources; overproduction suppresses the lethality at high temperature of a chs5 spa2 double null mutation; potential Cdc28p substrate, CSR2	2.1	3.02E-05
PDR5	Plasma membrane ATP-binding cassette (ABC) transporter, short-lived multidrug transporter actively regulated by Pdr1p; also involved in steroid transport,	2.0	3.66E-03

	cation resistance, and cellular detoxification during exponential growth, PDR5		
MUP3	Low affinity methionine permease, similar to Mup1p, MUP3	1.9	8.15E-04
YOR1	Plasma membrane ATP-binding cassette (ABC) transporter, multidrug transporter mediates export of many different organic anions including oligomycin, YOR1	1.7	8.81E-03
ALP1	Arginine transporter; expression is normally very low and it is unclear what conditions would induce significant expression, ALP1	1.2	3.81E-03
ZRT1	High-affinity zinc transporter of the plasma membrane, responsible for the majority of zinc uptake; transcription is induced under low-zinc conditions by the Zap1p transcription factor, ZRT1	-1.1	7.69E-03
PDR12	Plasma membrane ATP-binding cassette (ABC) transporter, weak-acid-inducible multidrug transporter required for weak organic acid resistance; induced by sorbate and benzoate and regulated by War1p; mutants exhibit sorbate hypersensitivity, PDR12	-1.5	8.27E-04
Redox processes			
JLP1	Fe(II)-dependent sulfonate/alpha-ketoglutarate dioxygenase, involved in sulfonate catabolism for use as a sulfur source, contains sequence that closely resembles a J domain (typified by the E. coli DnaJ protein), JLP1	6.7	1.80E-05
OYE3	Widely conserved NADPH oxidoreductase containing flavin mononucleotide (FMN), homologous to Oye2p with slight differences in ligand binding and catalytic properties; may be involved in sterol metabolism, OYE3	3.6	9.43E-05
IDP2	Cytosolic NADP-specific isocitrate dehydrogenase, catalyzes oxidation of isocitrate to alpha-ketoglutarate; levels are elevated during growth on non-fermentable carbon sources and reduced during growth on glucose, IDP2	3.1	1.51E-04
GPX1	Phospholipid hydroperoxide glutathione peroxidase induced by glucose starvation that protects cells from phospholipid hydroperoxides and nonphospholipid peroxides during oxidative stress, GPX1	3.0	8.70E-03
IRC15	Putative S-adenosylmethionine-dependent methyltransferase of the seven beta-strand family; null mutant displays increased levels of spontaneous Rad52 foci, ---	2.9	5.70E-05
NDE2	Mitochondrial external NADH dehydrogenase, catalyzes the oxidation of cytosolic NADH; Nde1p and Nde2p are involved in providing the cytosolic NADH to the mitochondrial respiratory chain, NDE2	2.7	9.11E-06
HMX1	ER localized, heme-binding peroxidase involved in the degradation of heme; does not exhibit heme oxygenase activity despite similarity to heme oxygenases; expression	2.5	9.76E-03

	regulated by AFT1, HMX1		
FMO1	Flavin-containing monooxygenase, localized to the cytoplasmic face of the ER membrane; catalyzes oxidation of biological thiols to maintain the ER redox buffer ratio for correct folding of disulfide-bonded proteins, FMO1	2.4	1.45E-04
GRE2	NADPH-dependent methylglyoxal reductase (D-lactaldehyde dehydrogenase); stress induced (osmotic, ionic, oxidative, heat shock and heavy metals); regulated by the HOG pathway, GRE2	2.2	3.38E-03
GTO1	Omega-class glutathione transferase; induced under oxidative stress; putative peroxisomal localization, GTO1	2.2	9.17E-05
CTT1	Cytosolic catalase T, has a role in protection from oxidative damage by hydrogen peroxide, CTT1	2.2	1.98E-04
GND2	6-phosphogluconate dehydrogenase (decarboxylating), catalyzes an NADPH regenerating reaction in the pentose phosphate pathway; required for growth on D-glucono-delta-lactone, GND2	2.1	1.28E-04
FRE5	Putative ferric reductase with similarity to Fre2p; expression induced by low iron levels; the authentic, non-tagged protein is detected in highly purified mitochondria in high-throughput studies, FRE5	2.1	9.73E-04
FMP46	Putative redox protein containing a thioredoxin fold; the authentic, non-tagged protein is detected in highly purified mitochondria in high-throughput studies, FMP46	2.0	5.29E-03
YHB1	Nitric oxide oxidoreductase, flavohemoglobin involved in nitric oxide detoxification; plays a role in the oxidative and nitrosative stress responses, YHB1	1.9	4.92E-03
OLE1	Delta(9) fatty acid desaturase, required for monounsaturated fatty acid synthesis and for normal distribution of mitochondria, OLE1	1.9	3.32E-04
MET8	Bifunctional dehydrogenase and ferrochelatase, involved in the biosynthesis of siroheme, a prosthetic group used by sulfite reductase; required for sulfate assimilation and methionine biosynthesis, MET8	1.9	4.47E-04
GDH3	NADP(+)-dependent glutamate dehydrogenase, synthesizes glutamate from ammonia and alpha-ketoglutarate; rate of alpha-ketoglutarate utilization differs from Gdh1p; expression regulated by nitrogen and carbon sources, GDH3	1.8	5.97E-04
MXR1	Peptide methionine sulfoxide reductase, reverses the oxidation of methionine residues; involved in oxidative damage repair, providing resistance to oxidative stress and regulation of lifespan, MXR1	1.8	1.94E-03
BDH2	Putative medium-chain alcohol dehydrogenase with similarity to BDH1; transcription induced by constitutively active PDR1 and PDR3; BDH2 is an essential gene, BDH2	1.7	3.83E-03
YKL107W	Putative protein of unknown function, ---	1.6	5.03E-

			04
TRX3	Mitochondrial thioredoxin, highly conserved oxidoreductase required to maintain the redox homeostasis of the cell, forms the mitochondrial thioredoxin system with Trr2p, redox state is maintained by both Trr2p and Glr1p, TRX3	1.6	2.39E-03
HBN1	Putative protein of unknown function; similar to bacterial nitroreductases; green fluorescent protein (GFP)-fusion protein localizes to the cytoplasm and nucleus, HBN1	1.5	2.10E-04
YDL124W	NADPH-dependent alpha-keto amide reductase; reduces aromatic alpha-keto amides, aliphatic alpha-keto esters, and aromatic alpha-keto esters; member of the aldo-keto reductase (AKR) family, ---	1.5	4.20E-04
ECM4	Omega class glutathione transferase; not essential; similar to Ygr154cp; green fluorescent protein (GFP)-fusion protein localizes to the cytoplasm, ECM4	1.4	2.94E-04
GUT2	Mitochondrial glycerol-3-phosphate dehydrogenase; expression is repressed by both glucose and cAMP and derepressed by non-fermentable carbon sources in a Snf1p, Rsf1p, Hap2/3/4/5 complex dependent manner, GUT2	1.3	4.40E-03
MCR1	Mitochondrial NADH-cytochrome b5 reductase, involved in ergosterol biosynthesis, MCR1	1.3	1.58E-03
RPH1	JmjC domain-containing histone demethylase which can specifically demethylate H3K36 tri- and dimethyl modification states; transcriptional repressor of PHR1; Rph1p phosphorylation during DNA damage is under control of the MEC1-RAD53 pathway, RPH1	1.3	7.43E-03
AAD6	Putative aryl-alcohol dehydrogenase with similarity to P. chrysosporium aryl-alcohol dehydrogenase, involved in the oxidative stress response, AAD6	1.2	7.73E-03
RNR3	Ribonucleotide-diphosphate reductase (RNR), large subunit; the RNR complex catalyzes the rate-limiting step in dNTP synthesis and is regulated by DNA replication and DNA damage checkpoint pathways via localization of the small subunits, RNR3	1.2	8.96E-03
GDH2	NAD(+)-dependent glutamate dehydrogenase, degrades glutamate to ammonia and alpha-ketoglutarate; expression sensitive to nitrogen catabolite repression and intracellular ammonia levels, GDH2	1.1	1.67E-03
OYE2	Widely conserved NADPH oxidoreductase containing flavin mononucleotide (FMN), homologous to Oye3p with slight differences in ligand binding and catalytic properties; may be involved in sterol metabolism, OYE2	1.1	4.40E-03
FRE6	Putative ferric reductase with similarity to Fre2p; expression induced by low iron levels, FRE6	1.1	7.08E-03
UGA2	Succinate semialdehyde dehydrogenase involved in the utilization of gamma-aminobutyrate (GABA) as a nitrogen source; part of the 4-aminobutyrate and	1.1	5.39E-03

	glutamate degradation pathways; localized to the cytoplasm, UGA2		
FAS2	Alpha subunit of fatty acid synthetase, which catalyzes the synthesis of long-chain saturated fatty acids; contains beta-ketoacyl reductase and beta-ketoacyl synthase activities; phosphorylated, FAS2	1.1	6.48E-03
PRX1	Mitochondrial peroxiredoxin (1-Cys Prx) with thioredoxin peroxidase activity, has a role in reduction of hydroperoxides; induced during respiratory growth and under conditions of oxidative stress; phosphorylated, PRX1	1.1	2.76E-03
GTT1	ER associated glutathione S-transferase capable of homodimerization; expression induced during the diauxic shift and throughout stationary phase; functional overlap with Gtt2p, Grx1p, and Grx2p, GTT1	1.0	9.16E-03
HTD2	Mitochondrial 3-hydroxyacyl-thioester dehydratase involved in fatty acid biosynthesis, required for respiratory growth and for normal mitochondrial morphology, HTD2	1.0	3.55E-03
LOT6	FMN-dependent NAD(P)H:quinone reductase that may be involved in quinone detoxification; gene expression increases in cultures shifted to a lower temperature, LOT6	0.9	5.86E-03
Biosynthesis of secondary metabolites			
FBP1	Fructose-1,6-bisphosphatase, key regulatory enzyme in the gluconeogenesis pathway, required for glucose metabolism, FBP1	5.5	7.81E-05
PDC6	Minor isoform of pyruvate decarboxylase, decarboxylates pyruvate to acetaldehyde, involved in amino acid catabolism; transcription is glucose- and ethanol-dependent, and is strongly induced during sulfur limitation, PDC6	4.3	3.70E-04
INO1	Inositol 1-phosphate synthase, involved in synthesis of inositol phosphates and inositol-containing phospholipids; transcription is coregulated with other phospholipid biosynthetic genes by Ino2p and Ino4p, which bind the UASINO DNA element, INO1	4.1	7.39E-07
AGX1	Alanine:glyoxylate aminotransferase (AGT), catalyzes the synthesis of glycine from glyoxylate, which is one of three pathways for glycine biosynthesis in yeast; has similarity to mammalian and plant alanine:glyoxylate aminotransferases, AGX1	3.1	8.96E-06
IDP2	Cytosolic NADP-specific isocitrate dehydrogenase, catalyzes oxidation of isocitrate to alpha-ketoglutarate; levels are elevated during growth on non-fermentable carbon sources and reduced during growth on glucose, IDP2	3.1	1.51E-04
IRC15	Putative S-adenosylmethionine-dependent methyltransferase of the seven beta-strand family; null mutant displays increased levels of spontaneous Rad52	2.9	5.70E-05

	foci, ---		
POT1	3-ketoacyl-CoA thiolase with broad chain length specificity, cleaves 3-ketoacyl-CoA into acyl-CoA and acetyl-CoA during beta-oxidation of fatty acids, POT1	2.8	5.84E-04
CTT1	Cytosolic catalase T, has a role in protection from oxidative damage by hydrogen peroxide, CTT1	2.2	1.98E-04
GND2	6-phosphogluconate dehydrogenase (decarboxylating), catalyzes an NADPH regenerating reaction in the pentose phosphate pathway; required for growth on D-glucono-delta-lactone, GND2	2.1	1.28E-04
MET8	Bifunctional dehydrogenase and ferrochelatase, involved in the biosynthesis of siroheme, a prosthetic group used by sulfite reductase; required for sulfate assimilation and methionine biosynthesis, MET8	1.9	4.47E-04
GAL3	Transcriptional regulator involved in activation of the GAL genes in response to galactose; forms a complex with Gal80p to relieve Gal80p inhibition of Gal4p; binds galactose and ATP but does not have galactokinase activity, GAL3	1.3	2.31E-03
MCR1	Mitochondrial NADH-cytochrome b5 reductase, involved in ergosterol biosynthesis, MCR1	1.3	1.58E-03
ACS1	Acetyl-coA synthetase isoform which, along with Acs2p, is the nuclear source of acetyl-coA for histone acetlyation; expressed during growth on nonfermentable carbon sources and under aerobic conditions, ACS1	1.2	2.15E-03
SDH4	Membrane anchor subunit of succinate dehydrogenase (Sdh1p, Sdh2p, Sdh3p, Sdh4p), which couples the oxidation of succinate to the transfer of electrons to ubiquinone, SDH4	1.1	4.66E-03
YNK1	Nucleoside diphosphate kinase, catalyzes the transfer of gamma phosphates from nucleoside triphosphates, usually ATP, to nucleoside diphosphates by a mechanism that involves formation of an autophosphorylated enzyme intermediate, YNK1	1.1	4.62E-03
SAM2	S-adenosylmethionine synthetase, catalyzes transfer of the adenosyl group of ATP to the sulfur atom of methionine; one of two differentially regulated isozymes (Sam1p and Sam2p), SAM2	0.9	8.18E-03
Small metobolic processes			
PDC6	Minor isoform of pyruvate decarboxylase, decarboxylates pyruvate to acetaldehyde, involved in amino acid catabolism; transcription is glucose- and ethanol-dependent, and is strongly induced during sulfur limitation, PDC6	4.3	3.70E-04
INO1	Inositol 1-phosphate synthase, involved in synthesis of inositol phosphates and inositol-containing phospholipids; transcription is coregulated with other phospholipid biosynthetic genes by Ino2p and Ino4p, which bind the UASINO DNA element, INO1	4.1	7.39E-07

YGP1	Cell wall-related secretory glycoprotein; induced by nutrient deprivation-associated growth arrest and upon entry into stationary phase; may be involved in adaptation prior to stationary phase entry; has similarity to Sps100p, YGP1	4.0	1.13E-07
PDR15	Plasma membrane ATP binding cassette (ABC) transporter, multidrug transporter and general stress response factor implicated in cellular detoxification; regulated by Pdr1p, Pdr3p and Pdr8p; promoter contains a PDR responsive element, PDR15	3.2	4.08E-04
AGX1	Alanine:glyoxylate aminotransferase (AGT), catalyzes the synthesis of glycine from glyoxylate, which is one of three pathways for glycine biosynthesis in yeast; has similarity to mammalian and plant alanine:glyoxylate aminotransferases, AGX1	3.1	8.96E-06
IDP2	Cytosolic NADP-specific isocitrate dehydrogenase, catalyzes oxidation of isocitrate to alpha-ketoglutarate; levels are elevated during growth on non-fermentable carbon sources and reduced during growth on glucose, IDP2	3.1	1.51E-04
POT1	3-ketoacyl-CoA thiolase with broad chain length specificity, cleaves 3-ketoacyl-CoA into acyl-CoA and acetyl-CoA during beta-oxidation of fatty acids, POT1	2.8	5.84E-04
URA10	One of two orotate phosphoribosyltransferase isozymes (see also URA5) that catalyze the fifth enzymatic step in the de novo biosynthesis of pyrimidines, converting orotate into orotidine-5'-phosphate, URA10	2.8	2.39E-03
NDE2	Mitochondrial external NADH dehydrogenase, catalyzes the oxidation of cytosolic NADH; Nde1p and Nde2p are involved in providing the cytosolic NADH to the mitochondrial respiratory chain, NDE2	2.7	9.11E-06
GRE2	NADPH-dependent methylglyoxal reductase (D-lactaldehyde dehydrogenase); stress induced (osmotic, ionic, oxidative, heat shock and heavy metals); regulated by the HOG pathway, GRE2	2.2	3.38E-03
GTO1	Omega-class glutathione transferase; induced under oxidative stress; putative peroxisomal localization, GTO1	2.2	9.17E-05
GND2	6-phosphogluconate dehydrogenase (decarboxylating), catalyzes an NADPH regenerating reaction in the pentose phosphate pathway; required for growth on D-glucono-delta-lactone, GND2	2.1	1.28E-04
MHT1	S-methylmethionine-homocysteine methyltransferase, functions along with Sam4p in the conversion of S-adenosylmethionine (AdoMet) to methionine to control the methionine/AdoMet ratio, MHT1	2.0	8.18E-04
PDR5	Plasma membrane ATP-binding cassette (ABC) transporter, short-lived multidrug transporter actively regulated by Pdr1p; also involved in steroid transport, cation resistance, and cellular detoxification during exponential growth, PDR5	2.0	3.66E-03

OLE1	Delta(9) fatty acid desaturase, required for monounsaturated fatty acid synthesis and for normal distribution of mitochondria, OLE1	1.9	3.32E-04
MET8	Bifunctional dehydrogenase and ferrochelatase, involved in the biosynthesis of siroheme, a prosthetic group used by sulfite reductase; required for sulfate assimilation and methionine biosynthesis, MET8	1.9	4.47E-04
GDH3	NADP(+)-dependent glutamate dehydrogenase, synthesizes glutamate from ammonia and alpha-ketoglutarate; rate of alpha-ketoglutarate utilization differs from Gdh1p; expression regulated by nitrogen and carbon sources, GDH3	1.8	5.97E-04
CAT2	Carnitine acetyl-CoA transferase present in both mitochondria and peroxisomes, transfers activated acetyl groups to carnitine to form acetylcarnitine which can be shuttled across membranes, CAT2	1.7	1.13E-04
YOR1	Plasma membrane ATP-binding cassette (ABC) transporter, multidrug transporter mediates export of many different organic anions including oligomycin, YOR1	1.7	8.81E-03
MET32	Zinc-finger DNA-binding protein, involved in transcriptional regulation of the methionine biosynthetic genes, similar to Met31p, MET32	1.6	4.12E-04
TRX3	Mitochondrial thioredoxin, highly conserved oxidoreductase required to maintain the redox homeostasis of the cell, forms the mitochondrial thioredoxin system with Trr2p, redox state is maintained by both Trr2p and Glr1p, TRX3	1.6	2.39E-03
THI4	Thiazole synthase, catalyzes formation of the thiazole moiety of thiamin pyrophosphate; required for thiamine biosynthesis and for mitochondrial genome stability, THI4	1.6	1.27E-04
MET28	Transcriptional activator in the Cbf1p-Met4p-Met28p complex, participates in the regulation of sulfur metabolism, MET28	1.6	1.74E-04
UBC8	Ubiquitin-conjugating enzyme that negatively regulates gluconeogenesis by mediating the glucose-induced ubiquitination of fructose-1,6-bisphosphatase (FBPase); cytoplasmic enzyme that catalyzes the ubiquitination of histones in vitro, UBC8	1.6	4.67E-03
MET30	F-box protein containing five copies of the WD40 motif, controls cell cycle function, sulfur metabolism, and methionine biosynthesis as part of the ubiquitin ligase complex; interacts with and regulates Met4p, localizes within the nucleus, MET30	1.6	2.18E-03
YKL151C	Putative protein of unknown function; green fluorescent protein (GFP)-fusion protein localizes to the cytoplasm, ---	1.6	2.19E-03
DAP1	Heme-binding protein involved in regulation of cytochrome P450 protein Erg11p; damage response	1.5	8.74E-03

	protein, related to mammalian membrane progesterone receptors; mutations lead to defects in telomeres, mitochondria, and sterol synthesis, DAP1		
MET2	L-homoserine-O-acetyltransferase, catalyzes the conversion of homoserine to O-acetyl homoserine which is the first step of the methionine biosynthetic pathway, MET2	1.5	1.79E-04
YDL124W	NADPH-dependent alpha-keto amide reductase; reduces aromatic alpha-keto amides, aliphatic alpha-keto esters, and aromatic alpha-keto esters; member of the aldo-keto reductase (AKR) family, ---	1.5	4.20E-04
ECM4	Omega class glutathione transferase; not essential; similar to Ygr154cp; green fluorescent protein (GFP)-fusion protein localizes to the cytoplasm, ECM4	1.4	2.94E-04
GSP2	GTP binding protein (mammalian Ranp homolog) involved in the maintenance of nuclear organization, RNA processing and transport; interacts with Kap121p, Kap123p and Pdr6p (karyophilin betas); Gsp1p homolog that is not required for viability, GSP2	1.4	6.29E-04
STF1	Protein involved in regulation of the mitochondrial F1F0-ATP synthase; Stf1p and Stf2p act as stabilizing factors that enhance inhibitory action of the Inh1p protein, STF1	1.3	1.16E-03
GUT2	Mitochondrial glycerol-3-phosphate dehydrogenase; expression is repressed by both glucose and cAMP and derepressed by non-fermentable carbon sources in a Snf1p, Rsf1p, Hap2/3/4/5 complex dependent manner, GUT2	1.3	4.40E-03
GSH1	Gamma glutamylcysteine synthetase catalyzes the first step in glutathione (GSH) biosynthesis; expression induced by oxidants, cadmium, and mercury, GSH1	1.3	5.85E-04
CKI1	Choline kinase, catalyzing the first step in phosphatidylcholine synthesis via the CDP-choline (Kennedy pathway); exhibits some ethanolamine kinase activity contributing to phosphatidylethanolamine synthesis via the CDP-ethanolamine pathway, CKI1	1.3	3.23E-03
MCR1	Mitochondrial NADH-cytochrome b5 reductase, involved in ergosterol biosynthesis, MCR1	1.3	1.58E-03
GTT2	Glutathione S-transferase capable of homodimerization; functional overlap with Gtt2p, Grx1p, and Grx2p, GTT2	1.2	1.15E-03
VHS3	Functionally redundant (see also SIS2) inhibitory subunit of Ppz1p, a PP1c-related ser/thr protein phosphatase Z isoform; synthetically lethal with sis2; putative phosphopantothenoylcysteine decarboxylase involved in coenzyme A biosynthesis, VHS3	1.2	3.03E-03
CAT8	Zinc cluster transcriptional activator necessary for derepression of a variety of genes under non-fermentative growth conditions, active after diauxic shift, binds carbon source responsive elements, CAT8	1.2	7.90E-03
PCA1	Cadmium transporting P-type ATPase; may also have a role in copper and iron homeostasis; S288C and most	1.2	7.40E-03

	other lab strains contain a G970R mutation which eliminates normal cadmium transport function, PCA1		
GDE1	Glycerophosphocholine (GroPCho) phosphodiesterase; hydrolyzes GroPCho to choline and glycerolphosphate, for use as a phosphate source and as a precursor for phosphocholine synthesis; may interact with ribosomes, GDE1	1.2	8.96E-03
RNR3	Ribonucleotide-diphosphate reductase (RNR), large subunit; the RNR complex catalyzes the rate-limiting step in dNTP synthesis and is regulated by DNA replication and DNA damage checkpoint pathways via localization of the small subunits, RNR3	1.2	8.96E-03
YNL200C	Putative protein of unknown function; the authentic, non-tagged protein is detected in highly purified mitochondria in high-throughput studies, ---	1.2	1.16E-03
ACS1	Acetyl-coa synthetase isoform which, along with Acs2p, is the nuclear source of acetyl-coA for histone acetylation; expressed during growth on nonfermentable carbon sources and under aerobic conditions, ACS1	1.2	2.15E-03
CHO1	Phosphatidylserine synthase, functions in phospholipid biosynthesis; catalyzes the reaction CDP-diaclyglycerol + L-serine = CMP + L-1-phosphatidylserine, transcriptionally repressed by myo-inositol and choline, CHO1	1.1	1.53E-03
CHO2	Phosphatidylethanolamine methyltransferase (PEMT), catalyzes the first step in the conversion of phosphatidylethanolamine to phosphatidylcholine during the methylation pathway of phosphatidylcholine biosynthesis, CHO2	1.1	3.97E-03
MSB3	GTPase-activating protein for Sec4p and several other Rab GTPases, regulates exocytosis via its action on Sec4p, also required for proper actin organization; similar to Msb4p; both Msb3p and Msb4p localize to sites of polarized growth, MSB3	1.1	2.29E-03
GDH2	NAD(+)-dependent glutamate dehydrogenase, degrades glutamate to ammonia and alpha-ketoglutarate; expression sensitive to nitrogen catabolite repression and intracellular ammonia levels, GDH2	1.1	1.67E-03
UGA2	Succinate semialdehyde dehydrogenase involved in the utilization of gamma-aminobutyrate (GABA) as a nitrogen source; part of the 4-aminobutyrate and glutamate degradation pathways; localized to the cytoplasm, UGA2	1.1	5.39E-03
FAS2	Alpha subunit of fatty acid synthetase, which catalyzes the synthesis of long-chain saturated fatty acids; contains beta-ketoacyl reductase and beta-ketoacyl synthase activities; phosphorylated, FAS2	1.1	6.48E-03
YNK1	Nucleoside diphosphate kinase, catalyzes the transfer of gamma phosphates from nucleoside triphosphates, usually ATP, to nucleoside diphosphates by a mechanism that	1.1	4.62E-03

	involves formation of an autophosphorylated enzyme intermediate, YNK1		
MET3	ATP sulfurylase, catalyzes the primary step of intracellular sulfate activation, essential for assimilatory reduction of sulfate to sulfide, involved in methionine metabolism, MET3	1.1	9.38E-03
ROM1	GDP/GTP exchange protein (GEP) for Rho1p; mutations are synthetically lethal with mutations in rom2, which also encodes a GEP, ROM1	1.0	5.61E-03
GTT1	ER associated glutathione S-transferase capable of homodimerization; expression induced during the diauxic shift and throughout stationary phase; functional overlap with Gtt2p, Grx1p, and Grx2p, GTT1	1.0	9.16E-03
HTD2	Mitochondrial 3-hydroxyacyl-thioester dehydratase involved in fatty acid biosynthesis, required for respiratory growth and for normal mitochondrial morphology, HTD2	1.0	3.55E-03
OPI3	Phospholipid methyltransferase (methylene-fatty-acyl-phospholipid synthase), catalyzes the last two steps in phosphatidylcholine biosynthesis, OPI3	1.0	6.83E-03
EHT1	Acyl-coenzymeA:ethanol O-acyltransferase that plays a minor role in medium-chain fatty acid ethyl ester biosynthesis; contains esterase activity; localizes to lipid particles and the mitochondrial outer membrane, EHT1	0.9	6.13E-03
INH1	Protein that inhibits ATP hydrolysis by the F1F0-ATP synthase, inhibitory function is enhanced by stabilizing proteins Stf1p and Stf2p; has similarity to Stf1p and both Inh1p and Stf1p exhibit the potential to form coiled-coil structures, INH1	0.9	8.93E-03
SAM2	S-adenosylmethionine synthetase, catalyzes transfer of the adenosyl group of ATP to the sulfur atom of methionine; one of two differentially regulated isozymes (Sam1p and Sam2p), SAM2	0.9	8.18E-03
Stress			
Multiple stress response			
SPI1	GPI-anchored cell wall protein involved in weak acid resistance; basal expression requires Msn2p/Msn4p; expression is induced under conditions of stress and during the diauxic shift; similar to Sed1p, SPI1	4.7	8.17E-04
PDR15	Plasma membrane ATP binding cassette (ABC) transporter, multidrug transporter and general stress response factor implicated in cellular detoxification; regulated by Pdr1p, Pdr3p and Pdr8p; promoter contains a PDR responsive element, PDR15	3.2	4.08E-04
DDR2	Multistress response protein, expression is activated by a variety of xenobiotic agents and environmental or physiological stresses, DDR2	2.7	1.11E-05
GRE2	NADPH-dependent methylglyoxal reductase (D-lactaldehyde dehydrogenase); stress induced (osmotic,	2.2	3.38E-03

	ionic, oxidative, heat shock and heavy metals); regulated by the HOG pathway, GRE2		
CTT1	Cytosolic catalase T, has a role in protection from oxidative damage by hydrogen peroxide,	2.2	1.98E-04
SRL3	Cytoplasmic protein that, when overexpressed, suppresses the lethality of a rad53 null mutation; potential Cdc28p substrate	2.0	0.003542
DCS2	Non-essential, stress induced regulatory protein containing a HIT (histidine triad) motif; modulates m7G-oligoribonucleotide metabolism; inhibits Dcs1p; regulated by Msn2p, Msn4p, and the Ras-cAMP-cAPK signaling pathway, similar to Dcs1p., DCS2	1.9	6.80E-04
FRT2	Tail-anchored endoplasmic reticulum membrane protein, interacts with homolog Frt1p but is not a substrate of calcineurin (unlike Frt1p), promotes growth in conditions of high Na+, alkaline pH, or cell wall stress; potential Cdc28p substrate, FRT2	1.7	3.36E-03
RPN4	Transcription factor that stimulates expression of proteasome genes; Rpn4p levels are in turn regulated by the 26S proteasome in a negative feedback control mechanism; RPN4 is transcriptionally regulated by various stress responses, RPN4	1.5	8.18E-03
MBR1	Protein involved in mitochondrial functions and stress response; overexpression suppresses growth defects of hap2, hap3, and hap4 mutants, MBR1	1.5	7.49E-03
UBI4	Ubiquitin, becomes conjugated to proteins, marking them for selective degradation via the ubiquitin-26S proteasome system; essential for the cellular stress response; encoded as a polyubiquitin precursor comprised of 5 head-to-tail repeats, UBI4	1.2	1.98E-03
HSP150	O-mannosylated heat shock protein that is secreted and covalently attached to the cell wall via beta-1,3-glucan and disulfide bridges; required for cell wall stability; induced by heat shock, oxidative stress, and nitrogen limitation, HSP150	1.0	6.70E-03
NTH1	Neutral trehalase, degrades trehalose; required for thermotolerance and may mediate resistance to other cellular stresses; may be phosphorylated by Cdc28p, NTH1	1.0	5.36E-03
Osmolarity stress			
SIP18	Protein of unknown function whose expression is induced by osmotic stress, SIP18	5.4	5.69E-08
STL1	Glycerol proton symporter of the plasma membrane, subject to glucose-induced inactivation, strongly but transiently induced when cells are subjected to osmotic shock, STL1	3.9	2.35E-03
PAI3	Cytop\lasmic proteinase A (Pep4p) inhibitor, dependent on Pbs2p and Hog1p protein kinases for osmotic induction; intrinsically unstructured, N-terminal half	3.7	5.86E-06

	becomes ordered in the active site of proteinase A upon contact, PAI3		
SMP1	Putative transcription factor involved in regulating the response to osmotic stress; member of the MADS-box family of transcription factors, SMP1	1.7	2.70E-03
GPH1	Non-essential glycogen phosphorylase required for the mobilization of glycogen, activity is regulated by cyclic AMP-mediated phosphorylation, expression is regulated by stress-response elements and by the HOG MAP kinase pathway, GPH1	1.4	2.25E-03
SSK22	MAP kinase kinase kinase of the HOG1 mitogen-activated signaling pathway; functionally redundant with, and homologous to, Ssk2p; interacts with and is activated by Ssk1p; phosphorylates Pbs2p, SSK22	1.2	5.15E-03
Heat shock			
HSP26	Small heat shock protein (sHSP) with chaperone activity; forms hollow, sphere-shaped oligomers that suppress unfolded proteins aggregation; oligomer activation requires a heat-induced conformational change; not expressed in unstressed cells, HSP26	4.4	2.95E-07
GAC1	Regulatory subunit for Glc7p type-1 protein phosphatase (PP1), tethers Glc7p to Gsy2p glycogen synthase, binds Hsf1p heat shock transcription factor, required for induction of some HSF-regulated genes under heat shock, GAC1	2.2	9.99E-05
TIP1	Major cell wall mannoprotein with possible lipase activity; transcription is induced by heat- and cold-shock; member of the Srp1p/Tip1p family of serine-alanine-rich proteins, TIP1	2.1	1.44E-04
HSP12	Plasma membrane localized protein that protects membranes from desiccation; induced by heat shock, oxidative stress, osmostress, stationary phase entry, glucose depletion, oleate and alcohol; regulated by the HOG and Ras-Pka pathways, HSP12	1.9	5.34E-04
UBC5	Ubiquitin-conjugating enzyme that mediates selective degradation of short-lived and abnormal proteins, central component of the cellular stress response; expression is heat inducible, UBC5	1.3	4.99E-04
Oxidative stress			
OYE3	Widely conserved NADPH oxidoreductase containing flavin mononucleotide (FMN), homologous to Oye2p with slight differences in ligand binding and catalytic properties; may be involved in sterol metabolism, OYE3	3.6	9.43E-05
GPX1	Phospholipid hydroperoxide glutathione peroxidase induced by glucose starvation that protects cells from phospholipid hydroperoxides and nonphospholipid peroxides during oxidative stress, GPX1	3.0	8.70E-03
GTO1	Omega-class glutathione transferase; induced under oxidative stress; putative peroxisomal localization, GTO1	2.2	9.17E-05

CTT1	Cytosolic catalase T, has a role in protection from oxidative damage by hydrogen peroxide,	2.2	1.98E-04
YHB1	Nitric oxide oxidoreductase, flavohemoglobin involved in nitric oxide detoxification; plays a role in the oxidative and nitrosative stress responses, YHB1	1.9	4.92E-03
MXR1	Peptide methionine sulfoxide reductase, reverses the oxidation of methionine residues; involved in oxidative damage repair, providing resistance to oxidative stress and regulation of lifespan, MXR1	1.8	1.94E-03
gsh1	Gamma glutamylcysteine synthetase catalyzes the first step in glutathione (GSH) biosynthesis; expression induced by oxidants, cadmium, and mercury, GSH1	1.3	5.85E-04
GTT2	Glutathione S-transferase capable of homodimerization; functional overlap with Gtt2p, Grx1p, and Grx2p, GTT2	1.2	1.15E-03
AAD6	Putative aryl-alcohol dehydrogenase with similarity to P. chrysosporium aryl-alcohol dehydrogenase, involved in the oxidative stress response, AAD6	1.2	7.73E-03
PRX1	Mitochondrial peroxiredoxin (1-Cys Prx) with thioredoxin peroxidase activity, has a role in reduction of hydroperoxides; induced during respiratory growth and under conditions of oxidative stress; phosphorylated, PRX1	1.1	2.76E-03
YAP5	Basic leucine zipper (bZIP) transcription factor	1.0	0.00598
GTT1	ER associated glutathione S-transferase capable of homodimerization; expression induced during the diauxic shift and throughout stationary phase; functional overlap with Gtt2p, Grx1p, and Grx2p, GTT1	1.0	9.16E-03
Cell wall integrity and PKC-pathway			
PIR3	O-glycosylated covalently-bound cell wall protein required for cell wall stability; expression is cell cycle regulated, peaking in M/G1 and also subject to regulation by the cell integrity pathway	5.0	9.39E-07
KDX1(MLP1)	Protein kinase implicated in the Slt2p mitogen-activated (MAP) kinase signaling pathway; associates with Rlm1p, ---	2.1	1.38E-03
BAG7	Rho GTPase activating protein (RhoGAP), stimulates the intrinsic GTPase activity of Rho1p, which plays a role in actin cytoskeleton organization and control of cell wall synthesis; structurally and functionally related to Sac7p	2.0	0.43253
HSP12	Plasma membrane localized protein that protects membranes from desiccation; induced by heat shock, oxidative stress, osmostress, stationary phase entry, glucose depletion, oleate and alcohol; regulated by the HOG and Ras-Pka pathways, HSP12	1.9	5.34E-04
DCS2	Non-essential, stress induced regulatory protein containing a HIT (histidine triad) motif; modulates m7G-oligoribonucleotide metabolism; inhibits Dcs1p; regulated by Msn2p, Msn4p, and the Ras-cAMP-cAPK signaling pathway, similar to Dcs1p.	1.9	6.80E-04

AFR1	Alpha-factor pheromone receptor regulator, negatively regulates pheromone receptor signaling; required for normal mating projection (shmoo) formation; required for Spa2p to recruit Mpk1p to shmoo tip during mating; interacts with Cdc12p, AFR1	1.9	1.81E-04
SLT2	Serine/threonine MAP kinase involved in regulating the maintenance of cell wall integrity and progression through the cell cycle; regulated by the PKC1-mediated signaling pathway	1.9	0.004729
PST1	Cell wall protein that contains a putative GPI-attachment site; secreted by regenerating protoplasts; up-regulated by activation of the cell integrity pathway, as mediated by Rlm1p; upregulated by cell wall damage via disruption of FKS1	1.9	0.004729
GSC2	Catalytic subunit of 1,3-beta-glucan synthase, involved in formation of the inner layer of the spore wall; activity positively regulated by Rho1p and negatively by Smk1p; has similarity to an alternate catalytic subunit, Fks1p (Gsc1p), GSC2	1.6	1.04E-03
RLM1	MADS-box transcription factor, component of the protein kinase C-mediated MAP kinase pathway involved in the maintenance of cell integrity; phosphorylated and activated by the MAP-kinase Slt2p, RLM1	1.2	1.44E-03
VHS3	Functionally redundant (see also SIS2) inhibitory subunit of Ppz1p, a PP1c-related ser/thr protein phosphatase Z isoform; synthetically lethal with sis2; putative phosphopantothenoylcysteine decarboxylase involved in coenzyme A biosynthesis, VHS3	1.2	3.03E-03
MTL1	Protein with both structural and functional similarity to Mid2p, which is a plasma membrane sensor required for cell integrity signaling during pheromone-induced morphogenesis; suppresses rgd1 null mutations	1.2	0.503124
ROM1	GDP/GTP exchange protein (GEP) for Rho1p; mutations are synthetically lethal with mutations in rom2, which also encodes a GEP, ROM1	1.0	5.61E-03
SDP1	Stress-inducible dual-specificity MAP kinase phosphatase, negatively regulates Slt2p MAP kinase by direct dephosphorylation, diffuse localization under normal conditions shifts to punctate localization after heat shock	1.0	0.695198
PTP2	Phosphotyrosine-specific protein phosphatase involved in the inactivation of mitogen-activated protein kinase (MAPK) during osmolarity sensing; dephosporylates Hog1p MAPK and regulates its localization; localized to the nucleus,	1.0	0.027224
SLT2	Serine/threonine MAP kinase involved in regulating the maintenance of cell wall integrity and progression through the cell cycle; regulated by the PKC1-mediated signaling pathway	0.9	0.057308
BCK2	Protein rich in serine and threonine residues involved in	0.8	0.03723

	protein kinase C signaling pathway, which controls cell integrity; overproduction suppresses pkc1 mutations		1
WSC3	Partially redundant sensor-transducer of the stress-activated PKC1-MPK1 signaling pathway involved in maintenance of cell wall integrity; involved in the response to heat shock and other stressors; regulates 1,3-beta-glucan synthesis	0.7	0.116598
PRM5	Pheromone-regulated protein, predicted to have 1 transmembrane segment; induced during cell integrity signaling	0.7	1
PKH2	Serine/threonine protein kinase involved in sphingolipid-mediated signaling pathway that controls endocytosis; activates Ypk1p and Ykr2p, components of signaling cascade required for maintenance of cell wall integrity; redundant with Pkh1p	0.6	0.600569
PKH3	Protein kinase with similarity to mammalian phosphoinositide-dependent kinase 1 (PDK1) and yeast Pkh1p and Pkh2p, two redundant upstream activators of Pkc1p; identified as a multicopy suppressor of a pkh1 pkh2 double mutant	0.6	0.822118
ROM2	GDP/GTP exchange protein (GEP) for Rho1p and Rho2p; mutations are synthetically lethal with mutations in rom1, which also encodes a GEP	0.6	1
GFA1	Glutamine-fructose-6-phosphate amidotransferase, catalyzes the formation of glucosamine-6-P and glutamate from fructose-6-P and glutamine in the first step of chitin biosynthesis	0.5	1
MID2	O-glycosylated plasma membrane protein that acts as a sensor for cell wall integrity signaling and activates the pathway; interacts with Rom2p, a guanine nucleotide exchange factor for Rho1p, and with cell integrity pathway protein Zeo1p	0.5	1
PTP3	Phosphotyrosine-specific protein phosphatase involved in the inactivation of mitogen-activated protein kinase (MAPK) during osmolarity sensing; dephosporylates Hog1p MAPK and regulates its localization; localized to the cytoplasm	0.4	1
TUS1	Guanine nucleotide exchange factor (GEF) that functions to modulate Rho1p activity as part of the cell integrity signaling pathway; multicopy suppressor of tor2 mutation and ypk1 ypk2 double mutation; potential Cdc28p substrate	0.4	1
BCK1	Mitogen-activated protein (MAP) kinase kinase kinase acting in the protein kinase C signaling pathway, which controls cell integrity; upon activation by Pkc1p phosphorylates downstream kinases Mkk1p and Mkk2p	0.3	1
RHO5	Non-essential small GTPase of the Rho/Rac subfamily of Ras-like proteins, likely involved in protein kinase C (Pkc1p)-dependent signal transduction pathway that controls cell integrity	0.3	1

| PKH1	Serine/threonine protein kinase involved in sphingolipid-mediated signaling pathway that controls endocytosis; activates Ypk1p and Ykr2p, components of signaling cascade required for maintenance of cell wall integrity; redundant with Pkh2p	0.3	1
PKC1	Protein serine/threonine kinase essential for cell wall remodeling during growth; localized to sites of polarized growth and the mother-daughter bud neck; homolog of the alpha, beta, and gamma isoforms of mammalian protein kinase C (PKC)	0.3	1
BNI1	Formin, nucleates the formation of linear actin filaments, involved in cell processes such as budding and mitotic spindle orientation which require the formation of polarized actin cables, functionally redundant with BNR1	0.3	1
SWI4	DNA binding component of the SBF complex (Swi4p-Swi6p), a transcriptional activator that in concert with MBF (Mbp1-Swi6p) regulates late G1-specific transcription of targets including cyclins and genes required for DNA synthesis and repair	0.2	1
MKK1	Mitogen-activated kinase kinase involved in protein kinase C signaling pathway that controls cell integrity; upon activation by Bck1p phosphorylates downstream target, Slt2p; functionally redundant with Mkk2p	0.2	1
MSG5	Dual-specificity protein phosphatase required for maintenance of a low level of signaling through the cell integrity pathway; regulates and is regulated by Slt2p; dephosphorylates Fus3p; required for adaptive response to pheromone	0.1	1
SEC3	Non-essential subunit of the exocyst complex (Sec3p, Sec5p, Sec6p, Sec8p, Sec10p, Sec15p, Exo70p, Exo84p) which mediates targeting of post-Golgi vesicles to sites of active exocytosis; Sec3p specifically is a spatial landmark for secretion	0.1	1
FKS3	Protein involved in spore wall assembly, has similarity to 1,3-beta-D-glucan synthase catalytic subunits Fks1p and Gsc2p; the authentic, non-tagged protein is detected in highly purified mitochondria in high-throughput studie	0.0	1
SAC7	GTPase activating protein (GAP) for Rho1p, involved in signaling to the actin cytoskeleton, null mutations suppress tor2 mutations and temperature sensitive mutations in actin; potential Cdc28p substrate	-0.1	1
BNR1	Formin, nucleates the formation of linear actin filaments, involved in cell processes such as budding and mitotic spindle orientation which require the formation of polarized actin cables, functionally redundant with BNI1	-0.2	1
BEM2	Rho GTPase activating protein (RhoGAP) involved in the control of cytoskeleton organization and cellular morphogenesis; required for bud emergence	-0.2	1
SKN7	Nuclear response regulator and transcription factor, part of a branched two-component signaling system; required	-0.3	1

	for optimal induction of heat-shock genes in response to oxidative stress; involved in osmoregulation		
RHO1	GTP-binding protein of the rho subfamily of Ras-like proteins, involved in establishment of cell polarity; regulates protein kinase C (Pkc1p) and the cell wall synthesizing enzyme 1,3-beta-glucan synthase (Fks1p and Gsc2p)	-0.3	1
SWI6	Transcription cofactor, forms complexes with DNA-binding proteins Swi4p and Mbp1p to regulate transcription at the G1/S transition; involved in meiotic gene expression; localization regulated by phosphorylation; potential Cdc28p substrate	-0.5	0.686307
FKS1	Catalytic subunit of 1,3-beta-D-glucan synthase, functionally redundant with alternate catalytic subunit Gsc2p; binds to regulatory subunit Rho1p; involved in cell wall synthesis and maintenance; localizes to sites of cell wall remodeling	-0.6	1
LRG1	Putative GTPase-activating protein (GAP) involved in the Pkc1p-mediated signaling pathway that controls cell wall integrity; appears to specifically regulate 1,3-beta-glucan synthesis	-0.8	0.185367
WSC2	Partially redundant sensor-transducer of the stress-activated PKC1-MPK1 signaling pathway involved in maintenance of cell wall integrity and recovery from heat shock; secretory pathway Wsc2p is required for the arrest of secretion response,	-1.2	0.454214
Sulfur metabolism			
JLP1	Fe(II)-dependent sulfonate/alpha-ketoglutarate dioxygenase, involved in sulfonate catabolism for use as a sulfur source, contains sequence that closely resembles a J domain (typified by the E. coli DnaJ protein), JLP1	6.7	1.80E-05
AGP3	Low-affinity amino acid permease, may act to supply the cell with amino acids as nitrogen source in nitrogen-poor conditions; transcription is induced under conditions of sulfur limitation, AGP3	5.1	3.92E-06
PDC6	Minor isoform of pyruvate decarboxylase, decarboxylates pyruvate to acetaldehyde, involved in amino acid catabolism; transcription is glucose- and ethanol-dependent, and is strongly induced during sulfur limitation, PDC6	4.3	3.70E-04
BDS1	Bacterially-derived sulfatase required for use of alkyl- and aryl-sulfates as sulfur sources, BDS1	3.2	7.60E-05
GTO1	Omega-class glutathione transferase; induced under oxidative stress; putative peroxisomal localization, GTO1	2.2	9.17E-05
MHT1	S-methylmethionine-homocysteine methyltransferase, functions along with Sam4p in the conversion of S-adenosylmethionine (AdoMet) to methionine to control the methionine/AdoMet ratio, MHT1	2.0	8.18E-04
MET8	Bifunctional dehydrogenase and ferrochelatase, involved	1.9	4.47E-

|			
	in the biosynthesis of siroheme, a prosthetic group used by sulfite reductase; required for sulfate assimilation and methionine biosynthesis, MET8		04
YLL058W	Putative protein of unknown function with similarity to Str2p, which is a cystathionine gamma-synthase important in sulfur metabolism; YLL058W is not an essential gene, ---	1.8	3.34E-03
MET32	Zinc-finger DNA-binding protein, involved in transcriptional regulation of the methionine biosynthetic genes, similar to Met31p, MET32	1.6	4.12E-04
THI4	Thiazole synthase, catalyzes formation of the thiazole moiety of thiamin pyrophosphate; required for thiamine biosynthesis and for mitochondrial genome stability, THI4	1.6	1.27E-04
MET28	Transcriptional activator in the Cbf1p-Met4p-Met28p complex, participates in the regulation of sulfur metabolism, MET28	1.6	1.74E-04
MET30	F-box protein containing five copies of the WD40 motif, controls cell cycle function, sulfur metabolism, and methionine biosynthesis as part of the ubiquitin ligase complex; interacts with and regulates Met4p, localizes within the nucleus, MET30	1.6	2.18E-03
MET2	L-homoserine-O-acetyltransferase, catalyzes the conversion of homoserine to O-acetyl homoserine which is the first step of the methionine biosynthetic pathway, MET2	1.5	1.79E-04
ECM4	Omega class glutathione transferase; not essential; similar to Ygr154cp; green fluorescent protein (GFP)-fusion protein localizes to the cytoplasm, ECM4	1.4	2.94E-04
GSH1	Gamma glutamylcysteine synthetase catalyzes the first step in glutathione (GSH) biosynthesis; expression induced by oxidants, cadmium, and mercury, GSH1	1.3	5.85E-04
GTT2	Glutathione S-transferase capable of homodimerization; functional overlap with Gtt2p, Grx1p, and Grx2p, GTT2	1.2	1.15E-03
YHR112C	Putative protein of unknown function; green fluorescent protein (GFP)-fusion protein localizes to the cytoplasm, ---	1.2	1.65E-03
MET3	ATP sulfurylase, catalyzes the primary step of intracellular sulfate activation, essential for assimilatory reduction of sulfate to sulfide, involved in methionine metabolism, MET3	1.1	9.38E-03
GTT1	ER associated glutathione S-transferase capable of homodimerization; expression induced during the diauxic shift and throughout stationary phase; functional overlap with Gtt2p, Grx1p, and Grx2p, GTT1	1.0	9.16E-03
SAM2	S-adenosylmethionine synthetase, catalyzes transfer of the adenosyl group of ATP to the sulfur atom of methionine; one of two differentially regulated isozymes (Sam1p and Sam2p), SAM2	0.9	8.18E-03

Iron ion homeostasis			
HMX1	ER localized, heme-binding peroxidase involved in the degradation of heme; does not exhibit heme oxygenase activity despite similarity to heme oxygenases; expression regulated by AFT1, HMX1	2.5	9.76E-03
SIT1	Ferrioxamine B transporter, member of the ARN family of transporters that specifically recognize siderophore-iron chelates; transcription is induced during iron deprivation and diauxic shift; potentially phosphorylated by Cdc28p, SIT1	2.3	1.28E-03
FIT2	Mannoprotein that is incorporated into the cell wall via a glycosylphosphatidylinositol (GPI) anchor, involved in the retention of siderophore-iron in the cell wall, FIT2	2.0	6.39E-05
ARN2	Transporter, member of the ARN family of transporters that specifically recognize siderophore-iron chelates; responsible for uptake of iron bound to the siderophore triacetylfusarinine C, ARN2	1.9	1.38E-03
FIT3	Mannoprotein that is incorporated into the cell wall via a glycosylphosphatidylinositol (GPI) anchor, involved in the retention of siderophore-iron in the cell wall, FIT3	1.7	5.54E-03
TIS11	mRNA-binding protein expressed during iron starvation; binds to a sequence element in the 3'-untranslated regions of specific mRNAs to mediate their degradation; involved in iron homeostasis, TIS11	1.4	3.07E-03
PCA1	Cadmium transporting P-type ATPase; may also have a role in copper and iron homeostasis; S288C and most other lab strains contain a G970R mutation which eliminates normal cadmium transport function, PCA1	1.2	7.40E-03
FRE6	Putative ferric reductase with similarity to Fre2p; expression induced by low iron levels, FRE6	1.1	7.08E-03
ATX1	Cytosolic copper metallochaperone that transports copper to the secretory vesicle copper transporter Ccc2p for eventual insertion into Fet3p, which is a multicopper oxidase required for high-affinity iron uptake, ATX1	1.1	9.51E-03

[a] The $\log_2$ ratio of treated/control.

[b] The Bonferroni-corrected p values.
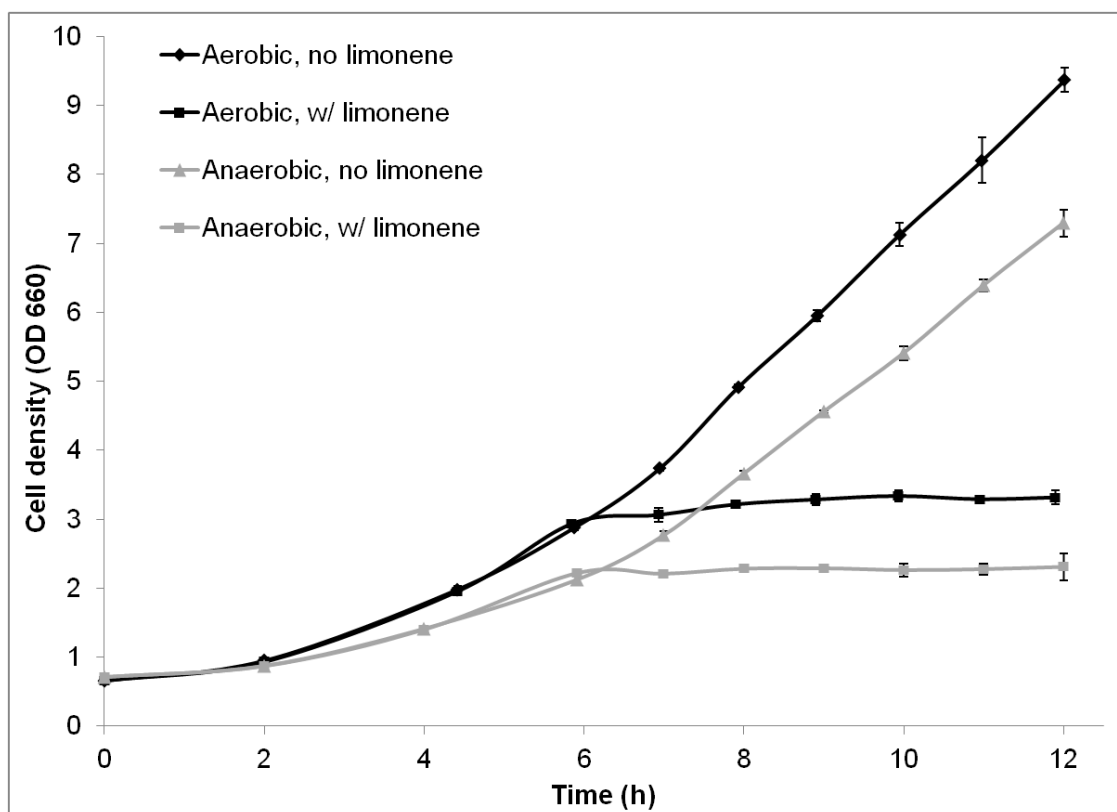
SI Fig 2. Anaerobic vs. aerobic growth curves. 107 mg/L of limonene was added at mid-exponential phase. Error bars represent one SD above and below the mean for biological triplicates.
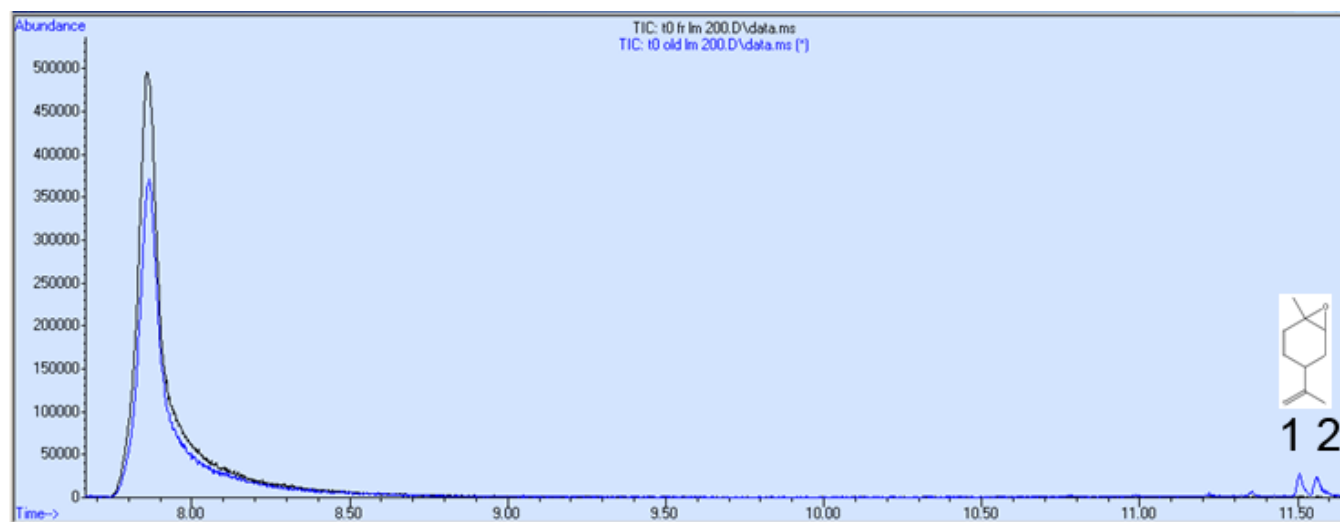
SI Fig 3. GC-MS chromatogram of limonene (RT = 7.9 min) sampled from challenged cultures after 6 h incubation at 30°C. The black line is limonene from anaerobic flasks (with no limonene oxide formation) and the blue line represents limonene from aerobic cultures (limonene oxide compounds at 11.5 min, peak 1 = limonene oxide, cis and peak 2 = limonene oxide, trans.). At 12 after inoculation (6 h after limonene addition), 1 mL of isopropyl

myristate (IPM) was added to the culture (~ 22 ml), vortexed and harvested (1 min, 4025 rcf). The top IPM phase containing limonene was removed and 1 μL was resuspended in 1 mL of a 1:4 toluene:hexane solution. The GC-MS analysis was carried out using the setting described in the Materials and Methods section with the following changes: 1 μL of sample was injected and the oven temperature was set to 70°C, held for 10 min then followed by a temperature ramp of 40 °C/min to 300°C and held for 3 min. Detection was achieved in scan mode at 9.26 scans/sec from 30-300 amu.

Glucose
↓↓↓
AcCoA
│ *ERG10* (0.10)
↓
AcAcCoA
│ *ERG13* (-0.43)
↓
HMG-CoA
│ *HMG2* (0.09)
↓ *HMG1* (0.56)
Mevalonate
│ *ERG12* (-0.07)
↓
Mevalonate-P
│ *ERG8* (-0.35)
↓
IPP
│ *MVD1* (0.53)
↓
GPP
│ *ERG20* (0.18)
↓
FPP
│ *ERG9* (0.79)
↓
Squalene
↓↓↓ *ERG4* (0.17)
     ERG6 (0.60)
Ergosterol
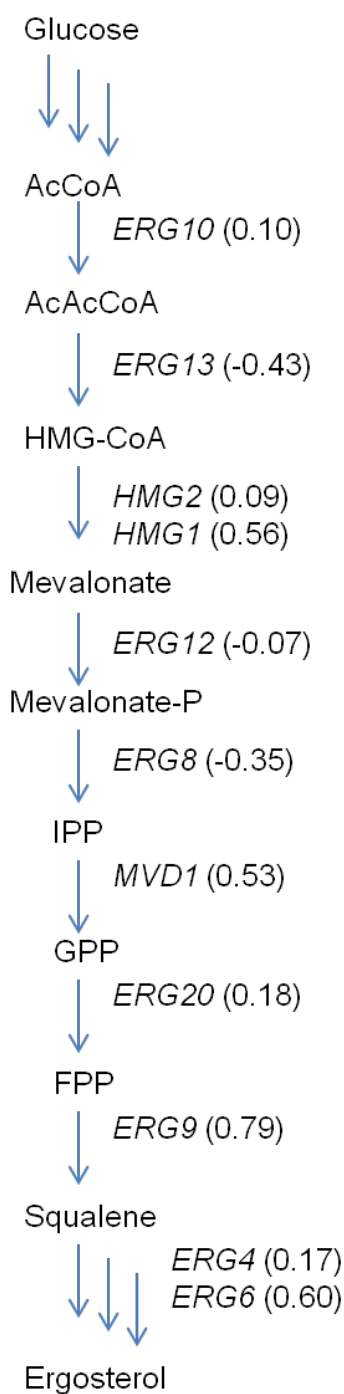
SI Fig 4. Transcript levels of genes associated with ergosterol biosynthesis. Numbers in the parenthesis represent the $\log_2$ fold changes of that particular gene (treated/control). None of these genes were differentially expressed (Bonferroni-corrected $p < 0.01$).
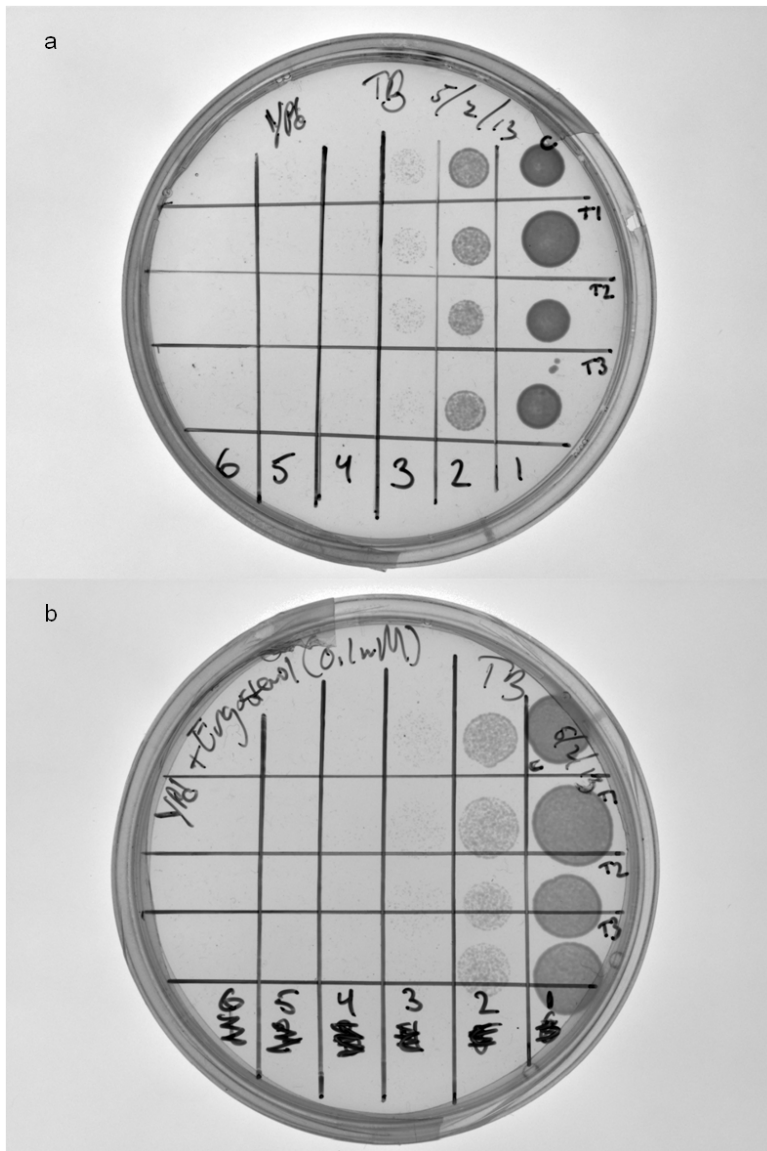
SI Fig 5. Effect of exogenous ergosterol on the growth and viability. Yeast cultures were dosed with limonene as described in the Materials and Methods. Cells were harvested and washed and diluted on rich medium (YPD) plates as described by Liu, et al (1). (a) YPD and (b) YPD + 0.1 mM ergosterol/Tween 80 (0.25% v/v). The top row of each plate is the untreated control and rows 2-4 represent biological replicates for limonene-treated cells at varying dilutions (10^{-1}-10^{-6}). Image was taken at 24 h. Tween 80 did cause spreading of the culture droplet on the surface in the ergosterol supplemented plate causing an increase in the diameter.
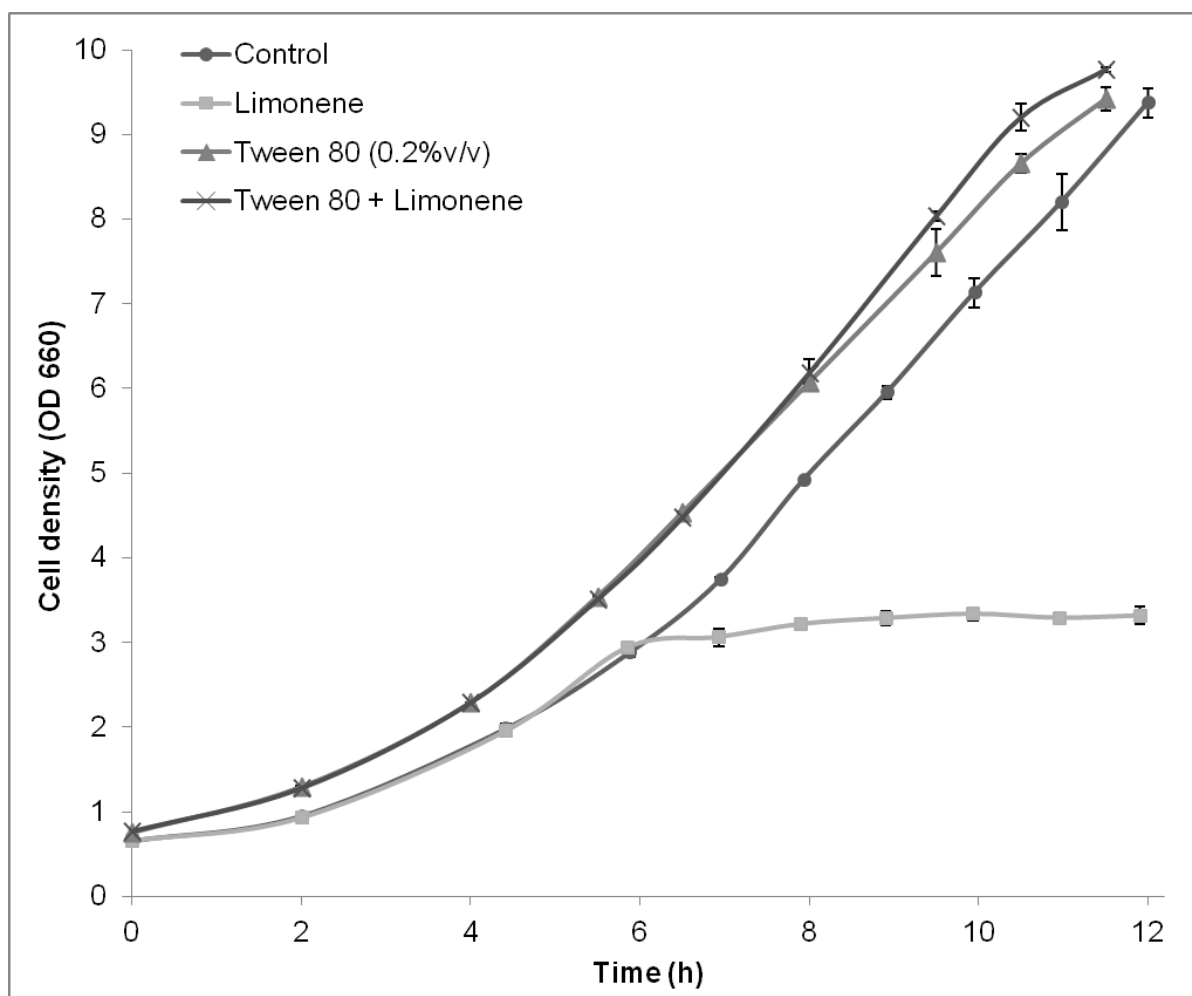
SI Fig 6. Dose response growth curves in the presence of limonene and limonene + surfactant. 107 mg/L of limonene was added at mid-exponential phase. Limonene was administered in the presence and absence of Tween 80 (0.2% v/v). Error bars represent one SD above and below the mean for biological triplicates.

References:

1.   **Liu, J., Y. Zhu, G. Du, J. Zhou, and J. Chen.** 2013. Exogenous ergosterol protects *Saccharomyces cerevisiae* from d-limonene stress. J. Appl. Microbiol. **114:**482-491.

Chapter 4 Supplementary information

Title: Evolutionary engineering improves tolerance towards jet fuel replacements in yeast
Authors: Timothy C. R. Brennan, Thomas C. Williams, Ben Schulz, Robin Palfreyman, Jens Kromer#, Lars K. Nielsen
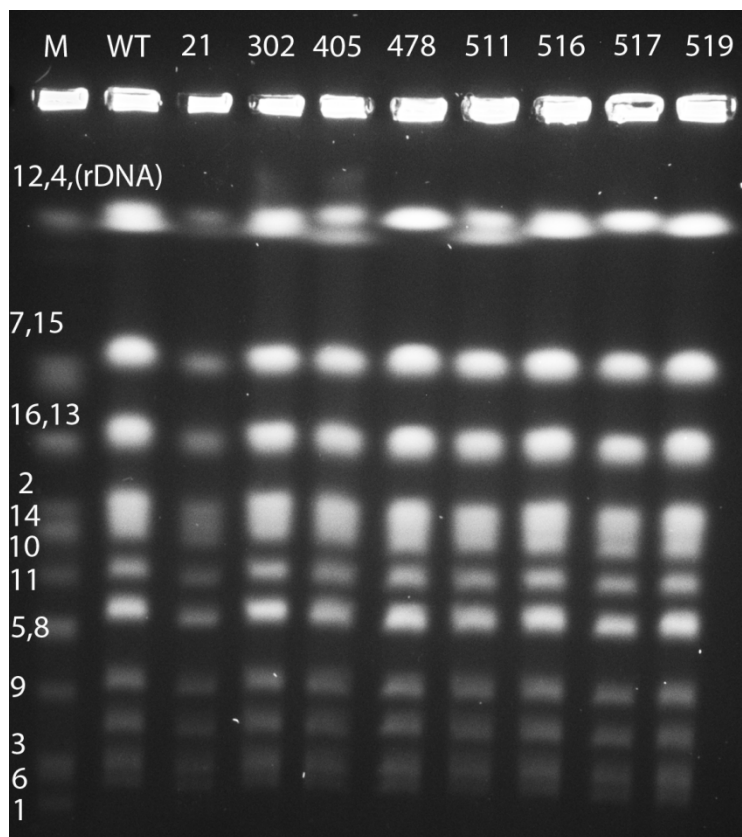

Fig S1. Pulsed-field gel electrophorogram of chromosomes from wild-type (WT) and evolved strains. M, yeast chromosome markers. Marker bands are labelled by chromosome.
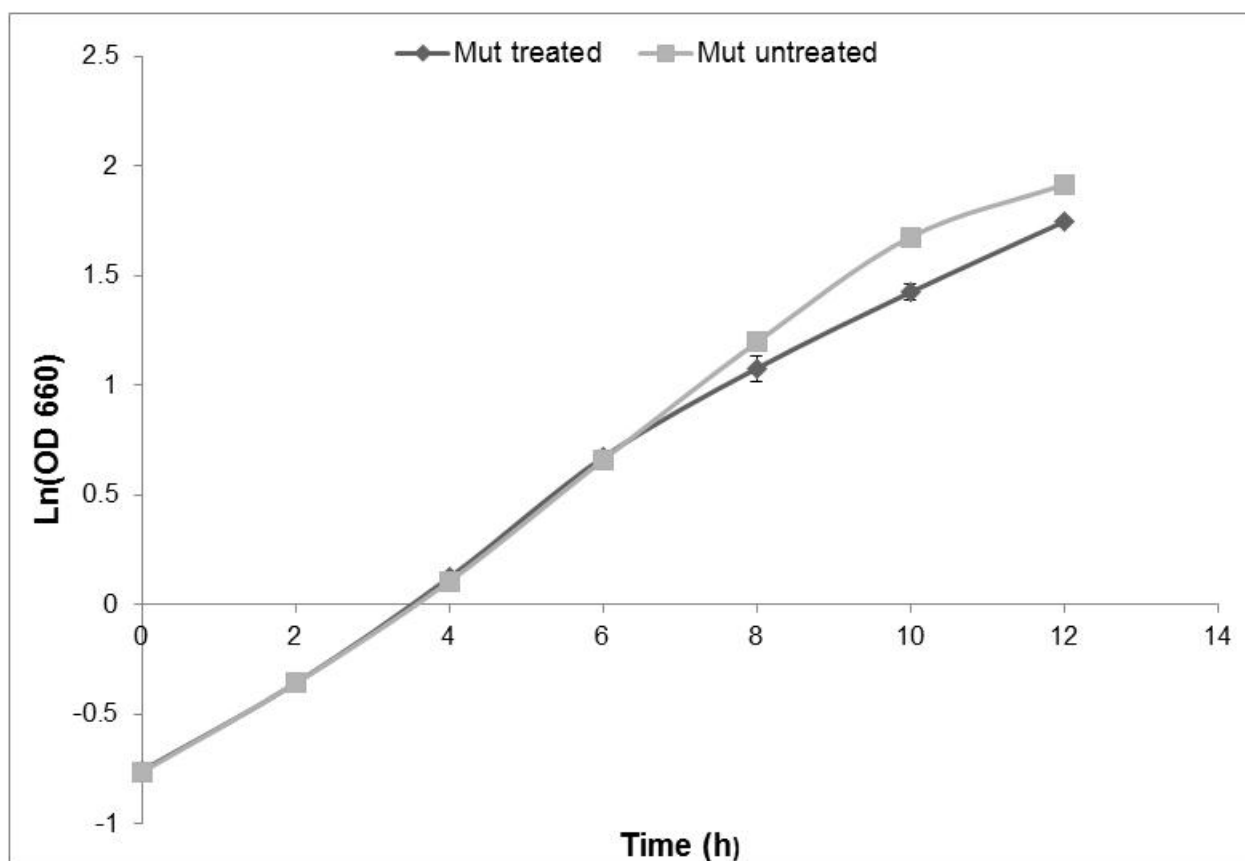
Fig S2. Single mutant (*tcb3-989*) growth during limonene treatment. The method followed Brennan et al. exactly [1]. At mid-exponential growth (6 h) 107 mg/l of limonene was dosed into the culture and growth was monitored. Total RNA was extracted 2 post limonene addition. All data was performed in triplicate.

Table S1. Overall Illumina whole-genome sequencing results and detection of mutations

Strain	Gen	Total no. Mapped PE reads	Genome percent reference coverage (%)	Average read depth	Total no. mutations	Total no. SNPs	Coding	Non-coding	Total no. INDELS	Coding	Non-coding	Limonene Recovery[b] (%)
TB21	88	56883018	99.02	350.9639	29	11	7	4	18	1	17	106±12
TB302	120	17106404	96.95	105.5452	39	4	2	2	35	8	27	128±9
TB405	160	20087733	98.01	123.9398	31	7	2	5	24	6	18	124±20
TB478	188	54674451	98.97	337.3372	31	10	7	3	21	2	19	138±7
TB511	200	18685198	98.3	115.2862	31	8	6	2	23	8	15	132±10
TB516	200	19656432	98.16	121.2787	39	7	2	5	32	7	25	136±7
TB517	200	18326663	98.12	113.0741	35	5	3	2	30	3	27	115±24
TB519	200	19444208	98.01	119.9693	42	9	6	3	33	4	29	141±17
TB23cs[a]	666	18480963	98.21%	114.0261	32	12	3	9	20	2	18	-

[a] Strain TB23cs was isolated from a chemostat culture.
[b] Recovery was calculated by taking the ratio of the peak area, determined by CG/MS, of limonene from the evolved strain to the control after 12 h of fermentation during the relative fitness assay. The control was carried out under identical conditions but in the absence of cells. For the WT strain the recovery was 119±5%. All data is in biological triplicate ± SD (*n* = 3).

Table S2. Primers used in this work.

Primer name	5′ to 3′ sequence

PDR3aF	ATGAAAGTGAAGAAATCAACTAG
PDR3aR	GTATTCTGGGCCTCCATGTCTTCTTTATGGTTAATGAATCCC
PDR3bF	GAATGCTGGTCGCTATACTGTTGTCTCGTTGGGAGTATTATG
PDR3bR	TCATAAGAAGGGATATGAAGTATTG
amdPF	GGGATTCATTAACCATAAAGAAGACATGGAGGCCCAGAATAC
amdPR	CATAATACTCCCAACGAGACAACAGTATAGCGACCAGCATTC
PDR3KIcheck F	CGCACTGAACACTACCTGGG
PDR3KIcheck R	ATGACGAGGACGCCACATTC
TCB3aF	ATGACTGGCATCAAAGCTC
TCB3aR	GTATTCTGGGCCTCCATGTCTAATACAACCAATAGGTTCGC
TCB3bF	GAATGCTGGTCGCTATACTGTTCGATGACAGAATGAATGG
TCB3bR	TTACTGCGTGTATTCTTGAGGAAC
amdTF	GCGAACCTATTGGTTGTATTAGACATGGAGGCCCAGAATAC
amdTR	CCATTCATTCTGTCATCGAACAGTATAGCGACCAGCATTC
TCB3KIcheck F	TCATTCCGTCTTTGCGACCT
TCB3KIcheck R	GCAGTAACAGGAGAGCGTTGA

Table S3. Differentially expressed (*P* < 0.05) gene list for single mutant (*tcb3-989*) for limonene treated vs. untreated cells.

Gene name	Protein stable ID	Gene description	log$_2$ FC	t	adj.P.Val
Upregulated					
INO1	YJL153C	Inositol-3-phosphate synthase, involved in synthesis of inositol phosphates and inositol-containing phospholipids; transcription is coregulated with other phospholipid biosynthetic genes by Ino2p and Ino4p, which bind the UASINO DNA element [Source:SGD;Acc:S000003689]	2.992	6.355	0.01287
ATF2	YGR177C	Alcohol acetyltransferase, may play a role in steroid detoxification; forms volatile esters during fermentation, which is important for brewing and winemaking [Source:SGD;Acc:S000003409]	1.735	19.381	0.00023
SIT1	YEL065W	Ferrioxamine B transporter, member of the ARN family of transporters that specifically recognize siderophore-iron chelates; transcription is induced during iron deprivation and diauxic shift; potentially phosphorylated by Cdc28p [Source:SGD;Acc:S000000791]	1.695	17.952	0.00027
YGP1	YNL160W	Cell wall-related secretory glycoprotein; induced by nutrient deprivation-associated growth arrest and upon entry into stationary phase; may be involved in adaptation prior to stationary phase entry; has similarity to Sps100p [Source:SGD;Acc:S000005104]	1.586	5.018	0.02646
AQY2	YLL052C	Water channel that mediates the transport of water across cell membranes, only expressed in proliferating cells, controlled by osmotic signals, may be involved in freeze tolerance; disrupted by a stop codon in many S. cerevisiae strains [Source:SGD;Acc:S000003975]	1.545	8.418	0.00474
PDR15	YDR406W	Plasma membrane ATP binding cassette (ABC) transporter, multidrug transporter and general stress response factor implicated in cellular detoxification; regulated by Pdr1p, Pdr3p and Pdr8p; promoter contains a PDR responsive element [Source:SGD;Acc:S000002814]	1.425	5.899	0.01619
HMX1	YLR205C	ER localized heme oxygenase, involved in heme degradation during iron starvation and in the oxidative stress response; expression is regulated by AFT1 and oxidative stress; relocates to the perinuclear region in the presence of oxidants [Source:SGD;Acc:S000004195]	1.367	10.505	0.00201
YLR346C	YLR346C	Putative protein of unknown function found in mitochondria; expression is regulated by transcription factors involved in pleiotropic drug resistance, Pdr1p and Yrr1p; YLR346C is not an essential gene [Source:SGD;Acc:S000004338]	1.358	7.188	0.00847

CAR1	YPL111W	Arginase, responsible for arginine degradation, expression responds to both induction by arginine and nitrogen catabolite repression; disruption enhances freeze tolerance [Source:SGD;Acc:S000006032]	1.353	4.835	0.02883
ARN1	YHL040C	Transporter, member of the ARN family of transporters that specifically recognize siderophore-iron chelates; responsible for uptake of iron bound to ferrirubin, ferrirhodin, and related siderophores [Source:SGD;Acc:S000001032]	1.323	18.501	0.00027
YLL053C	YLL053C	Putative protein; in the Sigma 1278B strain background YLL053C is contiguous with AQY2 which encodes an aquaporin [Source:SGD;Acc:S000003976]	1.296	7.615	0.00689
FIT2	YOR382W	Mannoprotein that is incorporated into the cell wall via a glycosylphosphatidylinositol (GPI) anchor, involved in the retention of siderophore-iron in the cell wall [Source:SGD;Acc:S000005909]	1.295	16.543	0.00029
FRE5	YOR384W	Putative ferric reductase with similarity to Fre2p; expression induced by low iron levels; the authentic, non-tagged protein is detected in highly purified mitochondria in high-throughput studies [Source:SGD;Acc:S000005911]	1.257	17.758	0.00027
ERG3	YLR056W	C-5 sterol desaturase, catalyzes the introduction of a C-5(6) double bond into episterol, a precursor in ergosterol biosynthesis; mutants are viable, but cannot grow on non-fermentable carbon sources [Source:SGD;Acc:S000004046]	1.161	16.588	0.00029
RSB1	YOR049C	Suppressor of sphingoid long chain base (LCB) sensitivity of an LCB-lyase mutation; putative integral membrane transporter or flippase that may transport LCBs from the cytoplasmic side toward the extracytoplasmic side of the membrane [Source:SGD;Acc:S000005575]	1.138	8.514	0.00467
YPL277C	YPL277C	Putative protein of unknown function; localized to the membranes; gene expression regulated by copper levels [Source:SGD;Acc:S000006198]	1.126	19.422	0.00023
ECL1	YGR146C	Protein of unknown function, affects chronological lifespan; induced by iron homeostasis transcription factor Aft2p; multicopy suppressor of temperature sensitive hsf1 mutant; induced by treatment with 8-methoxypsoralen and UVA irradiation [Source:SGD;Acc:S000003378]	1.125	9.330	0.00368
SMP1	YBR182C	Putative transcription factor involved in regulating the response to osmotic stress; member of the MADS-box family of transcription factors [Source:SGD;Acc:S000000386]	1.117	11.463	0.00145
PDR3	YBL005W	Transcriptional activator of the pleiotropic drug resistance network, regulates expression of ATP-binding cassette (ABC) transporters through binding to cis-acting sites known as PDREs (PDR responsive elements); post-translationally up-regulated in /.../lacking a functional mitochondrial genome [Source:SGD;Acc:S000000101]	1.098	27.746	0.00008
TIS11	YLR136C	mRNA-binding protein expressed during iron starvation; binds to a sequence element in the 3'-untranslated regions of specific mRNAs to mediate their degradation; involved in iron homeostasis [Source:SGD;Acc:S000004126]	1.096	28.455	0.00008
PRM7	YDL039C	Pheromone-regulated protein, predicted to have one transmembrane segment; promoter contains Gcn4p binding elements [Source:SGD;Acc:S000002197]	1.064	5.202	0.02350
TIR2	YOR010C	Putative cell wall mannoprotein of the Srp1p/Tip1p family of serine-alanine-rich proteins; transcription is induced by cold shock and anaerobiosis [Source:SGD;Acc:S000005536]	1.060	13.656	0.00070
YOR389W	YOR389W	Putative protein of unknown function; expression regulated by copper levels [Source:SGD;Acc:S000005916]	1.047	14.909	0.00048
FIT3	YOR383C	Mannoprotein that is incorporated into the cell wall via a glycosylphosphatidylinositol (GPI) anchor, involved in the retention of siderophore-iron in the cell wall [Source:SGD;Acc:S000005910]	1.022	17.051	0.00027
Down regulated					
Gene name	Protein stable ID	Gene description	logFC	t	adj.P.Val
WSC4	YHL028W	Endoplasmic reticulum (ER) membrane protein; involved in the translocation of soluble secretory proteins and insertion of membrane proteins into the ER membrane; may also have a role in the stress response but has only partial functional overlap with WSC1-3	-1.105	-4.962	0.027
DAL5	YJR152W	Allantoate permease; ureidosuccinate permease; also transports dipeptides, though with lower affinity than for allantoate and ureidosuccinate; expression is constitutive but sensitive to nitrogen catabolite repression	-1.260	-8.781	0.004
	YKR075C	Protein of unknown function; similar to Reg1p; expression regulated by glucose and Rgt1p; GFP-fusion protein is induced in response to the DNA-damaging agent MMS; YKR075C has a paralog, YOR062C, that arose from the whole genome	-1.479	-8.421	0.005

		duplication			
	YLR053C	Putative protein of unknown function	-1.113	-6.384	0.013
PUT4	YOR348C	Proline permease; required for high-affinity transport of proline; also transports the toxic proline analog azetidine-2-carboxylate (AzC); PUT4 transcription is repressed in ammonia-grown cells	-1.298	-13.886	0.001

Table S4. Differentially expressed ($p < 0.05$) cell wall protein list for single mutant (*tcb3-989*) and WT.

Untreated Mut/WT			
Protein	$\log_2$FC	T value	adj. p value
sp|P38616|YGP1_YEAST	0.5967	3.2832	0.00741
sp|P38248|ECM33_YEAST	-0.172	-3.487	0.0037
sp|P38288|TOS1_YEAST	-0.212	-2.82	0.02435
sp|Q03674|PLB2_YEAST	-0.314	-5.376	2.56E-06
sp|P47001|CIS3_YEAST	-0.415	-4.316	0.00029
sp|P36135|UTH1_YEAST	-0.582	-2.73	0.03036
sp|P39105|PLB1_YEAST	-0.624	-3.647	0.00319
WT +/- limonene treatment			
Protein	$\log_2$FC	T value	adj. p value
sp|P20840|SAG1_YEAST	1.1627	19.267	0
sp|P38616|YGP1_YEAST	0.8284	5.3917	7.32E-07
sp|P32329|YPS1_YEAST	0.8216	6.2453	4.42E-09
sp|Q03180|PIR3_YEAST	0.6543	4.2978	4.32E-05
sp|P46992|YJR1_YEAST	0.6413	4.5382	1.67E-05
sp|Q06325|YPS7_YEAST	0.6217	3.0185	0.00554
sp|Q04951|SCW10_YEAST	0.5038	5.7269	5.65E-08
sp|Q03178|PIR1_YEAST	0.4887	3.8011	0.0003
sp|P32478|HS150_YEAST	0.4724	5.5663	1.11E-07
sp|P53379|MKC7_YEAST	0.4587	4.6785	9.91E-06
sp|P52911|EXG2_YEAST	0.4142	5.7681	4.95E-08
sp|Q12355|PST1_YEAST	0.3914	2.2045	0.05032
sp|P15703|BGL2_YEAST	0.2267	2.202	0.04922
sp|Q03655|GAS3_YEAST	-0.391	-6.355	1.76E-09
sp|P28319|CWP1_YEAST	-0.606	-9.321	0
sp|P47001|CIS3_YEAST	-0.644	-4.671	1.08E-05
sp|O13547|CCW14_YEAST	-0.781	-9.11	0
sp|P36135|UTH1_YEAST	-0.95	-4.401	4.32E-05
Mutant +/- limonene treatment			
Protein	$\log_2$FC	T value	adj. p value
sp|Q06325|YPS7_YEAST	0.4939	2.4017	0.04365
sp|P47001|CIS3_YEAST	0.3433	2.9	0.01304
sp|Q03674|PLB2_YEAST	0.2655	4.4849	5.78E-05
sp|O13547|CCW14_YEAST	0.2296	2.8364	0.0138
sp|P38288|TOS1_YEAST	-0.245	-3.031	0.00931

Protein	log$_2$FC	T value	adj. p value
sp|Q03655|GAS3_YEAST	-0.25	-4.055	0.00026
sp|P28319|CWP1_YEAST	-0.293	-5.008	5.72E-06
sp|Q08193|GAS5_YEAST	-0.345	-5.666	3.58E-07
sp|P46992|YJR1_YEAST	-0.379	-2.292	0.05122
sp|P47033|PRY3_YEAST	-0.401	-2.45	0.03981
sp|P38616|YGP1_YEAST	-0.473	-2.254	0.05451
sp|P53189|SCW11_YEAST	-0.645	-3.721	0.00112
sp|Q12355|PST1_YEAST	-1.031	-6.155	3.58E-07
sp|P38248|ECM33_YEAST	-16.73	-4.097	0.00025
Limonene treatment Mut/WT			
Protein	log$_2$FC	T value	adj. p value
sp|O13547|CCW14_YEAST	1.0104	11.795	0
sp|P36135|UTH1_YEAST	0.8171	3.8901	0.0003
sp|P47001|CIS3_YEAST	0.5726	3.7131	0.00041
sp|P28319|CWP1_YEAST	0.2186	3.4781	0.00076
sp|P22146|GAS1_YEAST	-0.129	-2.441	0.01914
sp|Q08193|GAS5_YEAST	-0.305	-4.895	3.10E-06
sp|Q03180|PIR3_YEAST	-0.372	-2.543	0.01593
sp|P15703|BGL2_YEAST	-0.387	-3.604	0.00055
sp|P32478|HS150_YEAST	-0.408	-4.621	1.02E-05
sp|P32623|CRH2_YEAST	-0.422	-4.096	9.52E-05
sp|P39105|PLB1_YEAST	-0.426	-2.525	0.01658
sp|P52911|EXG2_YEAST	-0.539	-7.254	3.38E-12
sp|P38288|TOS1_YEAST	-0.539	-6.429	6.62E-10
sp|P47033|PRY3_YEAST	-0.556	-3.576	0.0006
sp|P53379|MKC7_YEAST	-0.627	-6.215	2.54E-09
sp|P38616|YGP1_YEAST	-0.704	-3.789	0.00039
sp|Q04951|SCW10_YEAST	-0.713	-7.928	4.00E-14
sp|P53189|SCW11_YEAST	-0.82	-4.361	4.92E-05
sp|P20840|SAG1_YEAST	-0.89	-14.43	0
sp|P32329|YPS1_YEAST	-1.016	-7.606	5.52E-13
sp|P46992|YJR1_YEAST	-1.249	-8.336	4.44E-15
sp|P23776|EXG1_YEAST	-1.269	-4.822	8.24E-06
sp|Q12355|PST1_YEAST	-1.524	-8.27	6.94E-12

Supplemental Materials and Methods:

GC/MS: After 12 h under limonene challenge (115 µg/l), 1 mL dodecane was added to the culture (~ 22 ml), vortexed and harvested (1 min, 4025 rcf). The top dodecane phase containing limonene was removed and stored for later analysis at -20°C. For GC/MS analysis, the dodecane-limonene mixture was diluted 1:100 in a 1:4 toluene:hexane solution. The GC-MS analysis was carried out using the settings described in Brennan et al. [1] with the following changes: 3 µL of sample was injected and the oven temperature

was set to 70°C, held for 10 min then followed by a temperature ramp of 40 °C/min to 300°C and held for 3 min. Detection was achieved in SIM acquisition mode for limonene using the following ions (m/z): 68.1, 93.1, 136.5 at 26.87 cycles/sec. The retention time for limonene was approximately 8 min.

Genomic Reconstruction: The mutant *PDR3* ORF was PCR amplified in two overlapping parts using primer pairs PDR3aF/PDR3aR and PDR3bF/PDR3bR (all primer sequences are listed in Table 1) from strain TB516 genomic DNA. The primers were located such that the 3' end of part 'a' contained 200bp of homology to the 5' end of part 'b'. The *amdSYM* marker expression cassette was amplified from the pUG-amdSYM plasmid (Euroscarf [2]) using primer pair amdPF/amdPR. The PCR amplified *amdSYM* marker was assembled between the two *PDR3* amplicons (part a and part b) using the Gibson Assembly method as in [3]. In order to facilitate part assembly the PDR3aR/amdPF and PDR3bF/amdPR primers shared 100% homology. The assembly product comprising of PDR3a-amdSYM-PDR3b was gel purified prior to PCR amplification using PDR3aF and PDR3bR primers. The PCR product was transformed into the S288C parent strain using the lithium acetate method as previously described [4] such that the native *PDR3* ORF was replaced with the PDR3a-amdSYM-PDR3b cassette. Transformants were selected on CBS plates with 0.6g/L acetamide as the sole nitrogen source in place of ammonium sulfate. Transformant colonies were screened for correct marker integration using PDR3KIcheckF and PDR3KIcheckR primers which anneal outside the knock in locus. Three positive transformants were grown in CBS media without acetamide selection to allow for *amdSYM* marker loop-out via recombination between the 200bp of homology shared between PDR3 part 'a' and part 'b'. After 24 hours of growth, cultures were plated on CBS media containing 2.3g/L fluoroacetamide for counter-selection of the amdSYM marker. Colonies were screened for loss of the *amdSYM* marker using PCR with primer pair PDR3KIcheckF/PDR3KIcheckR. Positive colonies had the full *PDR3* ORF sequenced to confirm the presence of the desired mutation and the absence of PCR generated errors. The *TCB3* mutation (frame shift at 989) was reconstructed in the S288C parent strain using the same approach as for *PDR3*, except that the knock in cassette containing the amdSYM marker was transformed in two parts (TCB3a-amdSYM and amdSYM-TCB3b). This difference arose because the Gibson Assembly product containing the two ORF parts and the *amdSYM* marker could not be obtained. Given that the TCB3a-amdSYM and amdSYM-TCB3b products were easily generated, they were co-transformed into the parent strain such that the native yeast homologous recombination machinery would

facilitate the completion of the knock-in cassette. Mutant *TCB3* DNA was amplified from TB516 genomic DNA using primer pairs TCB3aF/TCB3aR and TCB3bF/TCB3bR, while the amdSYM marker was amplified using amdTF and amdTR primers. Marker insertion and loop-out events were screened for using TCB3KIcheckF and TCB3KIcheckR primers, with all plate and growth manipulations carried out as for *PDR3*. A sequence confirmed *TCB3* strain (marker removed) was used to reconstruct the double mutant phenotype via transformation of the PDR3a-amdSYM-PDR3b knock in cassette and subsequent selection and marker removal as described above.

References

1.	Brennan, T.C.R., Krömer, J.O. & Nielsen, L.K. Physiological and Transcriptional Responses of Saccharomyces cerevisiae to d-Limonene Show Changes to the Cell Wall but Not to the Plasma Membrane. *Appl Environ Microbiol* **79**, 3590-3600 (2013).

2.	Solis-Escalante D Fau - Kuijpers, N.G.A. et al. amdSYM, a new dominant recyclable marker cassette for Saccharomyces cerevisiae.

3.	Gibson, D.G. et al. Enzymatic assembly of DNA molecules up to several hundred kilobases. *Nat Meth* **6**, 343-345 (2009).

4.	Daniel Gietz, R. & Woods, R.A. in Methods in Enzymology, Vol. Volume 350. (eds. G. Christine & R.F. Gerald) 87-96 (Academic Press, 2002).